CENTRO INTERNACIONAL DE ESTUDOS
DE DOUTORAMENTO E AVANZADOS
DA USC (CIEDUS)

TESE DE DOUTORAMENTO

INDUCED PLURIPOTENT STEM CELLS AS A NEW APPROACH IN THERAPY FOR STROKE

Esteban López Arias

ESCOLA DE DOUTORAMENTO INTERNACIONAL
PROGRAMA DE DOUTORAMENTO EN MEDICINA MOLECULAR

SANTIAGO DE COMPOSTELA
2019

USC
UNIVERSIDADE
DE SANTIAGO
DE COMPOSTELA

DECLARACIÓN DO AUTOR DA TESE

Induced pluripotent stem cells as a new approach in therapy for stroke

D. Esteban López Arias

Presento a miña tese, seguindo o procedemento axeitado ao Regulamento, e declaro que:

1) A tese abarca os resultados da elaboración do meu traballo.
2) De selo caso, na tese faise referencia ás colaboracións que tivo este traballo.
3) A tese é a versión definitiva presentada para a súa defensa e coincide coa versión enviada en formato electrónico.
4) Confirmo que a tese non incorre en ningún tipo de plaxio doutros autores nin de traballos presentados por min para a obtención doutros títulos.

Asdo. Esteban López Arias

En Santiago de Compostela, 23 de outubro de 2019

USC
UNIVERSIDADE
DE SANTIAGO
DE COMPOSTELA

AUTORIZACIÓN DO DIRECTOR / TITOR DA TESE

Induced pluripotent stem cells as a new approach in therapy for stroke

Dr. Tomás Sobrino Moreiras

Dr. Francisco Campos Pérez

Prof. José Castillo Sánchez

INFORMAN:

Que a presente tese, correspóndese co traballo realizado por D/Dna. ***Esteban López Arias****, baixo a miña dirección, e autorizo a súa presentación, considerando que reúne os requisitos esixidos no Regulamento de Estudos de Doutoramento da USC, e que como director desta non incorre nas causas de abstención establecidas na Lei 40/2015.*

En Santiago de Compostela, 23 de outubro de 2019

Directores

Tomás Sobrino Moreiras Francisco Campos Pérez José Castillo Sánchez

USC
UNIVERSIDADE
DE SANTIAGO
DE COMPOSTELA

Conflict of interest

The author and the directors of the work agreed to present the results in this Thesis and declare no conflict of interest.

USC
UNIVERSIDADE
DE SANTIAGO
DE COMPOSTELA

Research stay

During the development of the Thesis the PhD student performed a stay in an international laboratory, in the Lund Stem Cell Center in Lund, Sweden, with the Professor Zaal Kokaia from 15th of March to 15th of June 2017.

USC
UNIVERSIDADE
DE SANTIAGO
DE COMPOSTELA

Funding

This study was supported by the Spanish Ministry of Economy and Competitiveness (SAF2014-56336-R), *Xunta de Galicia* (*Consellería de Educación*: GRC2014/027 and *Axencia Galega de Innovación*), *Instituto de Salud Carlos III* (PI14/01879), Spanish Research Network on Cerebrovascular Diseases RETICS-INVICTUS (RD16/0019), and the European Union FEDER program.

The sponsors did not participate in study design, collection, analysis, interpretation of the data, writing the report, or the decision to submit the paper for publication.

USC
UNIVERSIDADE
DE SANTIAGO
DE COMPOSTELA

Agradecementos

Esta Tese non tería sido posible sen a dirección dos meus directores de tese, os Drs. Tomás Sobrino (tamén titor) e Francisco Campos, e o Prof. José Castillo. Tampouco sen a totalidade do *Laboratorio de Investigación de Neurociencias Clínicas*, que me deu a oportunidade de traballar en investigación, onde se desenvolveu a grande maioría do proxecto e onde atopei compañeiros que sempre botaron unha man, especialmente Clara Correa que traballou activamente nunha parte importante e David Barral, Juan Doval e Ramón Iglesias que se encargaron das resonancias.

Grazas tamén a tódolos laboratorios que participaron neste proxecto e que axudaron a completar os experimentos. Ó *Laboratorio de Células Madre en Cáncer y Envejecimiento* do Instituto de Investigación Sanitaria de Santiago de Compostela (IDIS) dirixido polo Dr. Manuel Collado, especialmente a Alba Ferreirós pola colaboración na obtención e caracterización de iPSCs. Ó Dr. Beiras do Servizo de Anatomía Patolóxica do Complexo Hospitalario Universitario de Santiago (CHUS) pola axuda cas imaxes de TEM. Ó *Grupo de investigación en Medicina Nuclear e Imagen Molecular* do IDIS, dirixido por Pablo Aguiar, pola axuda cos PET. Grazas ó *Lund Stem Cell Center* , dirixido polo Prof. Zaal Kokaia por acollerme na miña estadía internacional e ensinarme as técnicas de histoloxía, concretamente a Daniel Tornero. Grazas ó grupo de investigación *Bionanotools* do Centro Singular de Investigación en Química Biolóxica e Materiais Moleculares (CIQUS), dirixido por Pablo del Pino, pola axuda coa síntese e caracterización das nanopartículas de ouro.

USC
UNIVERSIDADE
DE SANTIAGO
DE COMPOSTELA

Summary

Ischemic and haemorrhagic stroke remain as diseases without treatment for recovery nor restauration of brain tissue, despite all the efforts of biomedical community to find out some neuroprotective or neurorestorative drug. Being the first cause of disability in Europe, stroke patients cost thousands of million euros per years to public health European cares; and not only as medical expenses but also direct and indirect social costs.

Many of efforts aimed to heal stroke focus on cell therapy, both in pre-clinical and clinical phases. Induced pluripotent stem cells (iPSCs) appeared in 2006 as a revolution in the way of getting stem cells. iPSCs are dedifferentiated as embryonic stem cells but can be obtained from somatic, adult and differentiated tissues. This open big opportunities in autologous grafts.

That is why we hypothesized that the systemic administration of iPSCs may improve the progress in stroke animal model, ischemic and haemorrhagic. As far as we know, we injected iPSCs intravenously in stroke animal models for the first time.

The first section presents the results of obtaining of iPSCs derived from primary mouse embryonic fibroblasts carrying a polycistronic cassette for the inducible expression of four reprogramming factors, and characterization of these cells by the standard methods.

In the second section of this study, we carried out a protocol to evaluate the potential therapeutic effect of intravenous administration of iPSCs in an ischemic stroke model in rats. The ischemic stroke was inducted by transient middle cerebral artery occlusion (tMCAO). The day after induction of cerebral ischemia, magnetic resonance imaging (MRI) and functional tests were performed. After this first follow-up, 3 million of iPSCs in 1 ml PBS were administrated in jugular vein in treated group (iv iPSCs) and 1 ml of PBS in control group. MRI and functional tests were repeated at 7, 14, 28 and 56 days. At 56 days we also acquired positron emission tomography (PET) images of whole body to check tumour

formation. And finally, rats were perfused and their brains extracted for histological analysis of neurogenesis and angiogenesis.

There were no differences in progression of lesion volumes between groups. iPSCs-treated group obtained better results in neurological tests, but not in motor test. Also, we found a greater neurogenesis in iv iPSCs group.

The third section is about the potential therapeutic effect of iPSCs administration in a haemorrhagic stroke model. The established protocol was similar to in the second section. The haemorrhage was inducted by injection of 5 µl collagenase in striatum. The first follow-ups consisted in MRI and functional tests same as in the previous section at 1, 7, 14, 28 and 56 days after model induction The treatments were administrated after first follow-up: 3 million of iPSCs in 1 ml PBS in jugular and 500000 iPSCs in 5 µl PBS in perihematoma (ic iPSCs). Control groups with injection of vehicle were also performed. PET images of whole body were acquired, and brains were extracted for histological study.

The hematoma volume progression did not show any differences between groups. ic iPSCs group presented worse punctuation in motor and neurological tests in comparison to its respective control, meanwhile iv iPSCs group obtained less deficit than its control in motor function. We observed an increased neuroblast positive area in ic iPSCs group compared to its control and enhanced activated neuroblasts in iv iPSCs group.

No differences were found in angiogenesis in any group, and PET studies did not reveal any tumour formation in both models.

In fourth section, cell tracking study was carried out to find where iPSCs travelled after systemic administration. iPSCs were labelled by 10 and 18 nm gold nanoparticles (AuNPs), apoptosis and pluripotency maintaining of labelled cells were evaluated to analyse the effect of AuNPs integration in cell metabolism. 18 nm-AuNPs-labelled cells were injected in ischemic rats in jugular vein. Organs were extracted and analysed by inductively coupled plasma mass spectrometry to measure quantity of gold. Most gold was found in liver (near to 80%) and to a lesser extent in spleen and lungs.

Resumo

As enfermidades cerebrovasculares, tanto o ictus isquémico coma o ictus hemorráxico, continúan a ser enfermidades sen tratamento para recuperación de funcións nin para a rexeneración do tecido cerebral, malia todos os esforzos da comunidade da investigación biomédica para atopar novos fármacos neuroprotectores e neurorrexeneradores. Dada a epidemioloxía e a previsión para as seguintes décadas deste tipo de enfermidades, o achado de terapias contra o ictus cobra especial importancia. As enfermidades cerebrovasculares constitúen a primeira causa de discapacidade en Europa e a segunda de mortalidade. Estes doentes supoñen un gasto de miles de millóns de euros cada ano nas sanidades públicas europeas, engadindo a isto custos sociais directos e indirectos.

Actualmente, os doentes hemorráxicos son tratados exclusivamente contra os síntomas, as consecuencias do dano cerebral pero non contra a enfermidade en si. E o único tratamento que os doentes isquémicos poden obter é a recanalización, farmacolóxica ou mecánica, do vaso sanguíneo ocluído, mais este procedemento só é eficiente nunha xanela terapéutica curta e ten varios posibles efectos secundarios non desexables. Moitos dos esforzos, tanto na investigación preclínica como na clínica, para atopar unha cura céntranse na terapia celular.

Un dos aspectos esenciais a ter en consideración no deseño dunha terapia celular é o tipo de células que se van administrar, xa que elas van ser as promotoras dos beneficios clínicos ou, pola contra, dos efectos secundarios negativos. Xa son moitos os tipos celulares empregados nos ensaios preclínicos e clínicos. A tendencia é usar células máis diferenciadas para obter efectos locais e células menos diferenciadas para obter efectos pleiotrópicos. As células nai pluripotentes inducidas (iPSCs, *induced pluripotent stem cells*) aparecen en 2006 como unha revolución no eido de obtención de células nai. As iPSCs son células indiferenciadas semellantes ás células embrionarias pero, a diferencia de estas, aquelas pódense obter de células somáticas, adultas e diferenciadas. Isto abre todo un abanico de posibilidades en enxertos autólogos.

É ben coñecido que as células excretan moléculas inmunolóxicas, exosomas e microvesículas que conteñen sinais inflamatorios e un amplo catálogo de moléculas que varía segundo o tipo celular de orixe. Xa que logo, as iPSCs tamén liberan microvesículas, a unha velocidade de 5000 por célula e hora, que conteñen determinados ARNm e factores de transcrición coma os propios do mantemento da pluripotencia (Oct3/4, Nanog, Klf4 e C-Myc). Ademais de manter o estado de pluripotencia, o conxunto de moléculas e corpos liberados polas células podería ter un efecto indutor da rexeneración en tecidos danados. En efecto, as microvesículas obtidas dun cultivo de iPSCs por si soas melloran a cicatrización nun modelo animal de fibrose pulmonar idiopática e son capaces de inhibir a apoptose causada por estrés oxidativo.

Considerando estes precedentes, a hipótese central desta tese é que a administración sistémica de iPSCs podería mellorar o prognóstico nos modelos animais de ictus isquémico e hemorráxico. O tipo de administración é a parte máis orixinal deste proxecto; xa que, segundo sabemos, nós vimos de inxectar por vez primeira iPSCs por vía intravenosa nun modelo animal de ictus.

Este estudo divídese en catro seccións. Na primeira delas se describe a obtención e caracterización das iPSCs. Foron extraídos fibroblastos primarios embrionarios dun rato transxénico portador dun casete policistrónico. Este casete codifica para os catro factores de reprogramación cara a pluripotencia (Oct4, Sox2, Klf4 e Nanog) mediante a indución por tetraciclina ou análogos coma a doxiciclina. Os fibroblastos foron cultivados e expandidos non máis aló do pase 3 e, posteriormente, cultivados con medio para iPSCs con doxiciclina. Tralo día 14 as colonias de iPSCs foron picadas e cultivadas con medio para iPSCs. A caracterización da pluripotencia das células baseouse en diferentes técnicas: tintura con fosfatasa alcalina; reacción en cadena da polimerasa con transcriptasa inversa cuantitativa para *Dlx3*, *GATA4* e *Oct3/4*; *western blot* para Sox2, Oct4 e β-Actin; citometría de fluxo para Oct4, Nanog e Sox2; formación de corpos embrionarios; e formación de teratomas *in vivo*.

A segunda sección analiza o potencial efecto terapéutico da administración intravenosa de iPSCs nun modelo de ictus isquémico en

ratas. A isquemia cerebral foi inducida mediante a oclusión transitoria da arteria cerebral media (tMCAO, *transient middle cerebral artery occlusion*). Este modelo comeza cunha incisión na liña media ventral do pescozo para expoñer a ramificación da arteria carótide logo de illar e separar os músculos esternocleidomastoideo e omohioide. Un filamento é introducido pola carótide externa e se leva ata a orixe da arteria cerebral media no polígono de Willis, onde oclúe o fluxo sanguíneo. A oclusión da MCAO mantívose durante 45 minutos.

Un día despois da oclusión da arteria cerebral media, fíxose un estudo de resonancia magnética (MRI, *magnetic resonance imaging*) co obxectivo de confirmar que existía infarto cerebral e que o tamaño deste era o adecuado co fin de reducir a variabilidade. Tamén se realizaron tests funcionais para establecer o déficit basal e a partir de este avaliar a progresión da recuperación funcional. Este seguimento composto por imaxe e tests repetiuse nos días 7, 14, 28 e 56 despois da isquemia. Logo de completar o primeiro seguimento completo administrouse o tratamento que consistiu en tres millóns de iPSCs diluídas en 1 ml de PBS no grupo tratado e o vehículo (1 ml de PBS) no grupo control; a administración foi feita por vía intravenosa, na xugular. Deste xeito, o primeiro seguimento foi realizado antes do tratamento e, polo tanto, serviu para obter resultados basais derivados da indución do modelo e non do tratamento.

Tralo último seguimento, os animais sometéronse a un estudio de tomografía por emisión de positróns (PET, *positron emission tomography*) usando o contraste 2-fluoro-2-desoxi-D-glucosa con flúor-18 (^{18}F-FDG) e escaneando todo o corpo. Esta glucosa é asimilada de forma normal polas células pero non pode ser metabolizada, así as células con máis requirimento metabólico van acumulando máis ^{18}F-FDG e, consecuentemente, emiten máis sinal. Neste estudo sinais anormalmente fortes indican con alta probabilidade a formación dun tumor. Todas as ratas do grupo tratado e algunha do grupo control foron analizadas mediante esta técnica.

Finalmente, os animais sacrificáronse, perfundíronse con PBS e formol 4%, e os seus cerebros foron extraídos para ser imbuídos en formol ata o día seguinte e en PBS con 30% de sacarosa ata que o

órgano deixe de flotar, para posteriormente facer estudos histolóxicos de neuroxénese e anxioxénese.

Na medición de volumes de infarto ó longo do seguimento de dous meses non se viron diferencias entre o grupo tratado e o grupo control. Sen embargo, os animais tratados con iPSCs tiveron mellores resultados nos tests neurolóxicos con respecto ó grupo control, non así no test motor. Nos estudos histolóxicos obtivemos diferencias entre os grupos na cuantificación da neuroxénese, os grupo tratado resultou con máis neuroblastos mitoticamente activos no hemisferio ipsilateral que o grupo control. Para avaliar a anxioxénese, cuantificamos a densidade de vasos no parénquima cerebral, mais non observamos diferencias entre os grupos. Nos estudos PET non se atopou ningún indicio de formación de tumores en ningunha das ratas, de feito a distribución do contraste polo corpo foi moi similar en todos os animais.

A terceira sección trata o estudo do potencial terapéutico da administración de iPSCs nun modelo de hemorraxia cerebral. O protocolo que seguimos nesta sección é semellante ó da sección anterior, despois da indución do modelo fixéronse seguimentos funcionais e de imaxe durante dous meses.

A hemorraxia cerebral foi xerada pola inxección de colaxenasa no estriado, 1 µl a unha taxa de 0,1 µl/min nas coordenadas -2,9 mm medial/lateral, +0,6 mm anterior/posterior, e -5,5 mm dorsal/ventral respecto de bregma; a inxección foi levada a cabo empregando un aparato estereotáxico. Unha hora despois do comezo da hemorraxia, adquiríronse imaxes de resonancia magnética para comprobar que o volume e a posición do hematoma fosen correctos e así poder reducir a variabilidade da lesión basal.

Coma na sección anterior, realizáronse seguimentos de MRI e tests funcionais nos días 1, 7, 14, 28 e 56 despois da indución do modelo, e de novo despois do seguimento do primeiro día aplicouse o tratamento. Neste caso deseñáronse catro grupos: o grupo tratado por vía intravenosa (con inxección na xugular de 3 millóns de iPSCs en 1 ml de PBS), o grupo control por vía intravenosa (inxección na xugular de 1 ml de PBS), o grupo tratado por vía intracerebral (inxección na zona perihematoma de 500000 iPSCs en 5 µl de PBS) e o grupo control por

vía intracerebral (inxección no rexión do perihematoma de 5 µl de PBS).

Ó finalizar os seguimentos, realizouse un estudo PET con ^{18}F-FDG como contraste para avaliar a posible formación de tumores e, por último, sacrificouse ó animal, perfundiuse con PBS e formol para posteriormente extraer o cerebro e reservalo ata o día seguinte en formol e despois en PBS con 30% de sacarosa. Cos cerebros leváronse a cabo estudos histolóxicos para avaliar neuroxénese e anxioxénsese.

A evolución do volume do hematoma ó longo dos dous meses non mostrou ningunha diferencia entre os grupos.

No test motor o grupo tratado con iPSCs intracerebralmente presentou unha peor puntuación con respecto ó seu control; por outra banda, o grupo tratado con iPSCs por vía intravenosa obtivo mellor resultado que o seu respectivo control na función motora, o que significa que a progresión do déficit motor foi reducido pola inxección de células por vía sistémica pero non por vía local. Nos tests neurolóxicos, unha vez máis o grupo tratado con células por vía intracerebral obtivo peores resultados con respecto ó seu grupo control. Os grupos tratados por vía intravenosa non presentaron diferencias na súa función motora nos dous meses de seguimento.

Como no modelo de isquemia, o grupo tratado con iPSCs por vía intravenosa presentou un número maior de neuroblastos activos con respecto ó seu control. Tamén o grupo tratado con iPSCs por vía intracerebral mostrou un área de neuroblastos ó redor da zona subventricular maior que o seu respectivo control nos dous hemisferios, isto quere dicir que as células rexeneradoras do tecido cerebral migraron máis, ata máis lonxe. Con todo, na cuantificación de vasos no parénquima cerebral non atopamos diferencias entre os grupos, así que concluímos que non houbo cambios na anxioxénese.

Unha vez máis os estudos PET non mostraron ningún tipo ou indicio de tumoroxénese.

Logo de comprobar o potencial terapéutico do tratamento sistémico de iPSCs en dous modelos de ictus, estudamos a distribución destas células polo corpo despois de seren inxectadas en xugular. Para poder levar a cabo este estudo é necesario ter algún tipo de marcador celular que nos permita rastrear as células unha vez estean espalladas polo

corpo. Deste xeito, a cuarta e última sección trata non só o estudo da biodistribución das iPSCs trala súa inxección en xugular, senón tamén o desenvolvemento dunha técnica que nos permitise a localización das células inxectadas.

A primeira técnica descrita é a marcaxe das células con nanopartículas (NPs, *nanoparticles*) magnéticas de ferro (MNPs, *magnetic nanoparticles*). Estas nanopartículas son captadas polas células de tal xeito que quedan integradas nelas.

A síntese das MNPs realizouse mesturando Fe (II) e Fe(III) a partes iguais en atmosfera de N_2 en condicións de temperatura controlada. Unha vez as nanopartículas estaban formadas engadiuse dextrano como cobertura (D-MNPs). Inspeccionáronse as D-MNPs por microscopio electrónico de transmisión (TEM, *transmission electron microscope*) e o seu diámetro resultou cunha media de 3,3 nm. Antes da incubación con células as D-MNPs deixáronse en axitación con poli-L-lisina para facilitar a captación destas polas células. Incubáronse as nanopartículas nos cultivos de iPSCs durante 24 horas a diferentes concentracións, mediante a tintura *Prussian Blue* comprobouse que efectivamente as células contiñan partículas de ferro, contrastando as imaxes cun control sen NPs. Tamén se adquiriron imaxes de TEM para corroborar que as nanopartículas estaban integradas no interior das células, con esta técnica observouse que as MNPs intégranse nas células formando agrupacións de diferentes tamaños.

Posteriormente, realizáronse análises de toxicidade para estudar o efecto da integración das nanopartículas nas iPSCs. Cuantificouse a proliferación celular logo de incubar as MNPs, tamén a diferentes concentracións; se ben observouse unha diminución da proliferación das células con nanopartículas con respecto ó control (células non incubadas previamente con MNPs), non se viron diferencias entre os diferentes grupos, con diferentes densidades de MNPs. Mediante citometría de fluxo analizáronse as porcentaxes de apoptose e necrose celular en mostras celulares con diferentes concentracións de MNPs. A marcaxe con Anexina, que identifica células apoptóticas, non deu diferencias entre as mostras con NPs e a mostra control. Sen embargo a marcaxe con ioduro de propidio deu unha porcentaxe de necrose máis elevada na mostra con maior concentración de MNPs que o control; non

dou diferencias, en cambio, co resto dos grupos. De todos os xeitos, a elevación da necrose, se ben estatisticamente significativa, non é tan grande como para comprometer a viabilidade da mostra. O test de LDH, que analiza o estrés celular, non mostrou diferencias entre o grupo control e os grupos incubados con MNPs.

Engadiuse un estudo *in vitro* de MRI, para comprobar que o ferro integrado nas células era capaz de captar sinal e, polo tanto, xerar un contraste para poderen ser rastreadas trala súa inxección *in vivo*. Efectivamente, obtivéronse medias de grises (a medida do sinal nas imaxes) nos mapas de T2 diminuídas nas mostras con máis ferro, tanto se comparamos diferentes concentracións de nanopartículas como se o facemos con números decrecentes de células e todas estas mostras cun control sen MNPs.

No estudo *in vivo* de MRI para localizar as células marcadas con ferro realizouse o mesmo protocolo de inxección que nas seccións anteriores, é dicir, tres millóns de iPSCs en 1 ml de PBS na xugular, pero neste caso as células foran incubadas previamente con 500 µg/ml de D-MNPs durante 24 horas e, tras lavar as nanopartículas do medio de cultivo, con medio normal durante polo menos 12 horas. Neste caso, as ratas foron sometidas ao modelo de isquemia descrito na sección segunda e se lles administraron as iPSCs-D-MNPs 24 horas despois da indución do modelo. Escaneouse o corpo enteiro e, especificamente, o cerebro dos animais xusto antes da inxección, xusto despois dela e dous días despois. Desafortunadamente, non se atoparon diferencias entre as imaxes nos diferentes tempos de seguimento, isto é, non se observou contraste causado polo ferro das MNPs. Concluímos, polo tanto, que malia que o ensaio *in vitro* conseguiu presentar diferencias no sinal das diferentes mostras con diferentes cantidades de ferro, esta captación de sinal non é suficiente para obter contraste nos estudos *in vivo* por mor do grande espallamento das células na distribución sistémica.

Ó descartar o seguimento das células marcadas con ferro por MRI, decidimos analizar a cantidade de ferro nos órganos de animais tratados con iPSCs-D-MNPs mediante espectrometría de masas con plasma acoplado inductivamente (ICP, *inductively coupled plasma mass spectrometry*). Para isto, usamos o protocolo de administración anteriormente descrito, é dicir, incubación con 500 µg/ml de D-MNPs

durante 24 horas, logo con medio normal durante polo menos 12 horas e inxección de tres millóns de iPSCs-D-MNPs en 1 ml de PBS en xugular logo de 24 horas tras indución do modelo de isquemia. As ratas foron sacrificadas e perfundidas con PBS 12, 24 e 48 horas despois da inxección e os seus órganos (cerebro, pulmóns, bazo, riles e fígado) extraídos. Medíronse os niveis de ferro en cada un dos órganos e comparáronse con niveis de ferro de ratas control (ratas isquémicas sen administración de células). Con esta técnica observamos uns niveis basais (os do grupo control) tan elevados que foi imposible poder identificar diferencias na cantidade de ferro nos distintos órganos. Por exemplo, no órgano con máis cantidade de ferro, o fígado, o nivel basal é de ó redor de 1500 µg e a cantidade total que se inxecta nos tres millóns de iPSCs-D-MNPs é de pouco máis de 20.

Posteriormente, debido ó resultado non satisfactorio da marcaxe das células con nanopartículas de ferro, procedemos a marcar as iPSCs con carboxifluoresceína succinimidil éster (CFSE), unha molécula fluorescente que é interiorizada polas células. Primeiramente, realizouse un ensaio *in vitro* para comprobar a marcaxe fluorescente e a súa identificación mediante citometría de fluxo. Incubáronse as células con CFSE seguindo o manual do fabricante e analizouse o seu sinal de fluorescencia xusto despois da marcaxe, 12, 24 e 48 horas despois diso. Observouse que preto do 100% das células ficaban marcadas e o sinal diminuía co tempo debido a división celular normal ata un 60% de células positivas ás 48 horas. Tres millóns de iPSCs marcadas con CFSE foron inxectadas nunha rata isquémica, 12 horas despois o animal foi sacrificado, perfundido con PBS e os seus órganos extraídos. As células dos órganos (pulmóns, bazo, riles e fígado) foron disgregadas, pasadas por un filtro para separalas e diluídas en PBS. Esta suspensión celular foi analizada por citometría de fluxo e comparada cunha suspensión celular de órganos dunha rata á que non se lle administrou nada, os histogramas de fluorescencia de todos os órganos das dúas ratas non mostraron diferencias. Polo tanto, non puidemos detectar presencia de células fluorescentes en ningún dos órganos e, consecuentemente, non foi posible obter resultados para definir unha biodistribución das iPSCs trala súa administración sistémica.

A seguinte proba consistiu en marcar células cun elemento radioactivo para seren detectadas en PET. Neste caso fíxose unha proba de concepto con células mesenquimais, que foron incubadas con ^{18}F-FDG. Sen embargo, en ningún caso, foron probadas diferentes condicións de cultivo, se conseguiu unha marcaxe suficientemente forte para poder levar este modelo ó seguinte paso, que sería o estudo *in vivo*.

Finalmente, optouse pola marcaxe das células con nanopartículas de ouro (AuNPs) co fin de detectar e medir as cantidades de ouro por ICP nos órganos trala inxección das células marcadas.

As AuNPs foron sintetizadas a partir de $HAuCl_4$ nunha solución de citrato de sodio e ácido cítrico, mediante a posterior adición en diferentes pasos de $HAuCl_4$ as NPs puidéronse crecer. Así obtivéronse AuNPs cun diámetro de media de 10-11 nm, as sementes, e outras de 18-19 nm, as NPs crecidas. Logo funcionalizáronse con albumina de soro bovino (BSA, *bovine serum albumin*) unida a rhodamina b; a BSA facilitará a captación de NPs por parte da célula e a rhodamina b, molécula fluorescente, permitiranos detectar e medir de forma relativa a marcaxe.

Os dous tamaños de nanopartículas foron incubadas en cultivos de iPSCs a diferentes tempos e concentracións. As iPSCs-AuNPs, posteriormente, foron analizadas no citómetro de fluxo co fin de coñecer que porcentaxe de células estaban marcadas con rhodamina b, é dicir, tiñan NPs integradas; e cal era a media de fluorescencia, isto é, cuantificar de forma relativa a cantidade de NPs integradas. Os mellores resultados tanto na porcentaxe positiva de iPSCs para rhodamina b como na media de fluorescencia obtivéronse co cultivo de 1 $mg_{AuNPs/ml}$ cunha de incubación de 24 horas das nanopartículas de 18 nm.

Coas mesmas condicións tamén se analizaron as porcentaxes de apoptose mediante a tintura con Anexina usando citometría de fluxo. Estes resultados non deron diferencias entre as diferentes condicións de incubación das AuNPs con respecto ó control (iPSCs baixo un cultivo normal).

Dado que a maior porcentaxe de células marcadas con NPs e a maior media de fluorescencia obtivéronse incubando as nanopartículas de 18 nm durante 24 horas a unha densidade de 1 mg/ml, foi esta a condición escollida para o ensaio de mantemento de pluripotencia. Utilizando un

kit de marcaxe de pluripotencia para citometría de fluxo (composto por marcadores para Oct3/4, Nanog e Sox2) comparáronse os niveis de pluripotencia dun cultivo normal de iPSCs cun cultivo de iPSCs trala incubación con AuNPs a diferentes tempos. En ningún caso a porcentaxe de células tripla positivas para os marcadores de pluripotencia foi menor nas iPSCs marcadas con NPs que nas iPSCs controis.

A análise da cantidade de ouro por ICP-MS dunha mostra de iPSCs-AuNPs deu como resultado que en tres millóns de células marcadas con nanopartículas (a cantidade de células que usamos anteriormente para as inxección por vía intravenosa) hai 114 µg de Au.

Finalmente, foron inxectadas tres millóns de iPSCs-AuNPs en ratas isquémicas, seguindo o mesmo protocolo que as administración sistémicas das seccións segunda e terceira. 24 horas despois da inxección os animais foron sacrificados e perfundidos, e os órganos (cerebro, riles, bazo, pulmóns e fígado) extraídos para cuantificar os niveis de ouro presentes en cada un e comparalos con órganos de ratas controis (sen inxección de células). A grande parte do ouro atopouse no fígado (87%), aínda que tamén os pulmóns e o bazo presentaron cantidades a ter en conta.

Polo tanto, concluímos que a biodistribución das iPSCs, a diferencia de outras células como as mesenquimales, céntrase no fígado e en menor medida en pulmóns e bazo.

INDEX

ABBREVIATIONS

^{18}F-FDG: ^{18}Fluor-fludeoxyglucose.

AMPA: α-amino-3-hydroxy-5-methyl-4-isoxazolepropionic acid.

AMPAr: α-amino-3-hydroxy-5-methyl-4-isoxazolepropionic acid receptor.

AP: Alkaline phosphatase.

ASA/AHA: Heart Association/American Stroke Association.

ATP: Adenosin trifosfato.

AuNPs: Gold nanoparticles.

AVM: Arteriovenous malformation.

BBB: Blood–brain barrier.

BCIP: 5-bromo-4-chloro-3-indolylphosphate.

BDNF: Brain-derived neurotrophic factor.

BMSCs: Bone marrow stem cells.

BSA: Bovine serum albumin.

CD: Cluster of differentiation.

CFSE: Carboxyfluorescein succinimidyl ester.

CI: Confidence interval.

CNS: Central nervous system.

COX-2: Cycloxigenase-2.

CT: Computed tomography.

DCX: Doublecortin.

DLS: Dynamic light scattering.

DMEN: Dulbecco's modified eagle medium.

D-MNPs: Dextran magnetic nanoparticles.

DNA: Deoxyribonucleic acid.

DPSCs: Dental pulp stem cells.

EDTA: Ethylenediamine tetraacetic acid.

EPO: Erythropoietin.

ESCs: Embryonic stem cells.

FBS: Fetal bovine serum.

FDG: Fludeoxyglucose.

FEEN: Fundación Española de Enfermedades Neurológicas (Neurological Diseases Spanish Foundation).

FOV: File of view.

GADPH: Glyceraldehyde 3-phosphate dehydrogenase.

GFAP: Glial fibrillary acidic protein.

HEK293T: Embryonic kidney 293.

HO: Heme oxygenase.

HRP: Horseradish peroxidase.

HUCBCs: Human cord blood cells.

i4F-MEFs: Inducible expression of the four reprogramming factors mouse embryonic fibroblasts.

ic: Intracranial.

ICAMs: Intercellular adhesion molecules.

ICH: Intracerebral haemorrhage.

ICP: Inductively coupled plasma.

ICP-MS: Inductively coupled plasma mass spectrometry.

IDIS: Instituto de Investigación Sanitaria de Santiago de Compostela (Health Research Institute of Santiago de Compostela).

IL: Interleukin.

INE: Instituto Nacional de Estadística (Statistics National Institute).

iNOS: Inducible NO synthase.

iPSCs: Induced pluripotent stem cells.

iv: Intravenous.

LDH: Lactate dehydrogenase.

LIF: Leukemia inhibitory factor.

MAPMTs: Multi-anode photomultiplier tubes.

MCA: Middle cerebral artery.

MenSCs: Stem cells isolated from menstrual fluid.

MGE: Multigradient-echo.

MLEM: Maximum likelihood expectation maximization.

MMPs: Metalloproteinases.

MNPs: Magnetic nanoparticles.

MRI: Magnetic resonance imaging.

mRNAs: Messenger ribonucleic acid.

MSCs: Mesenchymal stem cell.

MSME: Multi-slice multi-echo.
NBT: Nitro blue tetrazolium.
NES cells: Neuroepithelial-like stem cells.
NF-κB: Nuclear Factor kappa-light-chain-enhancer of activated B cells.
NIH: National Institutes of Health.
NMDA: N-methyl-D-aspartate glutamatergic.
NMDAr: N-methyl-D-aspartate glutamatergic receptors.
nNOS: Neuronal nitric oxide synthase.
NO: Nitric oxide.
NP: Nanoparticle.
NSCs: Neural stem cells.
OCT: Optimal Cutting Temperature.
OSKM: Oct-3/4, Sox2, Klf4 and c-Myc.
PBS: Phosphate-buffered saline.
PCR: Polymerase chain reaction.
PEI: Polyethylenimine.
PET: Positron emission tomography.
PI: Propidium iodide.
PI3-Akt: Phosphatidylinositol-3-kinase.
PLA2: Phospholipase A2.
PLL: Poly-lysine.
p-SCs: Placenta-derived stem cells.
PVDF: Polyvinylidene difluoride.
RIAIDT: Network of Infrastructures to Support Research and Technological Development.
RIPA: Radioimmunoprecipitation assay.
ROS: Reactive oxygen species.
rtPA: Recombinant tissue plasminogen activator.
RT-qPCR: Quantitative real time polymerase chain reaction.
SAH: Subarachnoid haemorrhage.
SD: Sprague-Dawley.
SDF-1: Stromal Cell-Derived Factor-1.
SEM: Standard error of the mean.
SPIO: Superparamagnetic iron oxide.
SVZ: Subventricular zone.

TEM: Transmission electron microscope.
tetOP: Tetracylin dependent promoter.
TIA: Transient ischemic attack.
TIE-2: Angiopoietin-2 receptor.
tMCAO: Transient middle cerebral artery occlusion.
TNF- α: Tumour necrosis factor-α.
TOAST: Trial of ORG 10172 in Acute Stroke Treatment.
TTBS: Tween-tris-buffered saline.
UV-Vis: Ultraviolet–visible spectroscopy.
VEGF: Vascular endothelial growth factor.
VEGFR: Vascular endothelial growth factor receptor.
WB: Western blot.

1. INTRODUCTION

USC
UNIVERSIDADE
DE SANTIAGO
DE COMPOSTELA

1.1.STROKE

1.1.1. DEFINITION OF STROKE

ASA/AHA (American Stroke Association/American Heart Association) defined stroke as a "neurological deficit attributed to an acute focal injury of the central nervous system (CNS) by a vascular cause, including cerebral infarction, intracerebral haemorrhage (ICH), and subarachnoid haemorrhage (SAH), and is a major cause of disability and death worldwide".(1)

In spite of different types of stroke, there is a set of common symptoms: weakness or numbness on one side of the body, difficulties of vision in one or both eyes, speaking or understanding language difficulty, headache more severe than usual and dizziness or instability, especially when associated with other symptoms above.(2) However many strokes are asymptomatic and are discovered only after an imaging test.

1.1.2. EPIDEMIOLOGY

According to the INE (*Instituto Nacional de Estadística*), stroke is the second cause of mortality in Spain that involved 7% (27850) of all deaths in 2013, and is the main cause in women, in fact 58.4% of deaths by stroke were women.(3) The 69% of stroke patients survive 4 years after stroke of any type, and the 55.4% of patients survive 10 years or more after ischemic stroke (**Figure 1**).(4)

The annual incidence of stroke is 120-350 per 100000 people (95% Confidence Interval (CI)), including both women and men.(5) The average of hospital stay due stroke is 13.6 days. However, 6 months after stroke, the 53% of patients have disability,(6) and 41.5% of them still have it after a year of follow-up.(7) Given these data, stroke is considered the most common cause of complex disability in adults.(8) In summary, the current scenario of the stroke in developed countries shows increased rates of incidence and prevalence, but a decreased in mortality (**Figure 2**).(9)

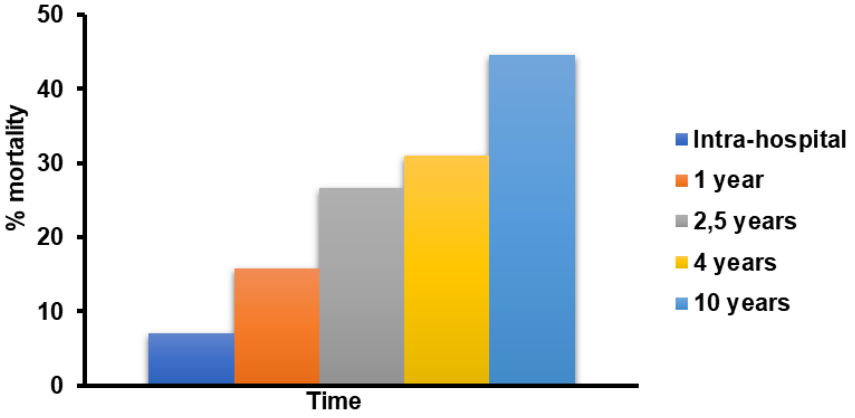

Figure 1: Cumulative death rate after stroke according to INE (self-created image).(3)

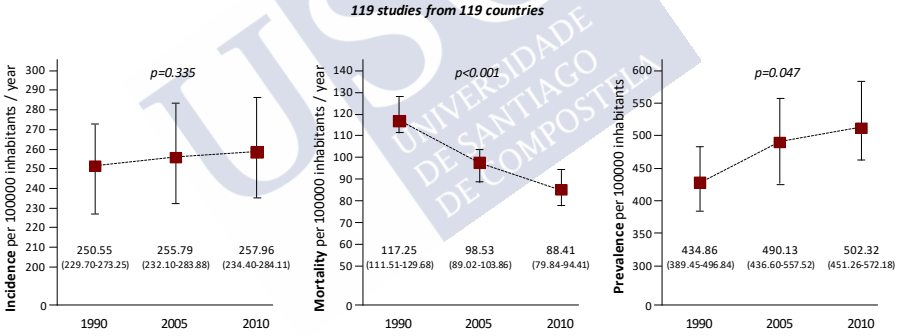

Figure 2: Age-adjusted annual incidence, mortality and prevalence in 1990, 2005, and 2010 according to Feigin *et al*. (self-created image).(9)

All Spanish studies about cost associated to stroke management show a huge public expenditure. FEEN (*Fundación Española de Enfermedades Neurológicas*) report(10) estimated that Spanish government spent about 1142 million euros in 2004 in stroke patients that means 13383 €/patient; nevertheless, this expenditure was lower than European average (16569 €/patient). Moreover, it is supposed that costs associated to stroke will increase in the following years; for example, the forecast for 2050 is estimated in 1900 million euros. The

study published by Carod-Artal *et al.* calculated that the cost of the follow up of stroke patients represent the 46% of whole expenditure during the first year;(11) another study by Beguiristain *et al.* estimated that the outpatient treatment means the 86.5% of total expenditure, 103 of 120 million euros in Basque Country in 2000.(12) But the most of total cost (53%) is spent in no healthy direct fee, including informal care and social cost programs. Importantly, during the first year after stroke, informal cares and indirect cost add up 58.3%, and this costs increase until the 72.4% of total public expenditure after the second year from stroke onset (**Figure 3**).(13)

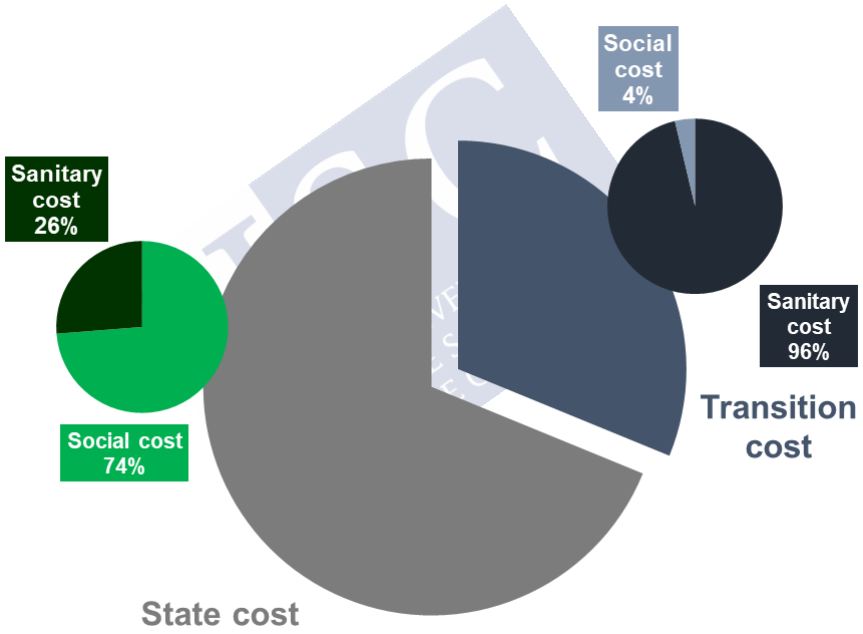

Figure 3: Distribution of expenditure caused by stroke in Basque Country according to Beguiristain *et al*. (self-created image).(12)

1.1.3. CLASSIFICATION AND PATHOPHYSIOLOGY OF STROKE

Stroke is mainly classified in ischemic and haemorrhagic stroke, depending on their nature. However, these two main groups of cerebrovascular diseases can be subdivide in accordance with other parameters such as stroke subtype, progression profile, neuroimaging characteristics, size and topography of the lesion, nature, mechanisms of induction, and aetiology.(2, 14)

1.1.3.1. Ischemic stroke

Ischemic stroke is produced by an obstruction of a cerebral blood vessel. This obstruction prevents blood flow in a specific region of the brain; therefore, the input of oxygen and glucose is decreased or cancelled. This type of stroke is the most common and represents about the 80% of all strokes.(2, 5, 15, 16) Ischemic stroke can be sub-classified as transient ischemic attack (TIA) or cerebral infarction. TIA is a focal cerebral dysfunction whose symptoms last for less than one hour, and is a vascular insufficiency due to an arterial thrombus or embolism.(17) A TIA is a risk factor for another major stroke. Cerebral infarction, by contrast, implies a long-lasting and intense blood flow deprivation with the consequent loss of brain parenchyma.

According to the aetiology, ischemic stroke was classified by the trial of ORG 10172 in Acute Stroke Treatment (TOAST) criteria,(16) in five subtypes: 1) large-artery atherosclerosis, 2) cardioembolism, 3) small-vessel occlusion, 4) stroke of other determined aetiology, and 5) stroke of undetermined aetiology:

- In **large-artery atherosclerosis** are included ischemic stroke patients with significant stenosis or occlusion (<50%) of a major brain artery or branch cortical artery.
- Ischemic stroke patients classified in **cardioembolic** category should have at least one cardiac source of risk of embolism.
- **Small-vessel occlusion** is that category for ischemic stroke patients with lacunar infarcts who should have a lesion with a diameter of less than 1.5 cm in brain imaging.

- Ischemic stroke patients with non-atherosclerosis vasculopathies, hypercoagulable states, or hematologic disorders are classified as acute ischemic stroke of **other determined aetiology**.
- Ischemic stroke of **undetermined aetiology** is for those patients with two or more causes identified, negative evaluation, or incomplete evaluation.

Despite TOAST criteria, there are other classifications such as Stroke Data Bank Subtype Classification or Oxfordshire Community Stroke Project Subtype Classification; however, TOAST is the most used classification in clinical practice and in clinical trials. Besides, it is a well-known classification, widely used in practice and literature and has got improved reliability.(18)

1.1.3.1.1. Pathophysiology of ischemic stroke

Ischemic stroke is induced by a decrease in cerebral blood flow by a thrombus/clot that occludes an artery in the brain. This process impacts on the normal cellular functions, but the extent of alterations depends on the severity of the reduction of flow, occlusion time, cerebral area and type of affected cells. Biochemical and metabolic paths associated to ischemic stroke are globally included in the concept "ischemic cascade" (**Figure 4**).

From beginning to end of ischemic cascade, several events take place: interruption of oxidative phosphorylation processes, deficient production of adenosine tri-phosphate (ATP), membrane depolarization, molecular imbalance, release of neurotransmitters, free radical generation, inflammatory process, early and late expression of genes, etc (**Figure 5**).(19) All these events induce cellular stress that finally may cause cell death.

In the case of an abrupt change of energy input, cell death will happen by necrosis. When homeostasis is lost, big and disordered changes occurs such as rupture of the cell membrane that provokes the cellular content empties into the intercellular space. On the other hand, those cells not undergoing necrosis go through slower and more controlled apoptotic process, where brain cells regulate the activation of specific genes in order to degrade cellular components in an organized way.

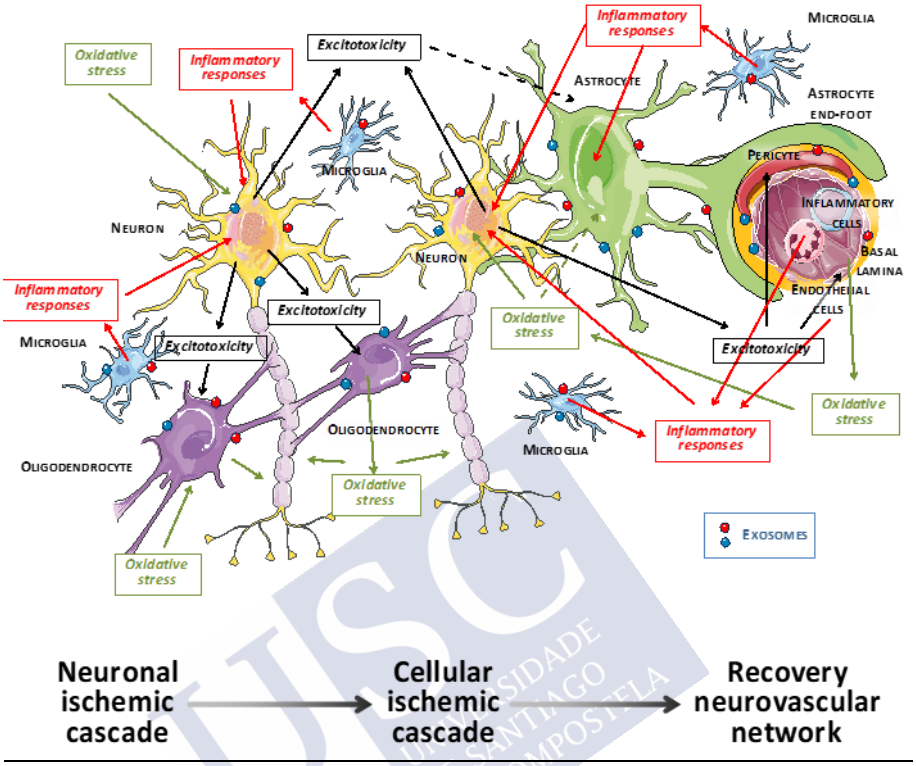

Figure 4: Biochemical pathways associated to ischemic cascade from the molecule to the neurovascular network (self-created image using elements with creative commons license).

At the beginning of ischemic stroke, lack of ATP and phosphocreatine alter ionic pumps in cell membrane and endoplasmic reticulum membrane. Pumps of neurons and glial cells stop, and ischemic depolarization happens; this depolarization englobes decrease of K^+ and increase of Ca^{2+}, Na^+ and H_2O levels inside cells; this process causes cytotoxic oedema. Furthermore, anaerobic acidogenic conversion of glucose also induces entry of Ca^{2+} inside the cells that mediated the release of glutamate and other excitatory neurotransmitters. Massive release of excitatory neurotransmitters has toxic effects in neurons by excitotoxicity processes. Additionally, release of noradrenalin and adenosine mediates the increase of Cl^-, Na^+

and H_2O permeability in glial cells; this process is called astrocytic oedema.(20)

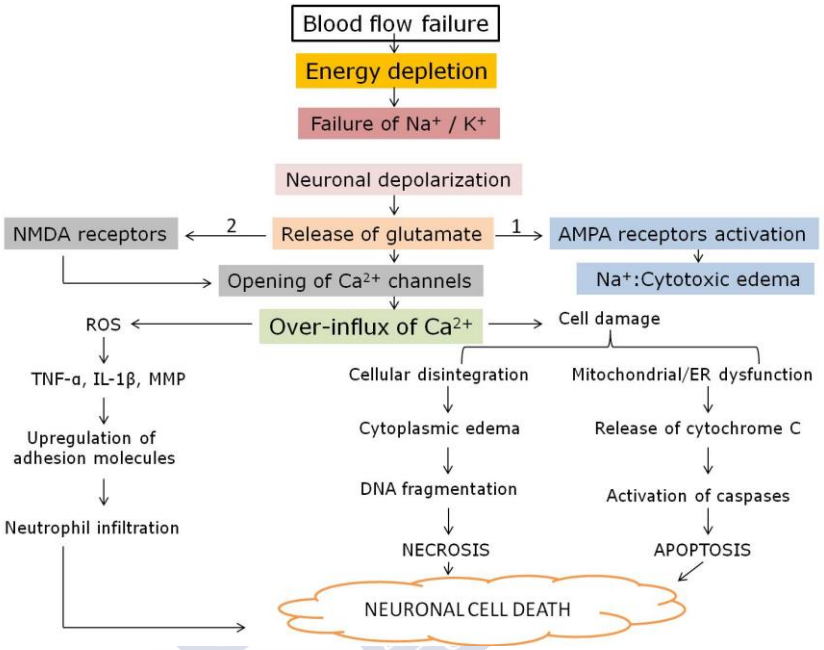

Figure 5: Sequence of main physiopathological events in cerebral ischemia (self-created image using elements with creative commons license).

Excess of intracellular Ca^{2+} levels actives several enzymes such as NO synthases, phospholipases, proteases, endonucleases, kinases and phosphatases.(21) This enzyme activation, together with the ion exchange and energetic failure increase extracellular glutamate levels that provokes the excitability of N-methyl-D-aspartate glutamatergic (NMDA) receptors (NMDAr), and α-amino-3-hydroxy-5-methyl-4-isoxazol propionic acid (AMPA) receptors (AMPAr), which positively feeds back the intracellular increase of Ca^{2+}. (**Figure 6**).(22-24)

This metabolic dysfunction generates free radicals. Specially, arachidonic acid and neuronal nitric oxide (NO) synthase (nNOS) at early stages, infiltration of neutrophils at intermediate stage, and inducible NO synthase enzymes (iNOS) and cycloxigenase-2 (COX-2)

induce production of oxygen reactive species (ROS) that induce oxidative stress increasing ischemic damage.(25, 26)

Finally, leucocytes adhesion to vessel wall and their transendothelial migration are promoted by several events: phospholipase A2 (PLA_2) activation; P-, E- and L- selectins and intercellular adhesion molecules (ICAMs) expression by endothelial cells; and reactive gliosis that increase cytokines, chemokines, growth factors and neuropeptides expression. All together provoke an inflammatory response, which if exacerbated, increases brain parenchymal damage induced by cerebral ischemia.

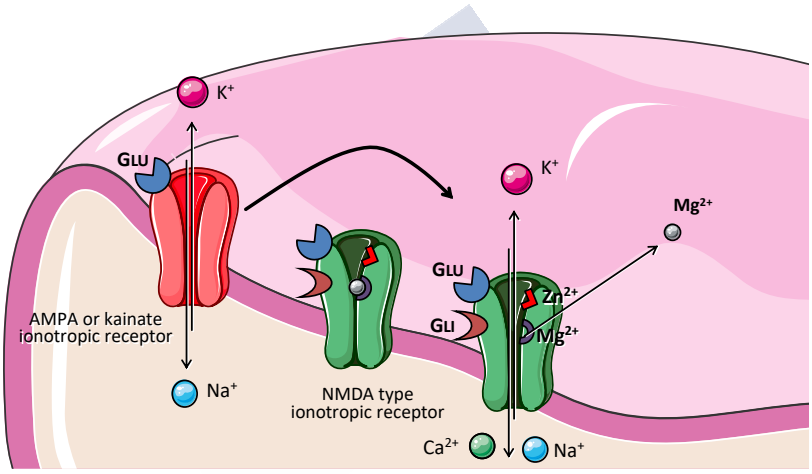

Figure 6: Role of glutamate on the stimulation of AMPA and NMDA receptors during cerebral ischemia (self-created image using elements with creative commons license).

As previously mentioned, depending on how controlled the cellular death is, this can occur by two different processes: necrosis and apoptosis.(27) In necrosis, the acute energetic failure provokes morphological cell changes ending in their lysis and subsequent necrosis.(28) By contrast, apoptosis is a programmed cell death; specific mechanisms of controlled degradation of cells are activated, and apoptosis occurs in an energy-dependent way.(29, 30)

Generally, in the early lesion there are two different regions caused by the heterogenicity of reduction of blood supply: core and

penumbra.(31) The ischemic core typically is located in the centre of the ischemic lesion and contains irreversibly injured cells. Cellular damage is metabolic and structural; therefore, cells are mortally injured and will become into necrotic cells. It was estimated that this process occurs with a blood flow less than 10 ml/100g·min.

On the other hand, collateral blood flow allows a residual input in the distal area of occluded vessel establishing the penumbra of stroke. This event creates a zone with reversible injured cells when blood flow is between 10 and 20 ml/100 g·min that may lead to apoptosis if brain tissue is not reperfused.(32)

The concept of ischemic penumbra was introduced by Astrup, Siesjö and Symon in 1981 and it was described as tissue around the centre of ischemia that has no electrical function, but extracellular concentration of potassium is normal or close to; then they placed it between two thresholds: "the upper threshold of electrical failure and the lower of energy failure and ion pump failure".(33) Over the span of more than 30 years the concept has being changed. Currently, inhibition of protein synthesis and maintaining of energy state is considered to define penumbra. In fact, it is showed that there is a zone in ischemic brain with intact ATP concentration but suppression of protein synthesis; moreover, the volume of this zone is decreased as the occlusion is longer (**Figure 7**).(34)

The length of occlusion and the magnitude of affected artery will mark the severity of ischemia. It is important to note that time is one of the most important factors.

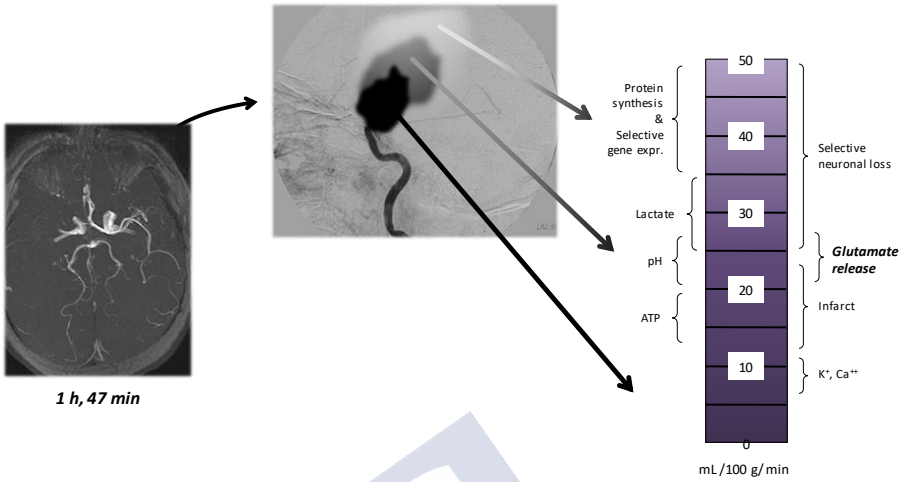

Figure 7: Representation of ischemic penumbra after cerebral ischemia (self-created image).

1.1.3.2. Haemorrhagic stroke

Among all cerebrovascular diseases, the pathologic group of haemorrhages corresponds to approximately 15% of all strokes. This percentage excludes those derived from cranioencephalic trauma. In essence, it consists in a blood extravasation, secondary to the breakage of a blood vessel, either arterial or venous, by diverse mechanisms.(2)

Intracerebral haemorrhage is classified into two types according to the cause. Primary intracerebral haemorrhage is spontaneous and more common than secondary one; and it is caused by arterial hypertension or amyloid angiopathy. Secondary intracerebral haemorrhage is due to rupture of abnormal vessels, or is associated to tumours, arteriovenous malformation, coagulation alterations, drug abuse.(35)

1.1.3.2.1. Pathophysiology of haemorrhagic stroke

Bleeding inside brain produces blood accumulation within cerebral parenchyma and an increase of intracranial pressure. Primary damage of tissue is related with the growth of hematoma and its consequent rupture of adjacent tissue and mass effect. Moreover, broken membranes from neurons and glial cells induce necrosis and cytotoxic

oedema by the release of excitotoxicity neurotransmitters. Furthermore, alterations of cell homeostasis produce rupture of blood-brain barrier (BBB), so damage is increased due to vasogenic oedema and uncontrolled passage of molecules, in special inflammatory cytokines.(36)

On the other hand, after bleeding, fragments of erythrocytes membranes release oxyhaemoglobin to the cerebral parenchyma that will be transform in methaemoglobin after few hours. In the cellular exterior, the heme group is converted in biliverdin, ferrous iron (Fe^{3+}), and CO by heme oxygenase (HO) enzyme; and biliverdin reductase convert biliverdin to bilirubin. From all these potential toxic molecules, Fe^{3+} is extremely toxic since reacts with H_2O_2 generating free radicals; CO relaxes vascular muscles and decrease vasospasm; low concentrations of bilirubin have antioxidant role, but high concentrations, as occurs in intracerebral haemorrhage, is neurotoxic. Degradation of haemoglobin within brain parenchyma damages proteins, DNA and lipids, active caspases and finally generate cellular death.(37)

Blood extravasation also permits the cross of coagulation factors to the brain parenchyma, as thrombin and tissue factor. Initially, thrombin is neuroprotector because limit hematoma; however, excessive accumulation of thrombin in cerebral parenchyma stimulate the expression of inflammatory cytokines, such as tumour necrosis factor-α (TNF- α) and metalloproteases by glial cells. These molecules induce degradation of extracellular matrix, BBB rupture and lysis of endothelial cells. Likewise, tissue factor damages vessels and inhibits normal function of coagulation mechanism that may mediate the formation of cerebral thrombus.

Additionally, nuclear factor kappa-light-chain-enhancer of activated B cells (NF-κB) actives several molecules such as adhesion molecules, cytokines, chemokines, metalloproteases, immune receptor, etc., increasing inflammation and, therefore, exacerbating damage.(38)

1.2.THERAPEUTIC APPROACHES FOR THE TREATMENT OF STROKE

1.2.1. THROMBOLYSIS AND NEURO-INTERVENTIONISM IN ACUTE PHASE OF STROKE

The therapeutic window in ischemic stroke is very short, so fast action is essential for the patient recovery. Pharmacological thrombolysis and mechanical thrombectomy, whose objective is to remove the clot and allow the blood flow supply again, are the gold-standard treatments in acute phase of ischemic stroke. Pharmacological thrombolysis is induced by recombinant tissue plasminogen activator (rtPA), an enzyme that catalyses the conversion of plasminogen to plasmin and constitutes the most common thrombolytic agent. Thrombectomy can be performed by several technics: aspiration, mechanical break up, ultrasound waves. Reperfusion therapies are effective within the first 4.5 hours (for thrombolysis with rtPA) and 6 hours (for thrombectomy) from stroke onset. However, thrombolysis with rtPA presents side-effects such as risk of haemorrhagic transformation and oedema development. Because of this, only 3-7% are treated with these technics.(39-43) For this reason, patients with intracranial haemorrhage and blood tests resulting haemorrhagic diathesis are excluded.(44) The therapeutic window may be extended by a discerning selection of patients with a large penumbra through neuroimaging techniques.(45)

On the other hand, haemorrhagic stroke patients are only treated for symptoms, maintaining constant vital functions, oxygenation, temperature and glycaemia, or controlling risk factors as hypertension. In some patients, decompressive craniotomy is performed in order to relieve mass effect; this surgery is possible if haemorrhage is not deep. Moreover, ICH must also be removed if it is associated with an AVM or tumour.(46)

Due to its limited treatments and its high prevalence with a great social impact, it is necessary to develop new therapeutic options for stroke.

1.2.2. NEUROPROTECTION

Neuroprotection is any therapeutic strategy or combination of them that prevents, interrupts, or slows down biochemical and molecular damage that could become irreversible after an ischemic or haemorrhagic brain event. Several compounds have been suggested and tested as neuroprotectors and most of them have shown good results in pre-clinical studies, though unfortunately none was shown to be an effective therapy in clinical trials.(47, 48)

Neuroprotective drugs can be mainly classified into different groups regarding their action mechanism.

a. Calcium blockers

The significant deleterious role of calcium in the ischemic cascade led to postulate calcium channel blockers as potential treatment against ischemic brain damage. Nimodipine is an example of calcium blocker. More than 250 preclinical studies of nimodipine in cerebral ischaemia have been published, but only 10 of them have shown positive results.(47) Other calcium channel blockers have been tested with similar negative results in clinical trials.

b. Glutamate antagonists

It is well established that glutamate, the major excitatory CNS neurotransmitter, is also capable of inducing excitotoxic neural injury in the setting of cerebral ischemia and other disorders. Glutamate and other related excitatory amino acids interact with several membrane receptors, which are relevant to neuroprotection. These mainly include NMDA and AMPA receptors.(48)

It has been reported that antagonists of NMDA receptors reduce infarct size and neurological deficit in animal models of focal cerebral ischemia, but its clinical use has showed several side effects, especially of cardiovascular and psychiatric origin. For example, selfotel, a competitive antagonist of NMDA receptors, has shown outcome improvement and no significant increase of mortality in a phase III study, but a high incidence of psychiatric adverse effects conditioned its withdrawal from clinical practice. Likewise, dextromethorphan and its metabolites dextrorphan and aptiganel were discontinued by an

unfavourable relationship between risk and benefit showing increased adverse effects. Eliprodil and gavestinel, other antagonists of NMDA receptors, showed excellent tolerance, but no efficacy.(49)

On the other hand, several AMPA antagonists showed neuroprotective effects in preclinical studies of both focal and global cerebral ischemia, but successful in larger clinical trials has not been reported.(48)

c. Antioxidants

Antioxidants were proposed as neuroprotective agents capable to prevent the oxidative stress generated by ischemic cascade. NXY-059, the most promising antioxidant drug, were tested in ischemic animals showing a great reduction of stroke volume. Although the first clinical trial was positive showing functional improvement of patients with acute ischemic stroke, a subsequent trial did not reproduce these beneficial effects.(50)

Another antioxidant that reached clinical phase is uric acid, another antioxidant that showed neuroprotective effects in preclinical models of ischemic stroke. A recent clinical trial(51) assessed whether uric acid therapy would improve functional outcomes at 90 days in patients with acute ischemic stroke. The results showed that uric acid treatment is safe but did not increase the proportion of patients who achieved excellent outcome after stroke compared with placebo.

d. Phospholipid precursors: citicoline

Citicoline stimulates structural phospholipids biosynthesis in neuronal membrane, specifically phosphatidylcholine (PC), inhibiting phospholipases and, therefore, the destruction of membrane lipids after ischemia, reducing free radicals production and excitotoxicity.(52, 53) In preclinical studies, citicoline treatment mediated a reduction of functional deficits at 28 days after induction of ischemia.(54) In 2002,(55) it was reported that citicoline treatment mediated functional recovery in one third of ischemic stroke patients; however, a more recent clinical trial(56) did not exhibit any neuroprotective effect in acute ischemic stroke patients.

e. Inhibitors of glutamate release

The inhibition of presynaptic glutamate release blocks ion channels activation and reduces the synthesis of nitric oxide, acting as a NMDA antagonist; and therefore it can be a potential neuroprotective in cerebral ischemia.(57) Lubeluzole, a benzothiazole derivative, is an example of this type of drugs that prevents the rising of extracellular glutamate as an indirect NMDA antagonist. In ischemic rats, lubeluzole treatment achieved neuroprotection at hippocampus level, maintaining the integrity of pyramidal neurons and decreasing cell death seven days after ischemia.(58) Nevertheless, clinical trials showed no effective effects in prevention of patients death or dependency.(59)

f. GABA agonists

The mechanism of action of GABA agonists involves potentiation of the activity of GABA, the brain´s major inhibitory neurotransmitter. GABA agonists attempt to counteract cellular depolarization caused by ischemia. Clinical trials with clomethiazole, which increases the activity of GABA, were negative in patients with total anterior circulation infarcts. Moreover, MaxiPost, a drug capable of inducing hyperpolarisation of neurons by opening potassium channels, also showed no benefit in clinical trials.(48)

g. Anti-inflammatory

The anti-inflammatory compounds act by inhibiting any of the mechanisms of extensive inflammatory cascade after cerebral ischemia. The enlimomab, a monoclonal antibody against ICAM-1 that inhibits leukocyte adhesion and migration through the vascular endothelium, was able to reduce infarct size in animal models of transient focal cerebral ischemia; however, a Phase III clinical trial showed negative effective results with a high number of complications. The UK279,276, a recombinant inhibitor protein of the CD11b/CD18 receptor, showed a low efficacy in clinical trial.(60)

h. Others

Other examples of neuroprotectors that have failed in clinical phases were BMS-204352 (an activator of potassium channel), piracetam (nootropic modulator of neurotransmitters), nalmefene

(long-acting opioid antagonist), or fibroblast growth factors.(48) Recently, scavengers of glutamate were also postulated as neuroprotector and tested in animals and ischemic stroke patients.(61)

1.2.3. NEUROREPAIR

Neurorepair is focused on the stimulation of neuronal plasticity, growth of neuronal and glial cells, and angiogenesis mechanisms with the consequent regeneration of damaged tissue. As endogenous repair mechanisms occur later than ischemic cascade, this therapeutic strategy, theoretically, has a larger therapeutic window. This approach can consist of enhancers of neurogenesis, angiogenesis, or synaptogenesis processes, as well as cellular therapy with stem cells, and others.

a. Neurogenesis

Neurogenesis is a normal process in an adult brain, by the division of neural stem cells,(62) localized in the subventricular region of the lateral ventricles (SVZ) and the dentate gyrus of the hippocampus. Damage to the brain as occurs in stroke promotes the generation of neural cells, neuroblasts, from these locations.(63) It is known that human neuroblasts migrate to regions close to lesion, but these new cells cannot integrate in the synaptic circuits.(64)

The enhancement of this natural process was the aim of testing erythropoietin (EPO) as a treatment for stroke, achieving increasing of neurogenesis and functional improvements in animal experimentation;(65) but unfortunately EPO testing in humans was cancelled at phase II of clinical trial.(66)

b. Angiogenesis

Angiogenesis is the formation of new blood vessels from pre-existing vessels and is a physiological process in embryonic development; in adult brain angiogenesis is induced by pathological conditions as ischemia. It was reported a proliferation of cerebral blood vessels after an ischemic insult between 2 and 28 days after ischemia induction.(67-70) Many molecules take part in the pathological angiogenesis at different times as vascular endothelial growth factor

(VEGF), its receptor (VEGFR) -generating new vascular ramifications- and angiopoietin 1 and 2 and their receptor (TIE-2) -maturating these new vessels.(71)

In animals it has been possible to increase angiogenesis after stroke by using these molecules as pharmacological drugs or with their indirect promotion with stem cells.(72)

c. Neurogenesis and angiogenesis

Neurogenesis and angiogenesis, as brain repair processes, act together, with neurogenesis assuming the regeneration of brain tissue and angiogenesis the carrier of nutrients and oxygen to the repaired regions after brain injury. Growth factors released by endothelial cells promote survival of neurons and cerebral tissue through different metabolic pathways. For example, matrix metalloproteinases (MMPs), stromal cell-derived factor-1 (SDF-1), or the abovementioned VEGF stimulate the migration of neural stem cells to damaged zones; and angiopoietin 2 and VEGFR2 increase the angiogenesis.(73)

This joint action was the target of several studies both *in vivo* and *in vitro*.(73, 74) It has been described that administration of neural progenitor stem cells (NPSCs) promote neurogenesis and angiogenesis improving function in animal models of stroke.(75, 76)

1.2.4. CELLULAR THERAPY

Cellular therapy is accepted as promising treatment due to its positive results in preclinical studies. Already in 1984, cells were transplanted to hypoxic rats; 20 days embryos cerebral cortex transplantation induces new cerebral connections.(77) From then on, publications about cellular therapy in stroke have had high increment.

Many types of stem cells were tested in animal models of stroke: embryonic stem cells (ESCs),(78) neural stem cells (NSCs),(79) bone marrow stem cells (BMSCs),(80) mesenchymal stem cell (MSCs),(81) dental pulp stem cells (DPSCs),(82) human cord blood cells (HUCBCs),(83) stem cells isolated from menstrual fluid (MenSCs),(84) and placenta-derived stem cells (p-SCs).(85) Some of them showed positive results.

Despite satisfactory studies, stem cells have several problems regarding their management. It is probable immune rejection. Availability of stem cells is restricted. Further, there are some ethical and legal problems.

Induced pluripotent stem cells (iPSCs) solve these obstacles. They are obtained from somatic, differentiated and adult cells and have capacity for dividing and differentiating to any type of cell except extraembryonic cells; therefore, ethic and legal problems for using embryos are avoided and grafted cells could be extracted from patient, so immune rejection is avoided too.

1.3.iPSCs

iPSCs were described for the first time by Takahashi and Yamanaka in 2006.(86) Since then, studies and publications about iPSCs only grew. It has been demonstrated that differentiated cells can be reprogrammed to an embryonic-like state by transfer of nuclear contents into oocytes or by fusion with ESCs. Takahashi and Yamanaka(44) demonstrated induction to pluripotent stem cells from mouse embryonic or adult fibroblasts by introducing four factors, Oct3/4, Sox2, c-Myc, and Klf4, under ESCs culture conditions (**Figure 8**). These iPSCs exhibit the morphology and growth properties of ESCs and express ESCs marker genes. Subcutaneous transplantation of iPSCs into nude mice resulted in tumours containing a variety of tissues from all three germ layers. These data demonstrate that iPSCs can be directly generated from differentiated cells and are promising cells for cellular therapy or modelling of disease (**Figure 8**).

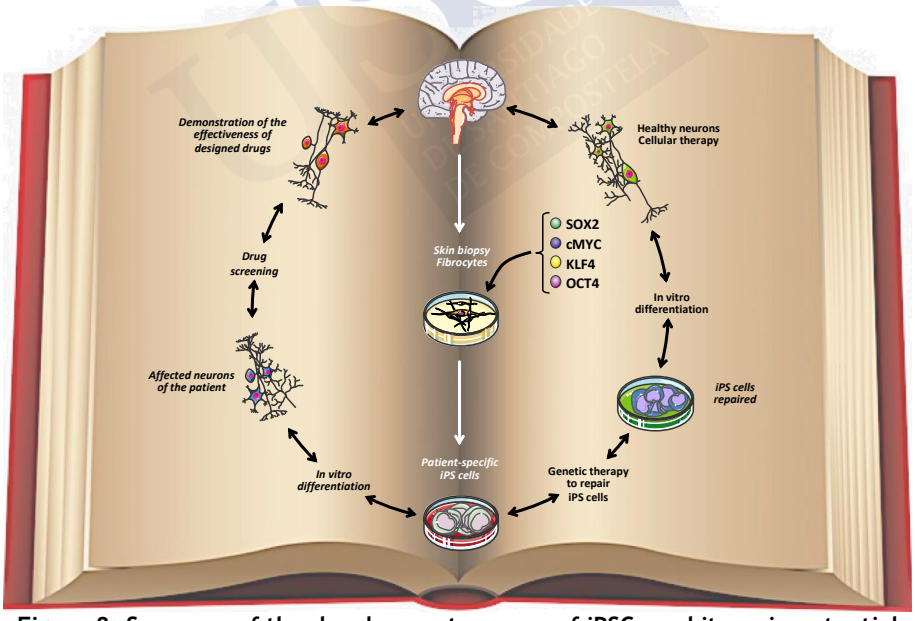

Figure 8: Summary of the development process of iPSCs and its main potential applications in neurological disorders, cellular therapy and modelling of disease (self-created image using elements with creative commons license).

1.3.1. iPSCs IN STROKE TREATMENT

Cellular therapy with iPSCs have been previously tested in preclinical studies of stroke with controversy results. The first study where iPSCs were transplanted in a stroke model was in 2010. Kawai *et al.*(87) directly injected iPSCs in striatum and cortex of ischemic rats. Results of this study showed that neuroblast and neurons were differentiated from iPSCs, but this treatment was not safe since teratomas were developed in the brain, and no neuroprotective effect was found. So, the main conclusion of this study was that iPSCs can be differentiate *in vivo*.

By contrast, Jiang *et al.*(88) demonstrated that the administration of human iPSCs into the striatum of ischemic rats induced smaller lesion and neurological recovery. This study also found the differentiation of neural cells derived from transplanted iPSCs.

Nevertheless, Jensen *et al.*(89) performed a preclinical study with a protocol close similar to that performed by Jiang,(32) but the obtained results were contradictory, since no protective effect was observed. A possible explanation of this contradictory results is the number of transplanted cells, much higher in Jiang's study (800000 vs. 250000). However, both studies found surviving and differentiated neuronal iPSCs-derived cells.

Regarding preclinical studies in intracerebral haemorrhage, grafts of iPSCs in an haemorrhagic animal model also showed functional recovery compared to vehicle and fibroblast control groups; furthermore, Qin *et al.*(90) found higher expression of BDNF and VEGF in brain after intracerebral administration of iPSCs. Besides, they observed survivor nestin, β-tubulin and glial fibrillary acidic protein (GFAP) positive iPSCs-derived cells at 28 days of follow-up.

In recent studies, iPSCs were derived to other cell lineages before transplantation. Yuan *et al.*(91) described survival, migration and differentiation of iPSCs-derived NSC injected into the striatum of ischemic mice; two weeks after iPSCs transplantation, neurons and astrocytes derived from iPSCs were identified. Other study that intracerebrally administered neuroepithelial-like stem cells (NES cells)-derived from iPSCs in ischemic mice showed functional recovery at 10 weeks after transplantation.(92) This same study found NeuN+

cells with electrophysiological functions that derived from transplanted cells. This NES cells lineage was also injected into the striatum of haemorrhagic rats,(93) observed better recovery, showing NES-derived cells around the hematoma.

All preclinical studies conducted to date have used the same route of administration. Cells were injected into the brain parenchyma that, nevertheless, is not a translational route to the clinical practice. Therefore, further studies testing other more translational administration routes are needed in order to probe efficacy of cellular therapy with iPSCs in stroke. In this regard, intravenous administration is the normal administration route for clinical procedures and was previously tested in other cell therapies with positive results. Furthermore, systemic administration would enable secreted molecules by iPSCs to be carried throughout whole body. In this sense, it is known that stem cells secrete cytokines, growth factors, anti-inflammatory molecules, etc., that can travel blood stream and may induce recovery through pleiotropic effects.

Given this gap, this study is focused on the intravenous route for iPSCs administration in two stroke animal models, ischemic and haemorrhagic stroke, in order to demonstrate therapeutic properties without side effects such us tumour formation.

USC
UNIVERSIDADE
DE SANTIAGO
DE COMPOSTELA

2. HYPOTHESIS

USC
UNIVERSIDADE
DE SANTIAGO
DE COMPOSTELA

Stroke is the main cause of disability and the second of death in Spain. Although some drugs had good and promising results in animal models, no pharmacological agent is currently been using in patients for neuroprotective or neurorestorative effect. Cell therapy is having hopeful results both in preclinical experiments as in clinical trials. In this regard, iPSCs have stood as new approach in cell therapy, but no conclusive results were found in preclinical models of stroke. Therefore, the hypothesis of this preclinical study are:

- The intravenous administration of iPSCs in an animal model of ischemic stroke mediates neuroprotective and neurorestorative effects implying functional and neurological recovery without adverse effects as tumour formation.
- The intracerebral and intravenous administrations of iPSCs in an animal model of haemorrhagic stroke mediates neuroprotective and neurorestorative effects involving functional and neurological recovery without adverse effects as tumour formation.

USC
UNIVERSIDADE
DE SANTIAGO
DE COMPOSTELA

3. OBJECTIVES

USC
UNIVERSIDADE
DE SANTIAGO
DE COMPOSTELA

The main objective of this study is to demonstrate the neuroprotective and neurorestorative effects of treatment with iPSCs in stroke animal models, both ischemic and haemorrhagic.

For this purpose, main objective was structured in specific objectives:

1) To demonstrate that iPSCs treatment mediates lesion volume reduction and functional and neurological recovery in stroke animal models.

2) To demonstrate that iPSCs administration mediates tissue regeneration, specifically through neurogenesis and angiogenesis mechanisms.

3) To analyse potential adverse effects of iPSCs therapy, in special tumour or teratomas development.

4) To determine the iPSCs biodistribution after its systemic administration in a stroke animal model.

USC
UNIVERSIDADE
DE SANTIAGO
DE COMPOSTELA

4. SECTION I: CULTURE AND CHARACTERIZATION OF iPSCs

USC
UNIVERSIDADE
DE SANTIAGO
DE COMPOSTELA

4.1.MATERIALS AND METHODS

4.1.1. iPSCs CULTURE

Obtaining and characterization of iPSCs were carried out in the *Laboratorio de Células Madre en Cáncer y Envejecimiento, Instituto de Investigación Sanitaria de Santiago de Compostela* (IDIS) as a collaboration with Dr. Manuel Collado's group. Primary mouse embryonic fibroblasts carrying a polycistronic cassette for the inducible expression of the four reprogramming factors (i4F-MEFs) were obtained from embryos at E13.5 of reprogrammable mice (the i4F transgenic mice).(94) These i4F-MEFs were cultured in standard DMEM (Dulbecco's modified eagle medium) (Sigma, San Luis, USA) supplemented with 10% FBS (fetal bovine serum) (Sigma, San Luis, USA), penicillin/streptomycin (Sigma, San Luis, USA) and L-glutamine (Sigma, San Luis, USA).

ES cells and iPS cells were cultured on top of mitomycin-C inactivated feeder cells on gelatin-coated plates in "iPSCs medium": DMEM supplemented with knockout serum replacement (KSR, 15%, LifeTechnologies, Carlsbad, CA, USA), LIF (leukemia inhibitory factor) 1000 u/ml (Millipore, Burlington, MA, USA), 1x non-essential amino acids (LifeTechnologies, Carlsbad, CA, USA), L-glutamine, penicillin/streptomycin , and 0.1 mM 2-mercaptoethanol (LifeTechnologies, Carlsbad, CA, USA).

For retroviral transduction, we transfected HEK293T (human embryonic kidney 293) cells ($5x10^6$ cells per 100-mm-diameter dish) with pBP-GFP (Addgene #14430; Watertown, MA, USA) and the ecotropic packaging vector, pCL-Eco (Addgene #12371; Watertown, MA, USA) using PEI (polyethylenimine) reagent. Retroviral supernatants were collected 3 times serially every 12 hours, starting 36 h after transfection. The supernatants were filtered through a 0.45 μm filter and polybrene was added at a final concentration of 8 μg/ml. The i4F-MEFs were plated ($1.4x10^6$ cells per 100-mm-diameter dish) the day before to the first round of transduction. One day after completing the retroviral transduction, the media was replaced by iPS cell medium containing doxycycline (Sigma, San Luis, USA) at 1μg/ml.

4.1.1.1. Reprogramming to iPSCs

For reprogramming to iPSCs, i4F MEFs transduced with the plasmid pBP-GFP were cultured in iPS cell medium (Sigma, San Luis, USA) in the presence of doxycycline at a concentration of 1 μg/ml. Medium was changed every 48 h during 14 days. The first iPSCs colonies appeared around day 7, and on day 14 the iPSCs colonies were picked and plated on top of mitomycin-C inactivated feeder cells on gelatin-coated plates in "iPSCs medium" without doxycycline. The clones were expanded and characterized.

4.1.2. CHARACTERIZATION OF iPSCS

4.1.2.1. Alkaline phosphatase staining

For alkaline phosphatase (AP) staining the iPSCs colonies were fixed with 4% paraformaldehyde and the alkaline phosphatase activity was detected with BCIP (5-bromo-4-chloro-3-indolyl-phosphate)/NBT (nitro blue tetrazolium) Color Development Substrate (Promega, Nigrán, PO, Spain) according to the manufacturer's instructions.

4.1.2.2. Quantitative real-time polymerase chain reaction

To measure the mRNA levels, total RNA was extracted from cells using the Nucleospin RNA kit (Macherey-Nagel, Düren, Germany) following the indications of the provider and with a DNAse treatment. After nanodrop RNA quantification, the RNA was retrotranscribed into cDNA according to the manufacturer's protocol (High-Capacity cDNA Reverse Transcription Kit, Applied Biosystems, Foster City, CA, USA). Quantitative real-time polymerase chain reaction (qRT-PCR) was performed using SYBR Green Power PCR Master Mix (Applied Biosystems, Foster City, CA, USA) in an Mx3005P RT-PCR system (Agilent technologies, Santa Clara, CA, USA). Relative quantitative RNA was normalized using the housekeeping gene *GADPH* (glyceraldehyde 3-phosphate dehydrogenase). Primer sequences are available from the authors upon request.

4.1.2.3. Western blot

For protein expression analysis, cell extracts were prepared using RIPA (radioimmunoprecipitation assay) buffer (LifeTechnologies, Carlsbad, CA, USA) (150 mM NaCl, 10 mM Tris-HCl pH 7.5, 0.1% SDS, 1% Triton X-100, 5 mM EDTA pH 8.0, 1% sodium deoxycholate containing protease inhibitors). After protein quantification using the DC Protein Assay (Bio-Rad, Hercules, CA, USA) the samples were adjusted to the same concentration and 20 µg of protein were electrophoresed in 12% polyacrylamide gels. Then the proteins were transferred to a PVDF (polyvinylidene difluoride) membrane that was blocked with 5% milk in TTBS (tween-tris-buffered saline) and incubated with the following primary antibodies: SOX2 (Santa Cruz Biotechnology, Dallas, TX, USA; sc-17320; 1:500), OCT4 (Santa Cruz Biotechnology, Dallas, TX, USA; sc-9081; 1:500), GFP (Clontech, Mountain View, CA, USA; 632375; 1:1000), β-ACTIN (ICN Biomedicals, Irvine, CA, USA; 1:2000), GADPH (Millipore, Burlington, MA, USA; MAB374; 1:2000) Incubation with the appropriate secondary antibodies conjugated to HRP (horseradish peroxidase) was followed by visualization using the ECL system (GEHealthcare, Chicago, IL, Estados Unidos).

4.1.2.4. Cytometry

The generated iPSCs were analysed using the BD Mouse Pluripotent Stem Cell Transcription Factor Analysis Kit according to the manufacturer's indications in a FACScalibur (Becton Dickinson, Franklin Lakes, NJ, USA) flow cytometer.

4.1.2.5. *In vitro* differentiation

In vitro embryoid body (EB) differentiation assay was performed to check the pluripotency of iPSCs by the hanging drop technique. For this, iPSCs were trypsinized and adjusted to a density of $2.5x10^5$ cells/ml in “embryoid body medium”: DMEM (LifeTechnologies, Carlsbad, CA, USA) supplemented with 10% FBS, streptomycin/penicillin, L-glutamine, 0.1 mM 2-mercaptoethanol, and

1X non-essential amino acids. Small volumes of 20 µl were placed as droplets on the lid of a petri dish and an average of 50 hanging drops were cultured over a cell culture dish containing PBS. After 3 days, droplets were collected and transferred to a petri dish and further cultured in embryoid body medium for 15 days before being harvested for RT-qPCR and histological analysis. For histological analysis the embryoid bodies were included in melted 0.2% agar and the resulting plug was fixed in buffered formalin and embedded in paraffin wax.

4.1.2.6. Teratoma formation

To test *in vivo* for pluripotency of the generated iPSCs, we performed teratoma formation assays. For this, iPSCs were adjusted to a concentration of $3x10^7$ cells/ml in PBS and were injected subcutaneously in nude mice (Janvier, Route du Genest, Le Genest-Saint-Isle, France) previously anesthetized with isoflurane (Baxter, Deerfield, IL, USA) 2% v/v O_2. We injected 100 µl of the cellular suspension on the back of the mouse, and after four weeks the mice were sacrificed by CO_2 asphyxiation and the teratomas were extracted and processed for histological analysis.

4.1.2.7. Immunohistochemistry

Tissue samples were fixed in formalin, embedded in paraffin wax, and sectioned at a thickness of 5 µm. Sections were stained with haematoxylin and eosin for pathological examination. The following primary antibodies were used: GFAP (rabbit polyclonal, Dako Agilent, Santa Clara, CA, USA), Desmin (mouse monoclonal, Clone D33, Dako Agilent, Santa Clara, CA, USA) and CKAE1/AE3 (mouse Monoclonal, Clone AE1/AE3, Dako Agilent, Santa Clara, CA, USA). Slides were then incubated with the corresponding secondary antibodies, EnVision System (Dako Agilent, Santa Clara, CA, USA).

4.2.RESULTS

4.2.1. REPROGRAMMING TO PLURIPOTENCY FROM i4F-MEFs

Figure 9 shows the main results on the pluripotency characterization of iPSCs derived from i4F-MEFs transducted with GFP. Colonies of iPSCs showed positive stained for AP (**Figure 9A**). Moreover, western blot (WB) analysis showed positive expression of pluripotency factors (Oct4 and Sox2) in iPSCs obtained from i4F-MEFs. Parental i4F-MEFs were shown as a negative control and ESCs as a positive control (**Figure 9B**). On the other hand, WB analysis of the expression of GFP after transduction of i4F-MEFS showed that iPSCs derived from these MEFs silence the expression of GFP during the pluripotent state (**Figure 9C**). Moreover, pluripotency factor (Oct4, Sox2, Klf4 and Nanog) mRNA expression was determine by RT-qPCR in iPSCs obtained from i4F-MEFs, using expression in ESCs as a positive control (**Figure 9D**). Finally, flow cytometry analysis of pluripotency factor (Oct4, Sox2 and Nanog) expression showed that undifferentiated Nanog+/Oct4+ cells composed 78.85% of the cell population, and Sox2+/Oct4+ cells composed 69.92 % of the cell population. Expression in ESCs was used as a positive control showing similar results (**Figure 9E**).

4.2.2. DIFFERENTIATION OF iPSCs

Figure 10 summarizes the main results on the differentiation characterization of iPSCs derived from i4F-MEFs transducted with GFP. **Figure 10A** shows a representative picture of an embryoid body (EB) in culture obtained after *in vitro* spontaneous differentiation of iPSCs. As expected, these EB derived from iPSCs showed a higher mRNA expression of differentiation factors (Dlx3, Nkx2.5, and Gfap) compared to iPSCs (all $p<0.0001$). Finally, immunohistochemistry analysis of teratomas obtained after injection in nude mice of iPSCs showed endodermal, mesodermal and ectodermal differentiation (CK AE1/AE3, desmin and GFAP of the 3 germ layers in teratomas).

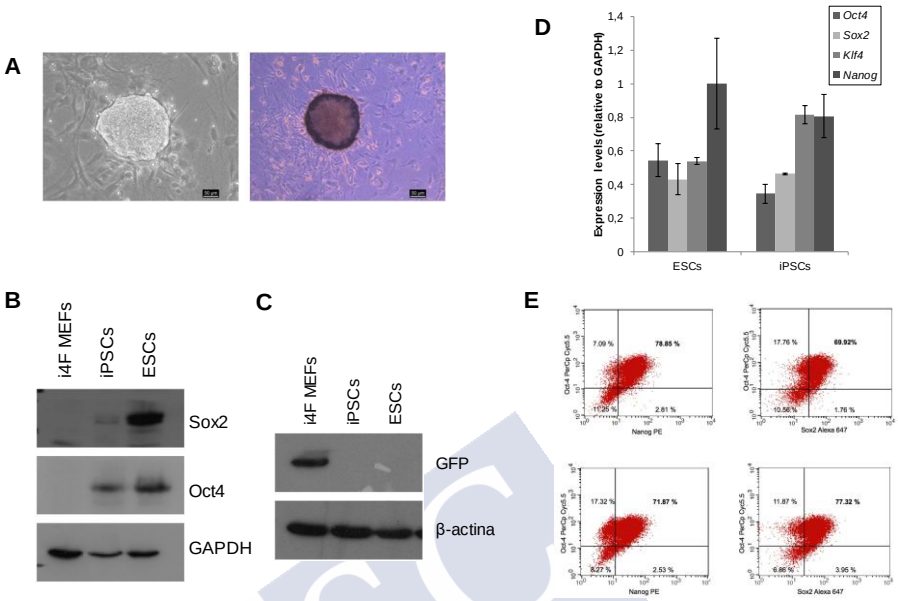

Figure 9: Pluripotency characterization of iPSCs derived from i4F-MEFs. (A) Representative pictures of iPSCs colonies derived from i4F-MEFs transduced with GFP (bright field) and stained for alkaline phosphatase (AP, right panel). (B) Western blot analysis of the expression of pluripotency factors (Oct4 and Sox2) in iPSCs obtained from i4F-MEFs. Parental i4F-MEFs were shown as a negative control and ESCs as a positive control. (C) Western blot analysis of the expression of GFP after transduction of i4F-MEFS. iPSCs derived from these MEFs silence the expression of GFP during the pluripotent state. (D) Pluripotency factor (Oct4, Sox2, Klf4 and Nanog) mRNA expression by qRT-PCR in iPSCs obtained from i4F-MEFs. Expression in ESCs was shown as a positive control. All data correspond to the average ± standard deviation (SD) of qRT-PCR data. (E) Graph showing the analysis of pluripotency factor (Oct4, Sox2 and Nanog) expression by flow cytometry. iPSCs (upper panels) were gated after cytometer setup. Undifferentiated Nanog+/Oct4+ cells composed 78.85% of the cell population (left panel) and Sox2+/Oct4+ cells composed 69.92 % of the cell population (right panel). Expression in ESCs (lower panels) was shown as a positive control. Undifferentiated Nanog+/Oct4+ cells composed 71.87 % of the cell population (left panel) and Sox2+/Oct4+ cells composed 77.32 % of the cell population (right panel).

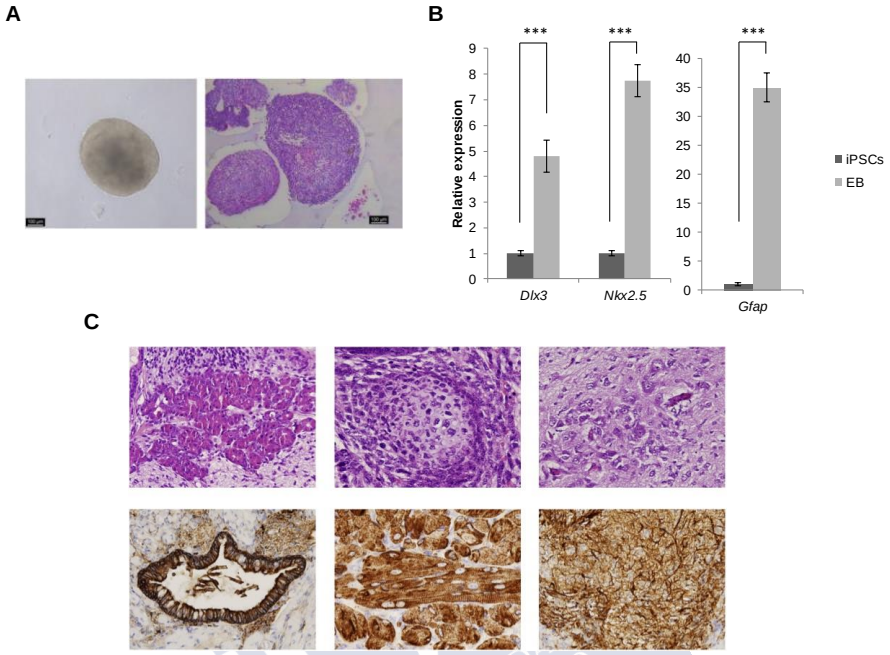

Figure 10: Differentiation of iPSCs. (A) Representative picture of an EB in culture (left panel) obtained after *in vitro* spontaneous differentiation of iPSCs. haematoxylin/eosin stained section of EBs embedded in paraffin (right panel). (B) Differentiation factors (Dlx3, Nkx2.5, and Gfap) mRNA expression by qRT-PCR in EB derived from iPSCs. Values are referred to the expression obtained for the corresponding iPSCs. All data correspond to the average ± SD of qRT-PCR data. Statistical significance was assessed by the two-tailed Student´s t-test: *** p<0.001. (C) Representative pictures of haematoxylin/eosin stained sections (upper panels) of teratomas obtained after injection in nude mice of iPSCs. Pictures show examples of endodermal, mesodermal and ectodermal differentiation (from left to right). Immunohistochemistry (lower panels) for markers of differentiation (CK AE1/AE3, desmin and GFAP) of the three germ layers in teratomas (from left to right).

USC
UNIVERSIDADE
DE SANTIAGO
DE COMPOSTELA

5. SECTION II: THERAPEUTIC EFFECTS OF iPSCs IN CEREBRAL ISCHEMIA

USC
UNIVERSIDADE
DE SANTIAGO
DE COMPOSTELA

5.1.MATERIALS AND METHODS

5.1.1. ANIMAL HANDLING

Experimental protocols and animal handling were approved by the chief of the *Servizo provincial da Gandaría* of the territorial department of *Consellería de medio Rural e do Mar* of province of A Coruña, being the main responsible PhD Francisco Campos Pérez. The animal experiments were conducted under the procedure number: 15010/2019/004 according to the Spanish and EU rules (86/609/CEE, 2003/65/CEE, 2010/63/EU, RD 1201/2005 and RD 53/2013).

All procedures were carried out in the Health Research Institute of Santiago de Compostela (IDIS), with the registration number: ES1507802928[01].

Male adult Sprague-Dawley (SD) rats (from Central Animal House of Universidade de Santiago de Compostela (USC), Spain) with a weight of 300 to 350 g were used. Rats were watered and fed ad libitum. Rats were kept in day/night cycles of 12/12 h at a mean temperature of 22 ± 1 °C and humidity of 60 ± 5% for one week previously to surgery and until the conclusion of the study protocol. For surgical procedures and magnetic resonance imaging (MRI) acquisitions, anaesthesia was induced by inhalation of 6% and maintained with 3-4% of sevoflurane in a nitrous oxide/oxygen mixture (70/30). During positron emission tomography (PET) acquisitions rats were anesthetized by inhalation of 3% of isoflurane in oxygen. Rectal temperature was maintained at 37 ºC by using a feedback-controlled heating pad only during the ischemic period.

5.1.2. SURGICAL PROCEDURES

Transient focal ischemia was induced in rats by transient middle cerebral artery occlusion (tMCAO) model of brain ischemia that is considered one of the best models to mimic human ischemic stroke and has been used in numerous studies.(95, 96) tMCAO was performed as previously described (95) with slight modifications (**Figure 11**). Rats were anesthetized as written above and their rectal temperature were

maintained at 37 ºC with a feedback-controlled heating system (1025 system, SA Instruments).

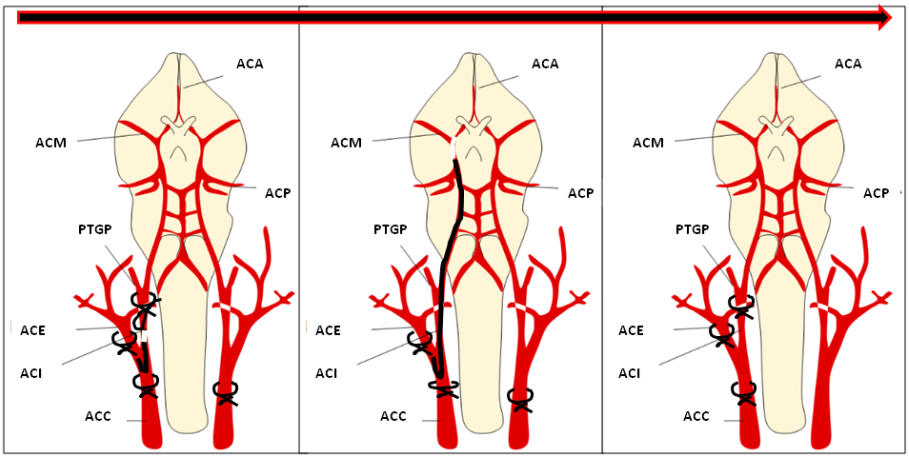

Figure 11: Schematic representation of tMCAO surgery (self-created image using elements with creative commons license).

Under a surgical microscope, an incision at middle line of ventral neck was performed to expose the common carotid, external carotid, and internal carotid arteries of the left side after setting aside the sternocleidomastoid and omohyoid muscle. The three arteries were separated and tied with 6-0 silk sutures. A silicon rubber-coated monofilament (403512PK5Re; Doccol Corporation, USA) was inserted through the external carotid into the left common carotid artery and advanced into the internal carotid until the origin of the MCA in the circle of Willis. Before the MCAO, the contralateral -right- common carotid artery was tied in order to reduce the total blood flow in brain and minimize collateral flow.

5 minutes before and during occlusion cerebral blood flow was measured with laser Doppler perfusion monitor (PeriFlux System 5000, Perimed, Sweden) connected to a probe (Probe 403, Perimed), that was placed on a notch made at temporal bone (over MCA region) (**Figure 12**).

After 45 minutes of occlusion, the filament was taken off, the right common artery untied, and all the incisions sutured. Finally, rats were unanaesthetised under infrared heat lamp.

Rats with less than 65% of blood flow reduction measured by Doppler, and rats without a clear reperfusion after removing the filament were excluded.

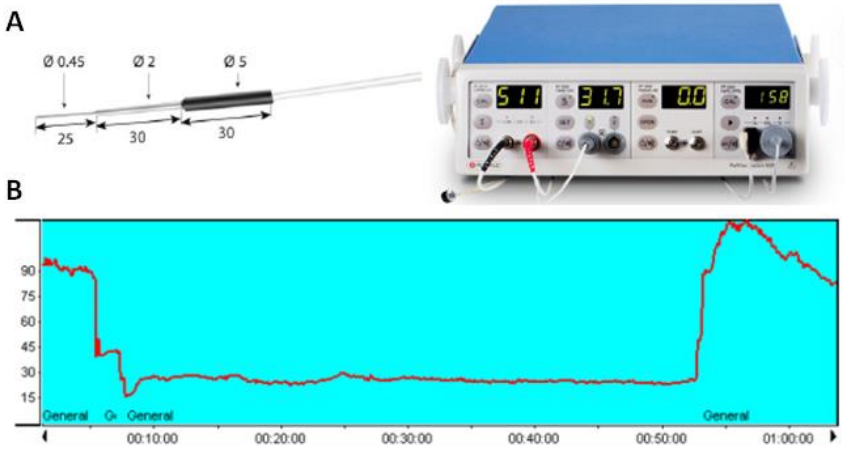

Figure 12: Doppler registration during occlusion of the middle cerebral artery. (A) Doppler probe. (B) Graphical representation of the doppler register. It represents the drop of blood flow during the occlusion of the tMCA and its subsequent rise during reperfusion. Self-created figure.

5.1.3. ANIMAL EXPERIMENTAL PROCEDURES

Experimental procedures were performed following six criteria derived from the Stroke Therapy Academic Industry Roundtable (STAIR) group guidelines for preclinical evaluation of stroke therapeutics:(97, 98) (1) cerebral blood flow was measured to confirm the vascular occlusion, as an index of the reliability of the ischemic model; (2) animals were randomly assigned to treatment groups of the study; (3) researchers were blinded to treatment administration; (4) researchers were blinded to treatments during outcome assessment; (5) temperature was controlled during the ischemic period; and (6) sample size power calculations were performed previous to the analysis.

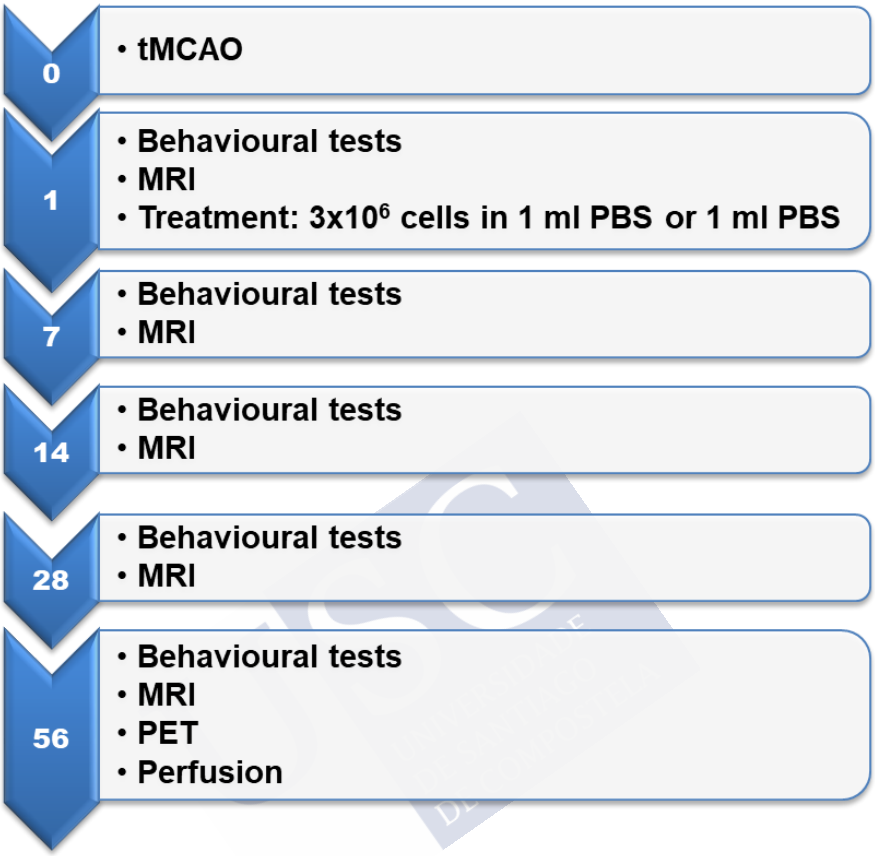

Figure 13: Study protocol indicating the analysis and tests performed during the 56-day follow-up period after tMCAO.

5.1.4. EXPERIMENTAL DESIGN

Two experimental groups were designed: (1) tMCAO control group (n = 12), intravenously treated with 1 ml of PBS; and (2) tMCAO group intravenously treated with $3x10^6$ iPSCs in 1 ml of PBS (n=12). Sample size was calculated by using the EPIDAT (http://dxsp.sergas.es/ApliEdatos/Epidat/cas/default.asp) with an alpha and beta errors of 0.05 and 0.2, respectively. Cells and vehicle treatments were intravenously administrated as previously descripted

(99) through jugular vein 24 h after tMCAO. We have chosen the dose of $3x10^6$ cells and the temporal profile of 24 h because this dose showed the greater therapeutic efficacy in several preclinical studies of cellular therapy in stroke.(100)

In all experimental groups, infarct volumes and behavioural test were performed at 1, 7, 14, 28 and 56 days after tMCAO. Furthermore, PET analysis for the evaluation of tumour formation, and brain immunofluorescence for cerebral neurogenesis and angiogenesis quantification were performed at the end of the follow-up period (56 days). A schematic representation of the study protocol is showed in **Figure 13.**

5.1.5. MAGNETIC RESONANCE IMAGE PROTOCOL

Infarct size was assessed by means of magnetic resonance imaging. MRI studies were conducted on a 9.4-T horizontal bore magnet MRI system, Biospec 94/20USR, (Bruker BioSpin, Germany) with a 20 cm wide actively shielded gradient coils (440 mT/m). Radiofrequency transmission was achieved with a birdcage volume resonator; signal was detected using a four-element surface coil, positioned over the head of the animal, which was fixed with a tooth bar, earplugs, and adhesive tape. Transmission and reception coils were actively decoupled from each other.

Gradient-echo pilot scans were performed at the beginning of each imaging session for accurate positioning of the animal inside the magnet bore. T2-weighted images were acquired using a RARE (factor n=4) sequence with the following acquisition parameters: field-of-view 19.2 x 19.2 mm^2, image matrix 192 x 192 (isotropic in-plane resolution of 0.1 mm/ pixel x 0.1 mm/ pixel), 14 consecutive slices of 1 mm thickness, repetition time = 3 seconds, effective echo time = 45 ms. T2-weighted images were acquired at 1, 7, 14, 28 and 56 days after MCAO. All images were processed, and maps were constructed with ImageJ (Rasband WS, ImageJ, US National Institutes of Health, Bethesda, MD, USA, http://rsb.info.nih.gov/ij/, 1997-2009). Infarct volumes were determined from T2 maps by manually selected areas of elevated

apparent diffusion coefficient/T2 values by a researcher blinded to animal handling.

5.1.6. BEHAVIOURAL TESTS

In all animals, a battery of behavioural tests was performed before tMCAO and 1, 7, 14, 28 and 56 days after MCAO by a researcher, who was blinded to the experimental groups during the darkness cycle. Cylinder test was performed to assess motor function and Bederson and Wahl's tests were performed to evaluate sensorimotor and neurological deficit.

5.1.6.1. Cylinder test

Cylinder test uses the exploratory behaviour of rats to assess forelimb motor deficit. Rats were placed in a cylinder and they were recorded for 10 minutes. Rats use to explore the cylinder touching the wall with their forelimbs. Placements of ipsilateral and contralateral forelimbs were counted, and asymmetry index were calculated for each rat by the formula: asymmetry index = 1 – (ipsilateral placements / (contralateral placements + ipsilateral placements)). More near to 1 is the asymmetry index, more severe is the motor deficit; normal healthy rats have got an asymmetry index around 0.5.(101)

5.1.6.2. Bederson and Whal´s tests

Bederson and Wahl's tests are validated scales with several items to evaluate neurological deficits. These tests are based in the presence or absence of a reflex or spontaneous activity of the animal.(102, 103) **Table 1** and **Table 2** show the items to explore and associated scores.

5.1.7. PET STUDY

At day 56, all ischemic rats included in iPSCs group were scanned by microPET/CT (micro-positron emission tomography-computed tomography). Likewise, 2 control rats were also scanned as negative control group. After, at least, 12 h of fast, rats were injected with ^{18}F-FDG (18Fluor-Fludeoxyglucose) in the vein of the tail. After that,

animals rested for 40 minutes and then PET/CT protocol was performed; whole bodies were scanned in order to find tumour formation.

Table 1: Items evaluated in Bederson test.

BEDERSON TEST	Normal	Deficit
Spontaneous movement	0-1	2-3
Circular spontaneous movement	0	1
Spontaneous flexion of contralateral forelimb	0	1
Circular movement when suspended	0	1
Extensor reflex when suspended	0	1
Corner detection	0	1
Total	**0-1**	**8**

Table 2: Items evaluated in Wahl test.

WAHL TEST	Normal	Deficit
Corner detection		
Forelimb	1	0
Hindlimb	1	0
Visual placing	1	0
Spontaneous flexion of contralateral forelimb	1	0
Spontaneous flexion of contralateral hindlimb	1	0
Circular spontaneous movement	1	0
Extensor reflex when suspended	1	0
Thoracic torsion when suspended	1	0
Total	**8**	**0**

PET/CT images were acquired by using an Albira PET/CT Preclinical Imaging System (Bruker Biospin, Woodbridge, Connecticut, USA). The PET subsystem comprises three rings of eight compact modules based on monolithic crystals coupled to multi-anode photomultiplier tubes (MAPMTs), forming an octagon with an axial FOV of 14.8 cm and a transaxial FOV of 8 cm in diameter. This system can create PET images with a spatial resolution of 1.2 mm and a sensitivity around 10%. The CT subsystem consists of a microfocus x-ray tube of 50 kVp and a CsI scintillator 2D pixelated flat panel detector that can generate images around 90 µm with a FOV of 7 cm.

PET/CT static acquisitions were performed, consisting of 20 min PET scan followed by 20 min CT scan. PET images were reconstructed using the maximum likelihood expectation maximization (MLEM) algorithm with 12 iterations and image pixel size of $0.4 \times 0.4 \times 0.4\ mm^3$, including scatter and random coincidences and no attenuation correction. The CT was centred in the abdominal region of each animal and the acquisition parameters were 35 kV for a tube current of 200 µA with 250 projections per bed.

All images were analysed using AMIDE software (http://amide.sourceforge.net/).(104)

5.1.8. IMMUNOFLUORESCENCE ANALYSIS

After the last follow-up (56 days after tMCAO), animals were sacrificed by overdose of anaesthesia and intracardially perfused with 50 ml of PBS and 200 ml of 4% formaldehyde. Immediately after, brains were extracted, immersed overnight in 4% formaldehyde and 24 h in 20% of sucrose PBS, embedded in OCT, cryopreserved and sectioned to 15-µm thickness.

To identify nuclei in active phase of cell cycle, monoclonal mouse antibody against Ki-67 (Dako, Santa Clara, USA) was used at a dilution of 1:50; to label immature neurons, rabbit polyclonal anti-DCX antibody (abcam, Cambridge, UK) was used at a dilution of 1:500; and rabbit polyclonal anti-CD31 antibody (abcam) at 1:50, for small vessels. Two double stainings were accomplished to detect neurogenesis (anti-Ki-67/anti-DCX) and angiogenesis (anti-Ki-67/

anti-CD31). These primary antibodies were incubated overnight. Biotinylated horse anti-mouse (Vector Laboratories, Peterborough, UK) was used as secondary antibody for anti-Ki-67 at a dilution of 1:200; while DyLight 488 goat anti-rabbit (Vector Laboratories, USA) was used as secondary for anti-DCX and anti-CD31 at a dilution of 1:300. The secondary antibodies were incubated for 1 hour. DyLight 594 streptavidin (Vector Laboratories) was used to label biotinylated secondary antibody at 1:500 with 30 min of incubation. Nuclei were detected with Hoechst 33342 (Invitrogen, Carlsbad, USA) that was incubated for 5 min at a dilution of 1:4000.

Before any incubation, antigen retrieval was performed with sodium citrate (pH 6.0) at 99 ºC for 20 min. In all incubations, slices were permeabilized with 0.2% X-100 triton in PBS and blocked with goat and horse serum (5% in primary incubation and 2% in secondary one).

The 15µm-slides were observed under Leica CTR6000 (Leica Microsystems) inverted microscope. Images were obtained by using LAS X Life Science software (Leica Microsystems).

Neurogenesis was quantified following previous well-described protocols.(105) DCX+ area and Ki-67+ cells from ipsilateral and contralateral subventricular zone were measured in the brains of at least 3 animals per group. Ki-67 density was calculated by the following formula: number of Ki-67+ cells/DCX+ area. To quantify angiogenesis, similar to previous protocols,(106) 6 fields of view of 200x in both cortex and striatum for both hemispheres were randomly chosen; the number of CD31+ vessels and Ki-67+ cells were counted, and proliferating cells densities were calculated by number of vessels or cells/mm^2.

5.1.9. STATISTICAL ANALYSIS

The results were expressed as average ± standard error of the mean (SEM), except for neurological scores that were discrete variables, so they were expressed as median [interquartile range].

Statistical analyses were made using Student t test assuming equal variances and with one tail. Significances of differences in discrete variables between groups were calculated by Mann–Whitney U test

with one tail. The statistical descriptions and tests were calculated by Microsoft Excel 365 ProPlus (Microsoft, Redmond, USA) with Real Statistics Resource Pack complement (Real Statistics Using Excel, http://www.real-statistics.com/ . All graphs were generated by Prism 5 for Windows, Version 5.01 (GraphPad Software, Inc, USA).

5.2.RESULTS

5.2.1. INCLUDED ANIMALS

A total of 73 SD rats were used in this study. Of all of them, 9 rats were excluded due death or surgery complications during the first 24 hours. Another 18 rats were excluded due to lack of occlusion or a cerebral blood flow reduction < 65%. Finally, 22 rats were excluded because of having an out of range lesion. Therefore, 24 rats were included and randomly assigned to iPSCs (n=12) and control (n=12) groups.

5.2.2. EFFECT OF iPSCs TREATMENT ON INFARCT VOLUME

As shown in **Figure 14** and **Figure 15**, no significant effects were observed on infarct volume for iPSCs treatment compared to the control group (all $p>0.05$) for any of the time points of the follow-up period. However, when we performed the comparison of lesion volumes adjusted to the basal one (24 h), we observed that the group treated with iPSCs showed a tendency to further reduce the volume of injury during the follow-up period, but this difference was not statistically significant (all $p>0.05$) (**Figure 16**).

In addition, lesion corrected by oedema, % lesion corrected by oedema respect to ipsilateral hemisphere volume, and % lesion corrected by oedema respect to whole brain volume were calculated (data not shown); no one of these calculations showed significant differences.

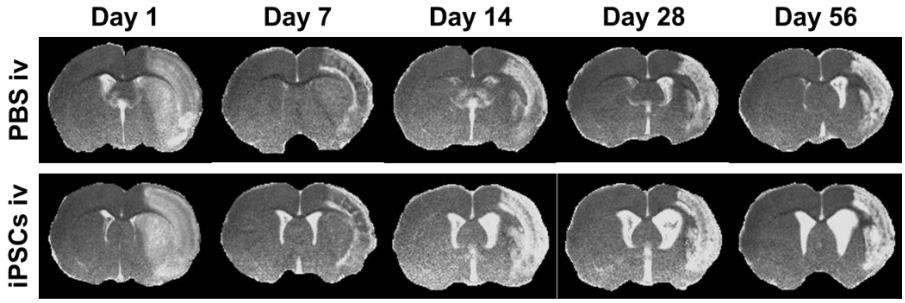

Figure 14: Representative MRI images of ischemic lesion for control and iPSCs group during the follow-up period of 56 days after tMCAO.

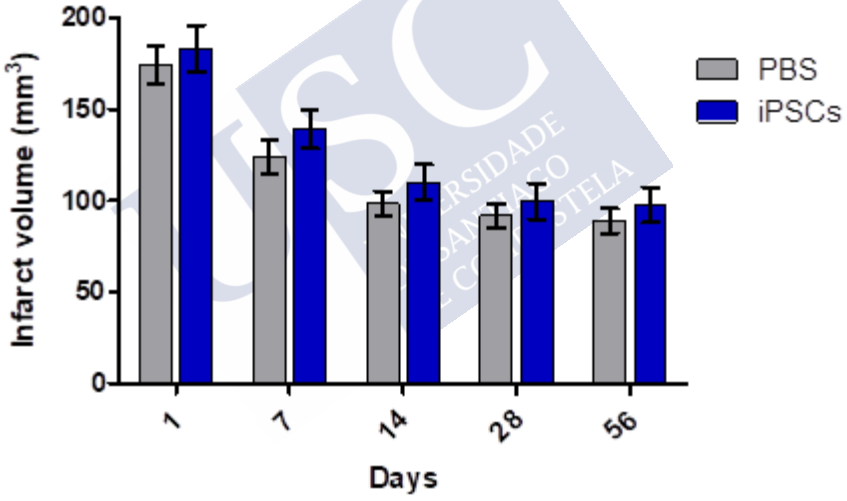

Figure 15: Comparison of absolute size of ischemic volumes for control and iPSCs group during the follow-up period of 56 days after tMCAO. Results are showed as mean ± SEM (n=12 animals per group). No differences were found between groups (all p>0.05).

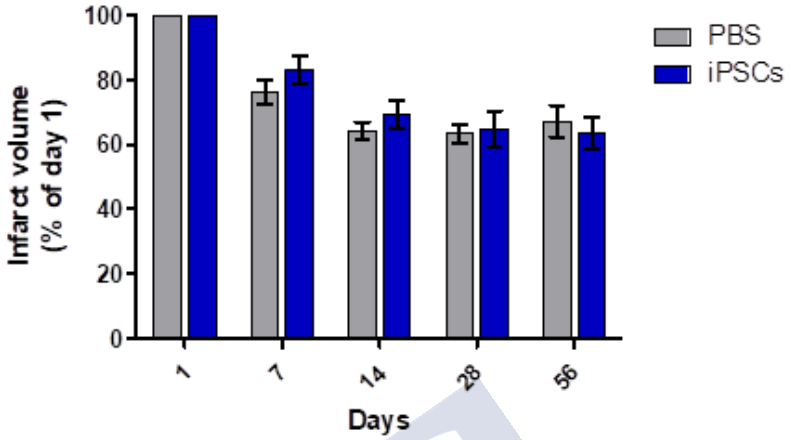

Figure 16: Comparison of lesion volumes adjusted to the basal one (24 h) for control and iPSCs group during the follow-up period of 56 days after tMCAO. Results are showed as mean ± SEM (n=12 animals per group). Although the group treated with iPSCs shows a tendency to further reduce the volume of injury during the follow-up period, this difference was not statistically significant (all p>0.05).

5.2.3. EFFECT OF iPSCs TREATMENT ON BEHAVIOURAL TESTS

5.2.3.1. Effect of iPSCs treatment on cylinder tests

Sensorimotor deficits after ischemic insult were quantified using laterality index. This index was close to 0.5 at 1 day before tMCAO for all animals. As shown in **Figure 17**, iPSCs group showed greater sensorimotor deficits from the beginning to the end of the follow-up period compared with the control group. This difference could be because the group treated with iPSCs had a greater volume of lesion at 24 hours after MCAO. To avoid this bias, we adjust the follow-up laterality indexes with respect to the baseline index at 24 hours. Performing this analysis, no significant differences were observed on functional recovery between groups (all p>0.05) for any of the time points of the follow-up period (**Figure 18**).

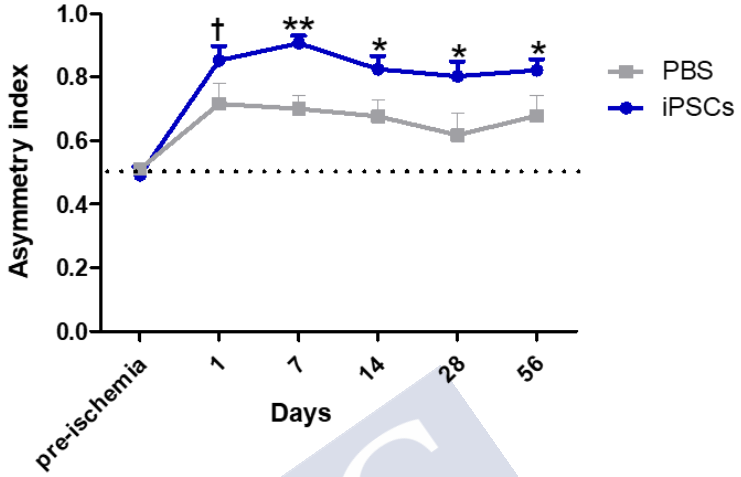

Figure 17: Effect of iPSCs treatment on somatosensory test. Sensorimotor deficits after ischemic insult were assessed using the cylinder test and quantified by laterality index. The iPSCs group showed greater sensorimotor deficits from the beginning to the end of the follow-up period compared with the control group. Results are showed as mean ± SEM (n=12 animals per group) (p<0.01, *p<0.05, †<0.1).**

5.2.3.2. Effect of iPSCs treatment on Bederson and Wahl´s tests

Unlike the functional recovery evaluated by the laterality index, the results of neurological deficit evaluation showed a greater recovery in the group treated with iPSCs. Specifically, iPSCs treated group showed better improvement in neurological outcome at the end of the follow-up period in both Bederson (**Figure 19**) and Wahl's (**Figure 21**) tests. In this regard, it is important to highlight that both experimental groups presented very similar scores in basal test, unlike the results of cylinder test, so there should not be any bias regarding to basal deficits. Even so, percentages respect to 1-day basal follow-up were calculated; and we observed that these neurological improvements for iPSCs group were maintained at last follow-up in both neurological tests (**Figure 20** and **Figure 22**).

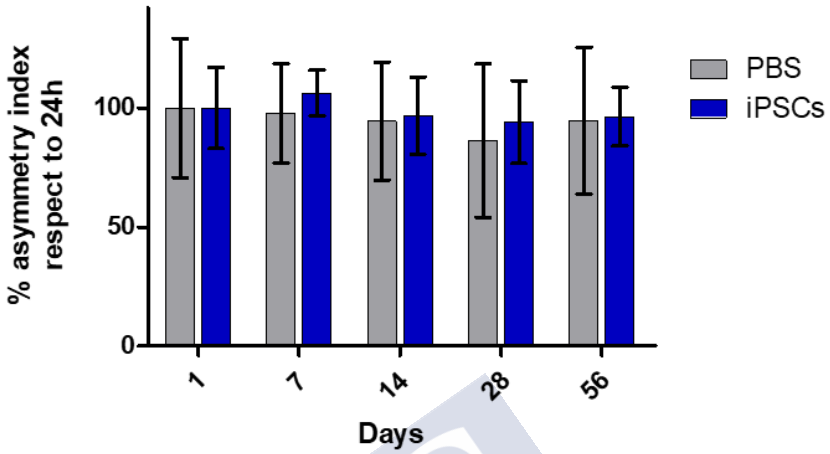

Figure 18: Percentage of asymmetry index respect to basal deficit at 24 h. Results are showed as mean ± SEM (n=12 animals per group). No significant differences were observed on functional recovery between groups (all p>0.05) for any of the time points of the follow-up period.

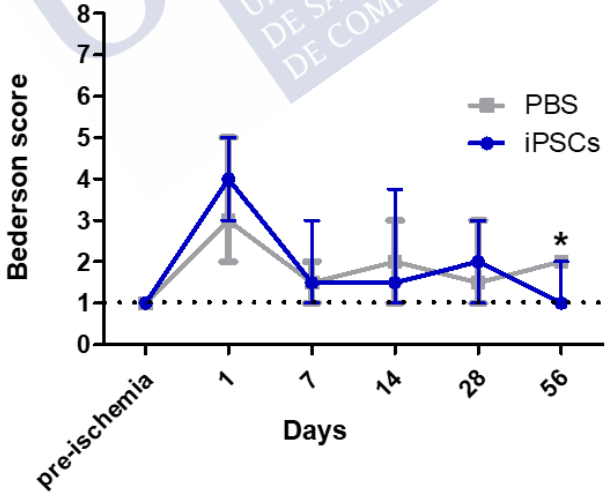

Figure 19: Effect of iPSCs treatment on neurological deficits evaluated by the Bederson test. The iPSCs group showed greater neurological improvement at the end of the follow-up period compared with the control group. Results are showed as mean ± SEM (n=12 animals per group) (*p<0.05).

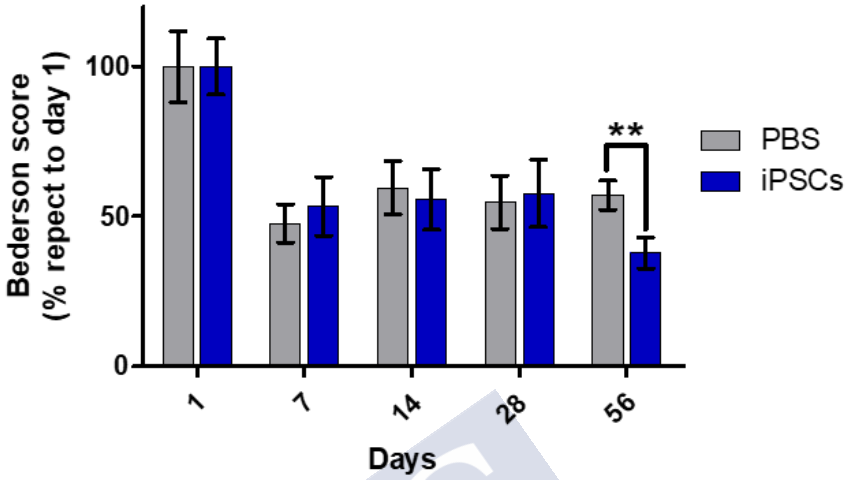

Figure 20: Progression of percentage of Bederson score respect to 1-day follow-up. The iPSCs group showed greater neurological improvement at the end of the follow-up period compared with the control group. Results are showed as mean ± SEM (n=12 animals per group) (*p<0.05).

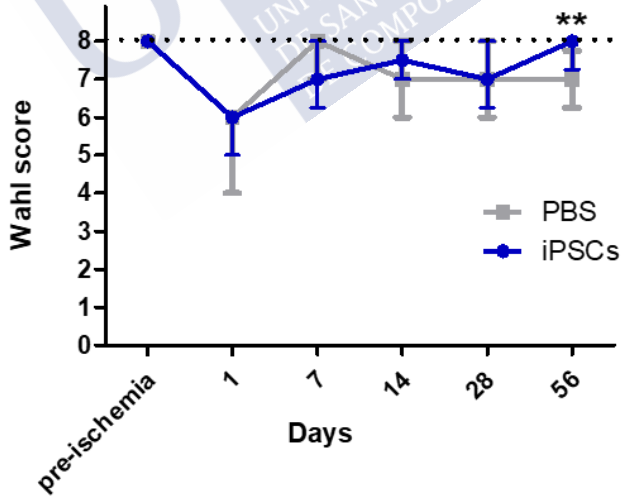

Figure 21: Effect of iPSCs treatment on neurological deficits evaluated by the Wahl test. The iPSCs group showed greater neurological improvement at the end of the follow-up period compared with the control group. Results are showed as mean ± SEM (n=12 animals per group) (p<0.01).**

5.2.4. EFFECT OF iPSCs TREATMENT ON CEREBRAL NEUROGENESIS AND ANGIOGENESIS

5.2.4.1. Effect of iPSCs treatment on cerebral neurogenesis

We analysed neurogenesis by immunofluorescence in brain slices obtained at 56 days after tMCAO. In the neurogenesis assay, area with DCX positive cells was measured in SVZ of both hemispheres to quantify the migration of neuronal precursor cells. We found a trend to higher DCX+ area in the ipsilateral SVZ for iPSCs treated group, but differences were not statistically significant (**Figure 23**).

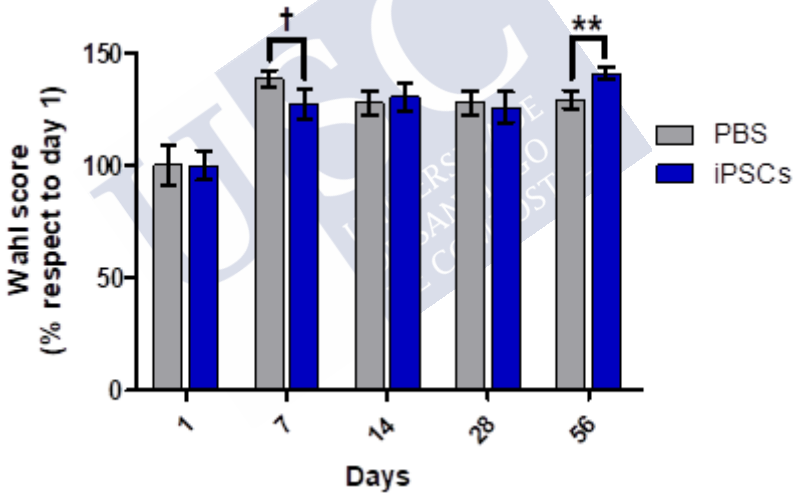

Figure 22: Progression of percentage of Wahl score respect to 1-day follow-up. The iPSCs group showed greater neurological improvement at the end of the follow-up period compared with the control group, although it had a greater deficit at 24 hours after the MCAO. Results are showed as mean ± SEM (n=12 animals per group) (p<0.01, †p<0.1).**

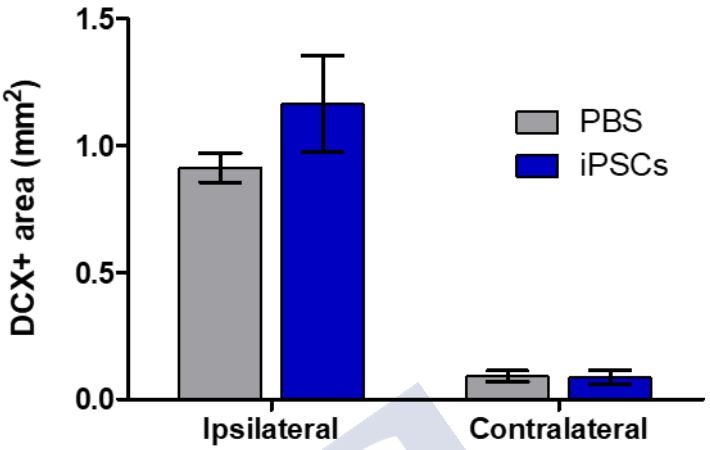

Figure 23: Comparison of DCX+ areas, measured in SVZ of both hemispheres, in iPSCs and control groups at 56 days after tMCAO. Results are showed as mean ± SEM (n=3 animals per group). Results showed a trend to higher DCX+ area in the ipsilateral SVZ for iPSCs treated group, but difference was not statistically significant (p>0.05).

In addition, Ki-67 positive cells were counted in DCX+ area in order to obtain the number of neuronal precursor cells in proliferation phase. We found more double positive cells (Ki-67+/DCX+) in ipsilateral hemisphere of the intravenous iPSCs treated group (**Figure 24**). Furthermore, a trend to a higher density of Ki-67+/DCX+ cells were also found in contralateral hemisphere for the iPSCs group (**Figure 24** and **Figure 25**).

Despite any differences are not statistically significant, we generally found a greater neurogenesis in ipsilateral hemisphere for iPSCs group compared to the control one in all measurements and computations of neurogenesis. Nonetheless, DCX+ areas in contralateral hemisphere were very similar in both groups, except in density of Ki-67^{+} cells (**Figure 26**).

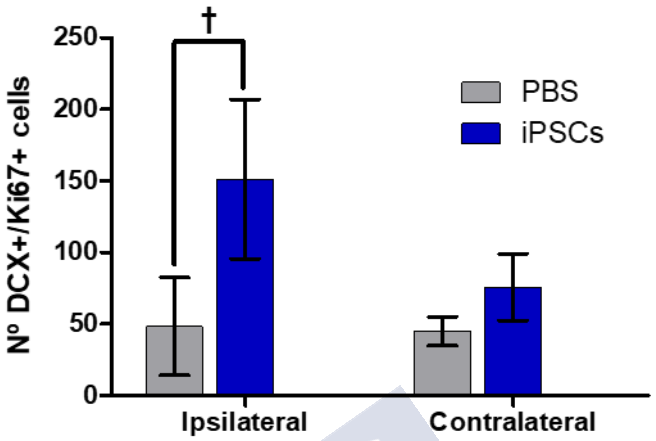

Figure 24: Number of Ki-67 positive cells in DCX positive area within SVZ in ipsilateral and contralateral hemispheres. Results are showed as mean ± SEM (n=3 animals per group). Results showed more neuronal precursor cells (Ki-67+/DCX+) in proliferation phase within the ipsilateral hemisphere for the intravenous iPSCs treated group (†p<0.1). Furthermore, a trend to a higher density of Ki-67+/DCX+ cells were also found in contralateral hemisphere of iPSCs group.

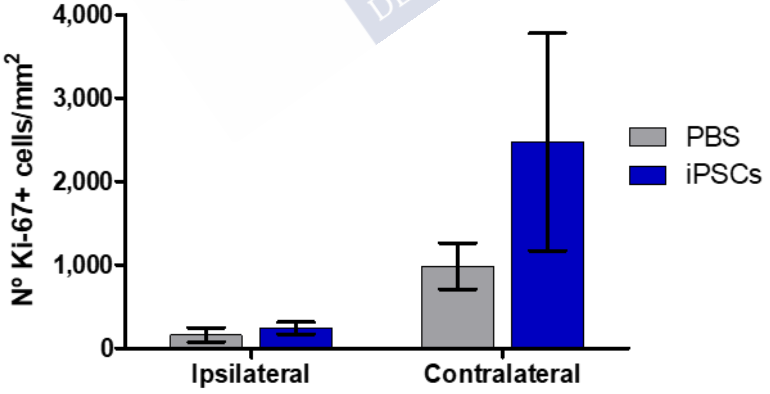

Figure 25: Density of Ki-67 positive cells, namely, the number of Ki-67+ cells within the DCX+ area in mm^2. Results are showed as mean ± SEM (n=3 animals per group). A trend to higher proliferation activity in iPSCs group was found especially within contralateral hemisphere.

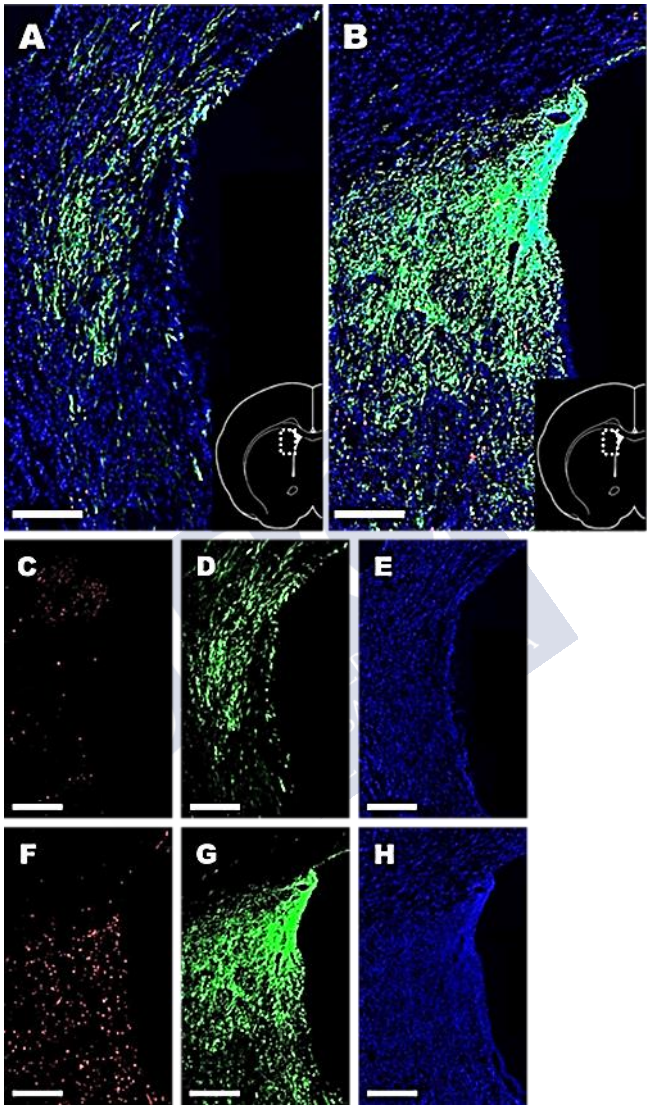

Figure 26: Images of ipsilateral SVZ 56 days after tMCAO. (A) SVZ of control rat, merge. (B) SVZ of iPSCs iv rat, merge. Scales in A and B are 200 µm. (C) detail of control SVZ, in red Ki-67 positive nucleus; D: detail of control SVZ stained DCX positive cells in green. (E) Hoechst staining of control SVZ. (F) red Ki-67 positive nuclei in treated rat. (G) detail of DCX+ area in iPSCs iv rat. (H) nuclei stained by Hoechst in treated SVZ. (C)-(H) scale is 400 µm.

5.2.4.2. Effect of iPSCs treatment on cerebral angiogenesis

Angiogenesis was analysed by immunofluorescence in brain slices obtained at 56 days after MCAO. In angiogenesis assay, the number of vessels (CD31+) and Ki67+ cells were counted. We didn't find any double positive cells. Moreover, we calculated the density of vessels. No differences were found in angiogenesis or number of vessels (**Figure 27** and **Figure 28**).

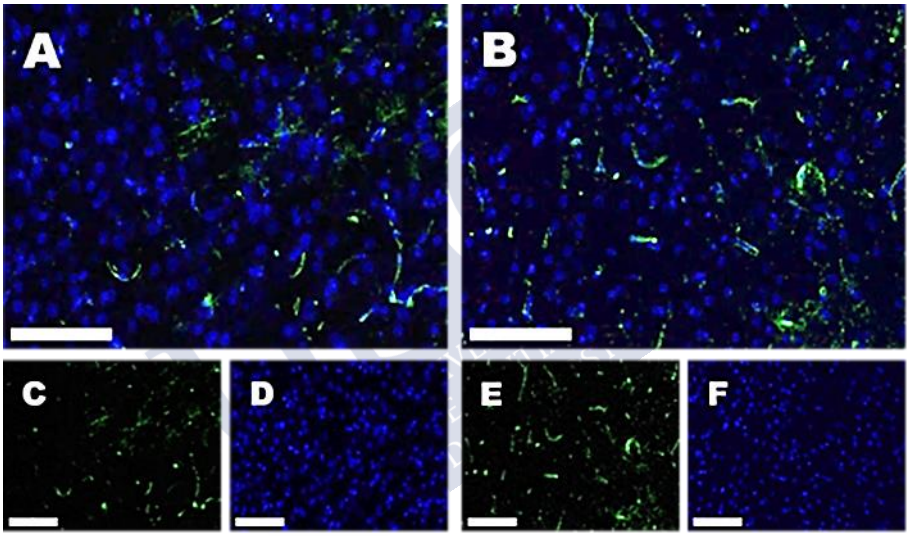

Figure 27: Images of cortex immunohistochemically stained for angiogenesis markers at 56 days after tMCAO, showing no differences between control and iPSCs treated group. (A) merge in control cortex; B: merge in iPSCs iv cortex. (C) CD31 positive in green of control. (D) Hoechst in blue of control. (E) CD31 positive vessels in green of iPSCs treated rat. (F) Hoechst in blue of transplanted rat. Scale in every microphotograph is 100 µm.

5.2.5. EFFECT OF iPSCs TREATMENT ON TUMOUR DEVELOPMENT

At day 56, all ischemic rats included in iPSCs group were scanned by microPET/CT. Likewise, 2 control rats were also scanned as negative control group. Whole bodies were scanned in order to find

tumour formation. PET images did not show tumour or teratoma formation in any case (**Figure 29**).

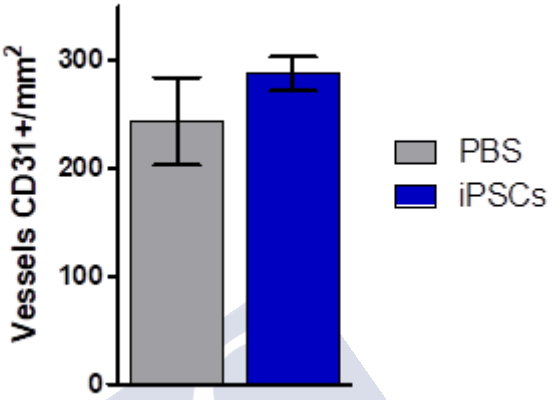

Figure 28: Density of vessels as number of vessels CD31+/mm^2 in control and iPSCs treated groups. Results are showed as mean ± SEM (n=3 animals per group). No differences were found between groups (p>0.05).

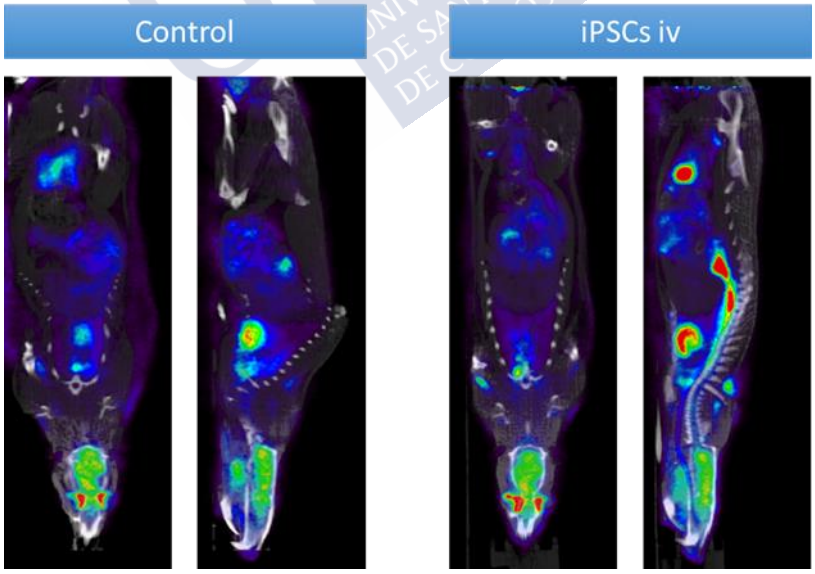

Figure 29: Representative PET/CT images for iPSCs and control groups, showing no evidence of tumour or teratomas formation at 56 days after MCAO.

6. SECTION III: THERAPEUTIC EFFECTS OF iPSCs IN INTRACEREBRAL HAEMORRHAGE

USC
UNIVERSIDADE
DE SANTIAGO
DE COMPOSTELA

MATERIALS AND METHODS

6.1.1. ANIMAL HANDLING

Experimental protocols and animal handling were approved by the chief of the *Servizo provincial da Gandaría* of the territorial department of *Consellería de medio Rural e do Mar* of province of A Coruña, being the main responsible PhD Francisco Campos Pérez. The animal experiments were conducted under the procedure number: 15010/2019/004 according to the Spanish and EU rules (86/609/CEE, 2003/65/CEE, 2010/63/EU, RD 1201/2005 and RD 53/2013).

All procedures were carried out in the Health Research Institute of Santiago de Compostela (IDIS), with the registration number: ES1507802928[01].

Male adult Sprague-Dawley rats (form Central Animal House of Universidade de Santiago de Compostela (USC), Spain) with a weight of 300 to 350 g were used for this study. Rats were watered and fed ad libitum. Rats were kept in day/night cycles of 12/12 h at a mean temperature of 22 ± 1 °C and humidity of 60% ± 5 for one week previously to surgery and until the conclusion of the study protocol. For surgical procedures and MRI acquisitions, anaesthesia was induced by inhalation of 6% and maintained with 3-4% of sevoflurane in a nitrous oxide/oxygen mixture (70/30). During PET acquisitions, rats were anesthetized by inhalation of 3% of isoflurane in oxygen. Rectal temperature was maintained at 37 ºC by using a feedback-controlled heating pad only during the ischemic period.

6.1.2. SURGICAL PROCEDURES

Intracerebral haemorrhages were provoked by injection of collagenase according to the Rosenberg's model.(107) A volume of 1 µl was injected estereotaxically with a 10 µl Hamilton syringe with 30G needle at the following coordinates from bregma: medial/lateral: -2.9 mm; anterior/posterior: +0.6 mm; and dorsal/ventral: -5.5 mm. The surgery was carried out with anesthetized rats with sevoflurane at 4% in a mixture of O_2:N_20 at 30:70.

After placing the rat at the stereotaxic, a cut in middle line of head was made to expose the skull, specifically the region around bregma. A mark in the particular location of injection was draw with bregma as reference and a subsequent trepanation of the skull was drilled. The needle was placed vertically at the site of trepanation. The descent of needle lasted 9 minutes until -6 mm, then needle was elevated 0.5 mm for 1 minute and 1 µl of 0.2 U/µl type VII collagenase (from *Clostridium histolyticum*, Sigma) was injected over 10 minutes. After injection we waited 10 minutes in order to allow spread the enzyme. The elevation of needle lasted 10 minutes. Once finished the induction of model, bone wax was placed in the trepanation and the cut was sutured.

Local analgesic (lidocaine Xilonibsa, Inibsa Dental, Spain) was sprayed on the incision. All animals were awaked under red lamp to prevent hypothermia at awakening.

6.1.3. ANIMAL EXPERIMENTAL PROCEDURES

Experimental procedure was performed following six criteria derived from the Stroke Therapy Academic Industry Roundtable (STAIR) group guidelines for preclinical evaluation of stroke therapeutics:(97, 98) (1) hematoma was evaluated at 1 h, before treatment, by T2-weighted MRI to confirm ICH, as an index of the reliability of the haemorrhagic model; (2) animals were randomly assigned to treatment groups of the study; (3) researchers were blinded to treatment administration; (4) researchers were blinded to treatments during outcome assessment; (5) temperature was controlled during the surgical period; and (6) sample size power calculations were performed previous to the analysis.

6.1.4. EXPERIMENTAL DESIGN

In this section we designed four groups: (1) iPSCs iv group (n=8): $3x10^6$ iPSCs intravenous administration in 1 ml of PBS; (2) control iv group (n=8): 1 ml of PBS intravenous administration; (3) iPSCs ic group (n=8): $5x10^5$ iPSCs intracerebral administration in 5 µl of PBS; (4) control ic group (n=8): 5 µl of PBS intracerebral administration.

Animals were distributed randomly in the four groups and the treatment (iPSCs or PBS) was administrated by a blind operator.

In the previous section we only used intravenous administration via, because is a common drug administration via. But, in some clinical cases, haemorrhagic strokes were managed with decompressive craniotomy; in these particular cases an intracranial administration wouldn't be so cumbersome, then we decided to include the intracranial administration too.

Required sample size was calculated from the basis of previous studies using the same model,(108) in order to be able of detecting an 25% effect size on hematoma growth vs controls. Eight animals per group are required to detect this difference with a power (1-β) of 0.8 and $\alpha = 0.05$. N was calculated using EPIDAT (http://dxsp.sergas.es/ApliEdatos/Epidat/cas/default.asp).

Cells and vehicle treatments were intravenously or intracerebral administrated as previously descripted(99) through jugular vein and into the perihematomal zone at 24 h after hematoma induction, respectively. The suggested doses and the temporal profile of 24 h were chosen because these doses showed the greater therapeutic efficacy in several preclinical studies of cellular therapy in stroke.(100)

In all experimental groups, hematoma volumes and behavioural test were performed previously any procurement and at 1, 7, 14, 28 and 56 days after hematoma induction. Likewise, MRI at one hour after collagenase injection was acquired in order to check whether the place and size of basal hematoma are the correct ones. Furthermore, PET analysis for the evaluation of tumour formation, and immunofluorescence of brain slices for neurogenesis and angiogenesis quantification were performed at the end of the follow-up period (56 days). A schematic representation of the study protocol is showed in **Figure 30.**

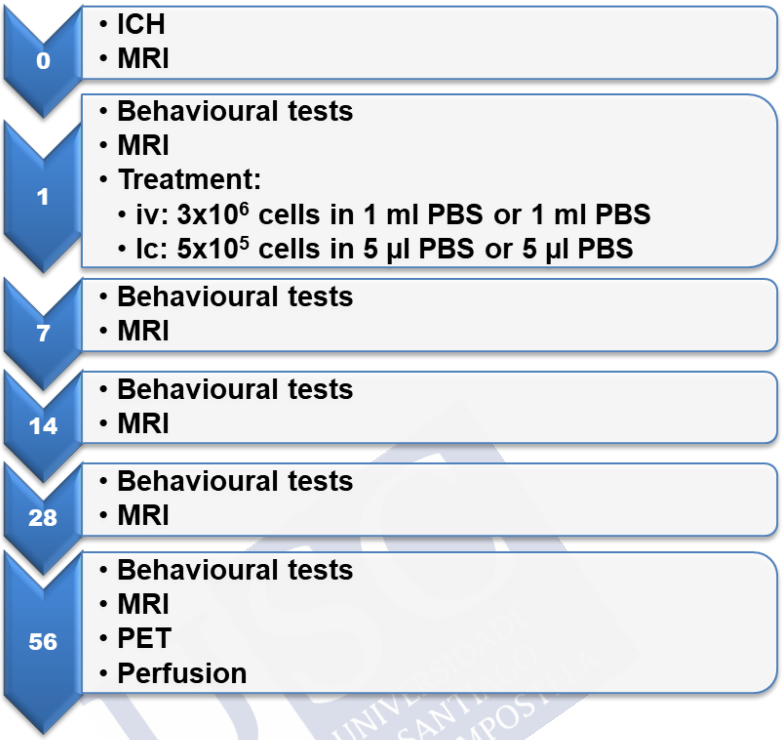

Figure 30: Study protocol indicating the analysis and tests performed during the 56-day follow-up period after hematoma induction.

6.1.5. MAGNETIC RESONANCE IMAGE PROTOCOL

Hematoma volumes were assessed basal (1 hour after collagenase injection) and at 1, 7, 14, 28 and 56 days after ICH induction by means of MRI conducted on a 9.4-T horizontal bore magnet MRI system (Biospec 94/20USR, Bruker BioSpin, Germany) with a 20 cm wide actively shielded gradient coils (440 mT/m), as previously described.(108) Radiofrequency transmission was achieved with a birdcage volume resonator and signal was detected using a four-element surface coil, positioned over the head of the animal. Gradient-echo pilot scans were performed at the beginning of each imaging session for accurate positioning of the animal inside the magnet bore. Multislice

axial T2-weighted imaging was performed at baseline (1 h after IHC induction), and at days 1, 7, 14, 28 and 56 after ICH. T2-weighted images were acquired using a RARE (factor n=4) sequence with the following acquisition parameters: field-of-view 19.2 x 19.2 mm^2, image matrix 192 x 192 (isotropic in-plane resolution of 0.1 mm/ pixel x 0.1 mm/ pixel), 18 consecutive slices of 0.5 mm thickness.

MR data analysis was performed using Para Vision (Bruker Medical, Ettlingen, Germany) and images were processed with ImageJ (Rasband WS, NIH, Bethesda, MD, USA, http://rsb.info.nih.gov/ij). The analysed region of interest was the hematoma and lesion region. Hematoma volumes (basal, days 1 and 7) as well as lesion volume at days 14, 28 and 56 were manually traced from T2 maps and the mean signal intensity was measured by 2 well-trained imaging analysts, blind to the experimental conditions.

6.1.6. BEHAVIOURAL TESTS

In all animals, a battery of behavioural tests was performed before ICH and at 1, 7, 14, 28 and 56 days after model induction by a researcher, who was blinded to the experimental groups during the darkness cycle. The battery of tests consisted of the cylinder test and modified Bederson's test that were previously fully explained in section 5.1.6.

6.1.7. PET STUDY

At day 56, all rats included in iPSCs treatment groups were scanned by microPET/CT. Likewise, 2 rats from each control group were also scanned as negative control group. PET/CT protocol was previously fully explained in section 5.1.7.

6.1.8. IMMUNOFLUORESCENCE ANALYSIS

After the last follow-up (56 days after ICH), animals were sacrificed by overdose of anaesthesia and intracardially perfused with 50 ml of PBS and 200 ml of 4% formaldehyde. Immediately, brains were extracted, immersed overnight in 4% formaldehyde and 24 h in

20% of sucrose PBS, embedded in OCT, cryopreserved and sectioned to 15-µm thickness. Immunofluorescence analysis for evaluation of neurogenesis and angiogenesis were previously fully explained in section 5.1.8.

6.1.9. STATISTICAL ANALYSIS

The results were expressed as average ± SEM, except for neurological scores that were discrete variables, so they were expressed as median [interquartile range].

Statistical analyses were made using Student t test assuming equal variances and with one tail. Significances of differences in discrete variables between groups were calculated by Mann–Whitney U test with one tail. The statistical descriptions and tests were calculated by Microsoft Excel 365 ProPlus (Microsoft) with Real Statistics Resource Pack complement (Real Statistics Using Excel, http://www.real-statistics.com/) . All graphs were generated by Prism 5 for Windows, Version 5.01 (GraphPad Software, Inc).

6.2.RESULTS

6.2.1. INCLUDED ANIMALS

A total of 35 SD rats were used in this study. Of all of them, one rat was excluded due death or surgery complications during the first 24 hours. Another one rat was excluded due to lack of hematoma. Finally, 1 rat was also excluded because of having an out of range lesion. Therefore, 32 SD rats were included and randomly assigned to intravenous (n=8) and intracerebral (n=8) iPSCs groups, and intravenous (n=8) and intracerebral (n=8) control groups.

6.2.2. EFFECT OF iPSCs TREATMENTS ON HEMATOMA VOLUMES

Hematoma size was quantified by MRI at 1 hour after ICH induction (basal hematoma), and at day 1, 7, 14, 28 and 56 post-ICH. As shown in **Figure 31** and **Figure 32**, hematoma presented its maximum size at 24 hours after collagenase injection, following by a continuous decrease that is more evident during the 1-to-7-days step.

As shown in **Figure 32**, no significant effects were observed on haematoma volumes for both iPSCs treatment, intravenous and intracerebral, compared to the control groups (all $p>0.05$) for any of the time points of the follow-up period. However, we found a trend to bigger haematoma in iv iPSCs group at baseline (1h) and at 1-day follow-up. Therefore, in order to avoid bias, we have calculated the percentage of lesion volume respect to basal ones (at 1 h and 1 day after ICH induction) (**Figure 33** and **Figure 34**, respectively). When we performed the comparison of lesion volumes adjusted to the basal ones, we observed that the group treated with iv iPSCs shows a tendency to further reduce the volume of injury during the follow-up period, but this difference was not statistically significant (all $p>0.05$) (**Figure 33** and **Figure 34**). By contrast, intracerebral iPSCs treated group trends to increase lesion volume during follow-up period, but again any difference was not statistically significant.

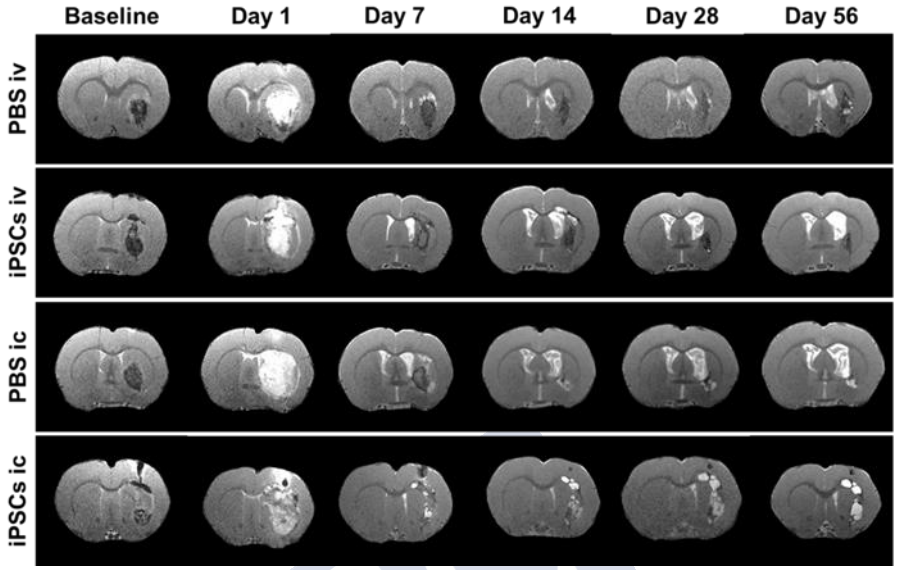

Figure 31: Representative MRI images of ICH lesions for control and iPSCs groups, both intravenous and intracerebral, during the follow-up period of 56 days after ICH induction.

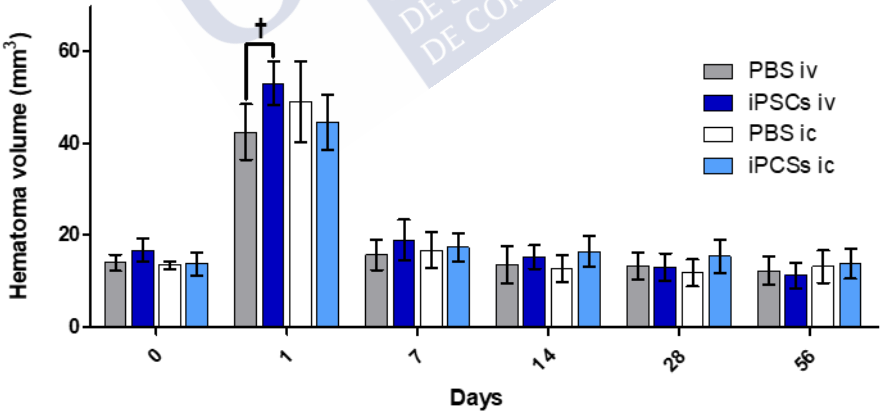

Figure 32: Comparison of absolute size of hematoma volumes for control and iPSCs groups during the follow-up period of 56 days after ICH. Results are showed as mean ± SEM (n=8 animals per group). No differences were found between groups (all p>0.05). However, a trend to bigger haematoma volume was found for iv iPSCs group both at baseline (1h) and at 1-day follow-up (†p<0.1).

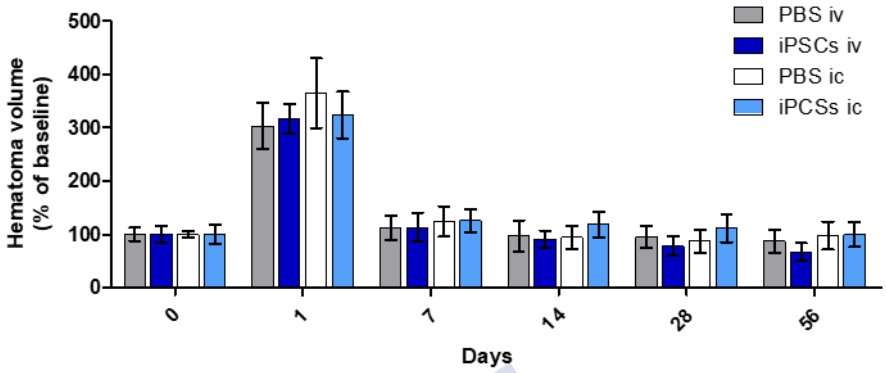

Figure 33: Comparison of lesion volumes adjusted to the basal one (1h) for control and iPSCs groups during the follow-up period of 56 days after ICH. Results are showed as mean ± SEM (n=8 animals per group). We observed that the group treated with iv iPSCs shows a tendency to further reduce the lesion volume during the follow-up period, but this difference was not statistically significant (all p>0.05).

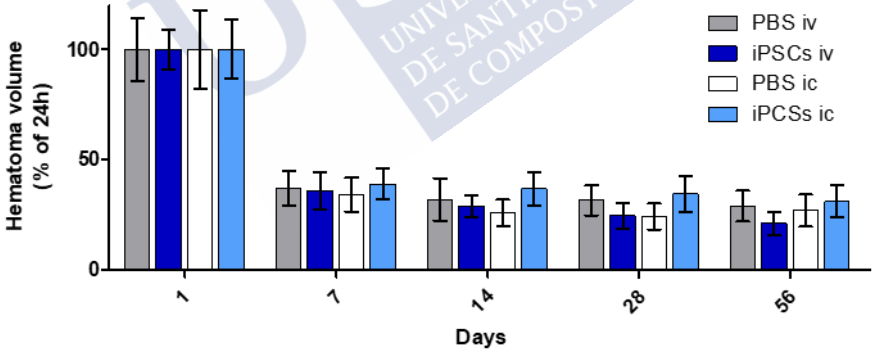

Figure 34: Comparison of lesion volumes adjusted to the basal at 1 day for control and iPSCs groups during the follow-up period of 56 days after ICH. Results are showed as mean ± SEM (n=8 animals per group). We observed that the group treated with iv iPSCs shows a trend to further reduce the lesion volume during the follow-up period, but this difference was not statistically significant (all p>0.05). By contrast, intracerebral iPSCs treated group trends to increase lesion volume during follow-up period, but again any difference was not statistically significant (p>0.05).

6.2.3. EFFECT OF iPSCs TREATMENT ON BEHAVIORAL TESTS

6.2.3.1. Effect of iPSCs treatment on cylinder tests

Sensorimotor deficits after ICH were quantified using laterality index. This index was close to 0.5 at 1 day before model induction for all experimental groups. As shown in **Figure 35**, iv iPSCs group showed greater sensorimotor recovery at day 28 post-ICH compared with the control group ($p<0.05$). By contrast, ic iPSCs group showed greater functional impairment compared to the control group at day 7 ($p<0.05$) (**Figure 35**). This difference could be because the group treated with ic iPSCs had a higher increment of ICH volume during the first 24 hours after haematoma induction. Besides, this assessment was done before any treatment, so this difference is not due to the iPSCs administration. In any case, to avoid this bias, we adjust the follow-up laterality indexes with respect to the baseline index at 24 hours (**Figure 36**)**.** Performing this analysis, we observed a better functional recovery for iPSCs groups (both ic and iv administration) at day, 14 and 28 post-ICH (all $p<0.05$) and a trend at day 7 ($p<0.01$) (**Figure 36**).

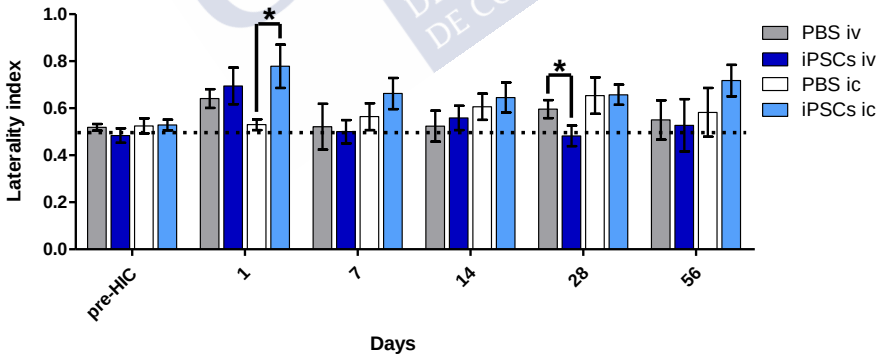

Figure 35: Effect of iPSCs treatment on somatosensory test. Sensorimotor deficits after ICH were assessed using the cylinder test and quantified by laterality index. The iv iPSCs group showed greater sensorimotor recovery at day 28 post-ICH compared with the iv control group. By contrast, ic iPSCs group showed greater functional impairment compared to its control group. Results are showed as mean ± SEM (n=8 animals per group) (*p< 0.05).

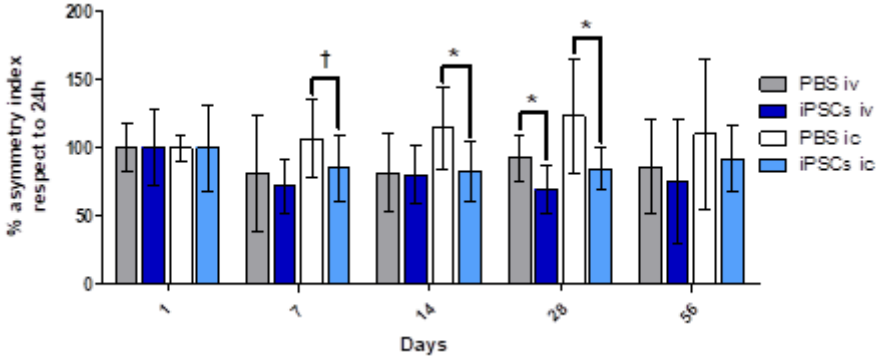

Figure 36: Percentage of asymmetry index respect to basal deficit at 24 h. Results are showed as mean ± SEM (n=8 animals per group). We observed a better functional recovery for iPSCs groups (both ic and iv administration) at day 7, 14 and 28 post-ICH (†p<0.1, *p<0.05).

6.2.3.2. Effect of iPSCs treatment on Bederson´s tests

Because the scores of the Bederson and Wahl's tests showed an excellent correlation (r = 0.89) in the study in cerebral ischemia, we decided to analyse only the Bederson test for the ICH study. Surprisingly, unlike the functional recovery evaluated by the laterality index, the results of neurological deficit evaluation showed a further deterioration in the group treated with iv iPSCs at day 7, although no differences were found in subsequent follow-ups (**Figure 37**). Likewise, percentages respect to 1-day basal follow-up were calculated; and we observed that these neurological deficits for both iPSCs treated groups were maintained at day 7 and 14 for ic iPSCs group (all $p<0.05$), although no differences were obtained at last follow-up period (**Figure 38**).

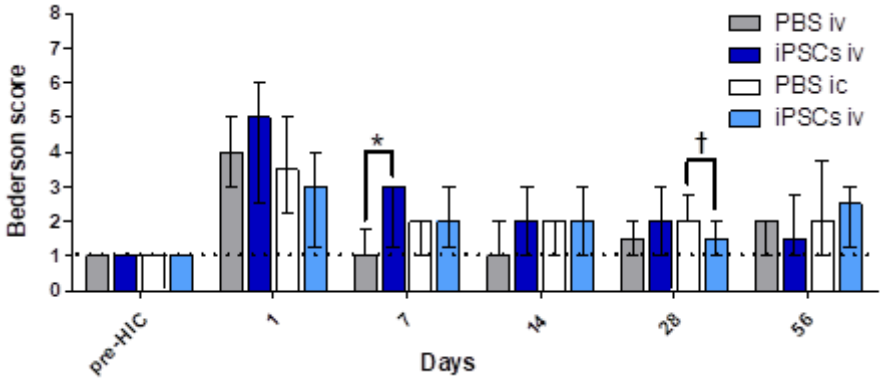

Figure 37: Effect of iPSCs treatment on neurological deficits evaluated by the Bederson test. The iPSCs iv group showed further deterioration at day 7, although no differences were found in subsequent follow-ups. Results are showed as mean ± SEM. (n=8 animals per group). (†p<0.1. *p<0.05).

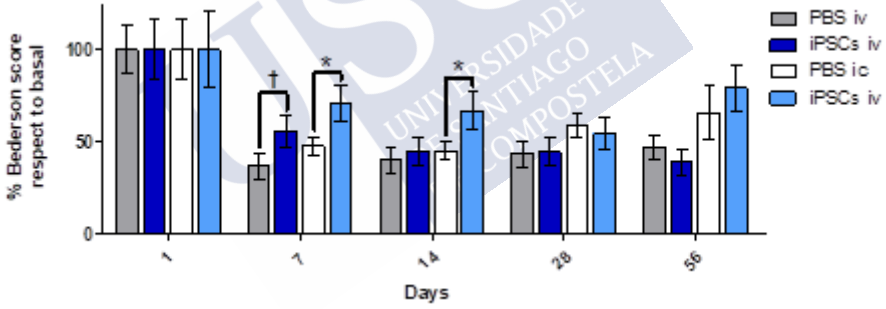

Figure 38: Progression of percentage of Bederson score respect to 1-day follow-up. Higher neurological deficits for both iPSCs treated groups were found at day 7 and 14 for ic iPSCs group, although no differences were obtained at last follow-up period. Results are showed as mean ± SEM. (n=8 animals per group). (†p<0.1. *p<0.05).

6.2.4. EFFECT OF iPSCs TREATMENT ON CEREBRAL NEUROGENESIS AND ANGIONESIS

6.2.4.1. Effect of iPSCs treatment on cerebral neurogenesis

We analysed neurogenesis by immunofluorescence in brain slices obtained at 56 days after ICH. In the neurogenesis assay, area with DCX positive cells was measured in SVZ of both hemispheres to quantify the migration of neuronal precursor cells. The ic iPSCs group showed a great increase of DCX positive area compared with its control group in both hemispheres. Moreover, the iv iPSCs group also exhibited neuronal precursor cells marker gain, but the difference with its control group was lower and not statistically significant (**Figure 39** and **Figure 40**).

In addition, Ki-67 positive cells were counted in DCX+ area in order to obtain the number of neuronal precursor cells in proliferation phase. Interestingly, we found more double positive cells (Ki-67+/DCX+) in ipsilateral hemisphere for the iv iPSCs treated group ($p<0.05$). Furthermore, a trend to a higher density of Ki-67+/DCX+ cells were also found in all iPSCs treated groups in both hemispheres compared with their respective control groups (**Figure 41**).

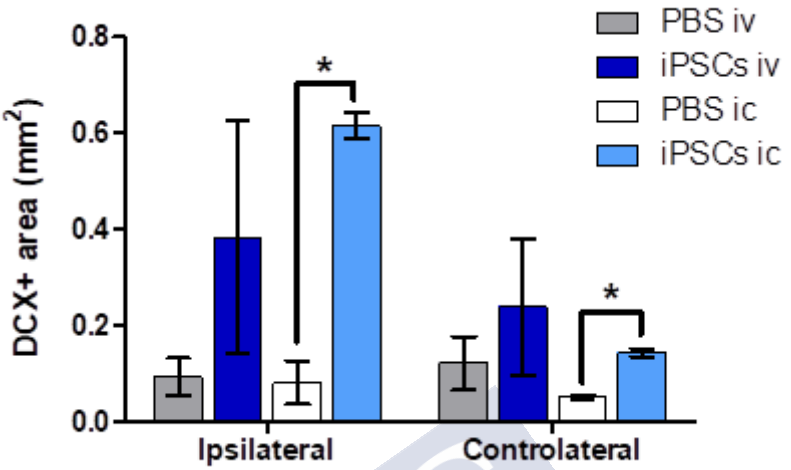

Figure 39: DCX+ area in mm^2. The ic iPSCs group showed a great increase of DCX positive area compared with its control group in both hemispheres. Moreover, the iv iPSCs group also exhibited neuronal precursor cells marker gain, but the difference with its control group was lower and not statistically significant. Results are showed as mean ± SEM. (*p<0.05).

6.2.4.2. Effect of iPSCs treatment on cerebral angiogenesis

Angiogenesis was analysed by immunofluorescence in brain slices obtained at 56 days after ICH. In angiogenesis assay, the number of vessels (CD31+) and Ki-67+ cells were counted. We didn't find any double positive cells. Moreover, we calculated the density of vessels. No differences were found in angiogenesis or number of vessels between groups (**Figure 42** and **Figure 43**).

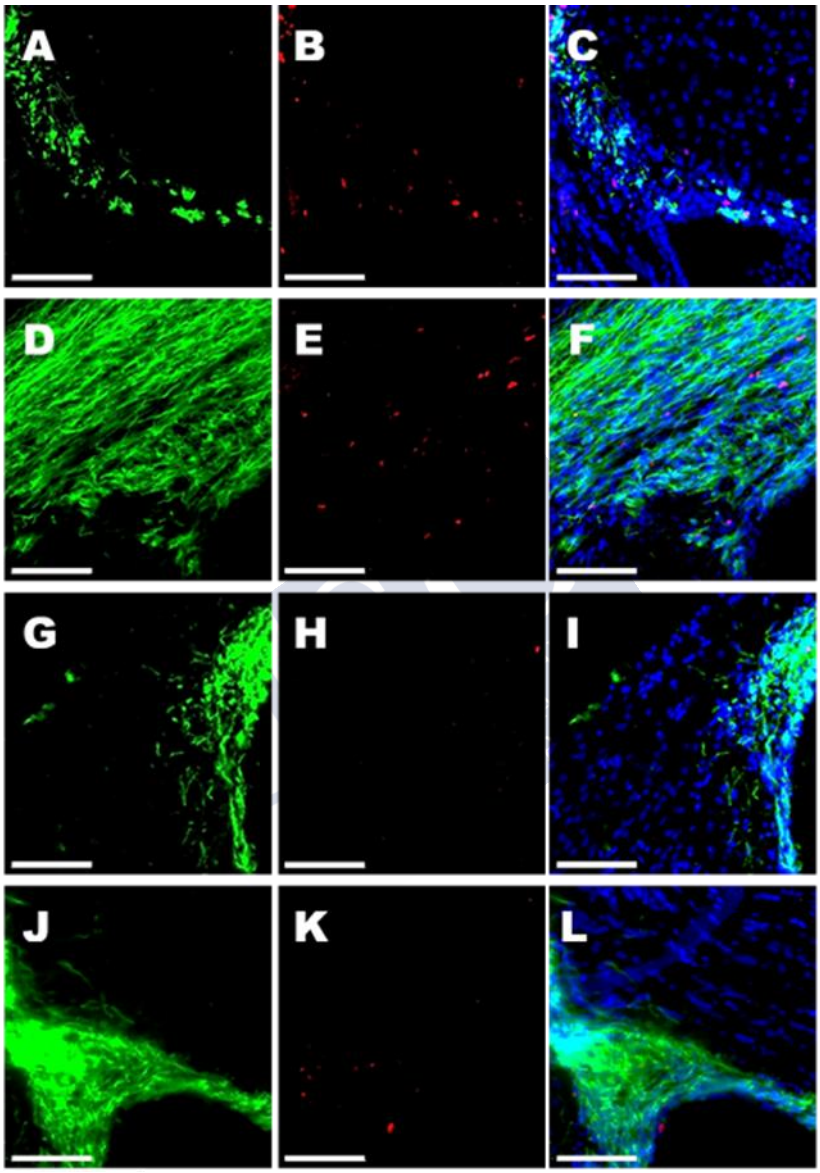

Figure 40: Images of neurogenesis in ipsilateral SVZ at 56 days after ICH. (A), (B) and (C) control ic. (D), (C) and (F) iPSCs ic. (G), (H) and (I): control iv. (J), (K) and (L) iPSCs iv. Green represents DCX positive cells; red is Ki-67 positive nucleus; in blue nucleus stained by Hoechst. Scale: 100 µm.

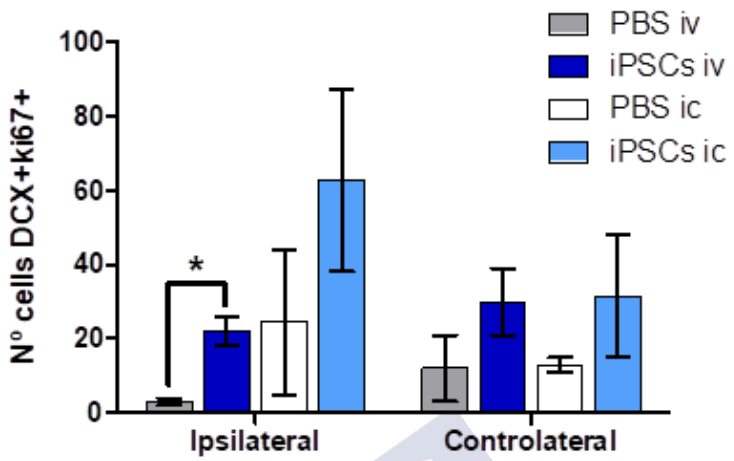

Figure 41: Number of Ki-67 positive cells in DCX positive area within SVZ in ipsilateral and contralateral hemispheres. Results are showed as mean ± SEM (n=3 animals per group). Results showed more neuronal precursor cells in proliferation phase (Ki-67+/DCX+) within the ipsilateral hemisphere for the iv iPSCs treated group (*p<0.05). Furthermore, a trend to a higher density of Ki-67+/DCX+ cells were also found in both hemispheres for all iPSCs treated groups.

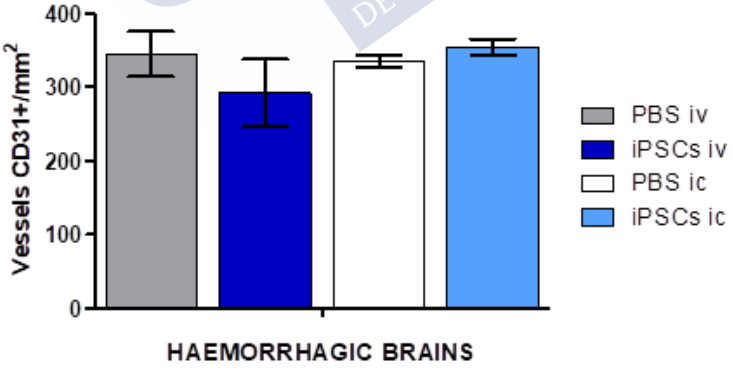

Figure 42: Density of vessels as number of vessels CD31+/mm^2 in control and iPSCs treated groups. Results are showed as mean ± SEM (n=3 animals per group). No differences were found between groups (p>0.05).

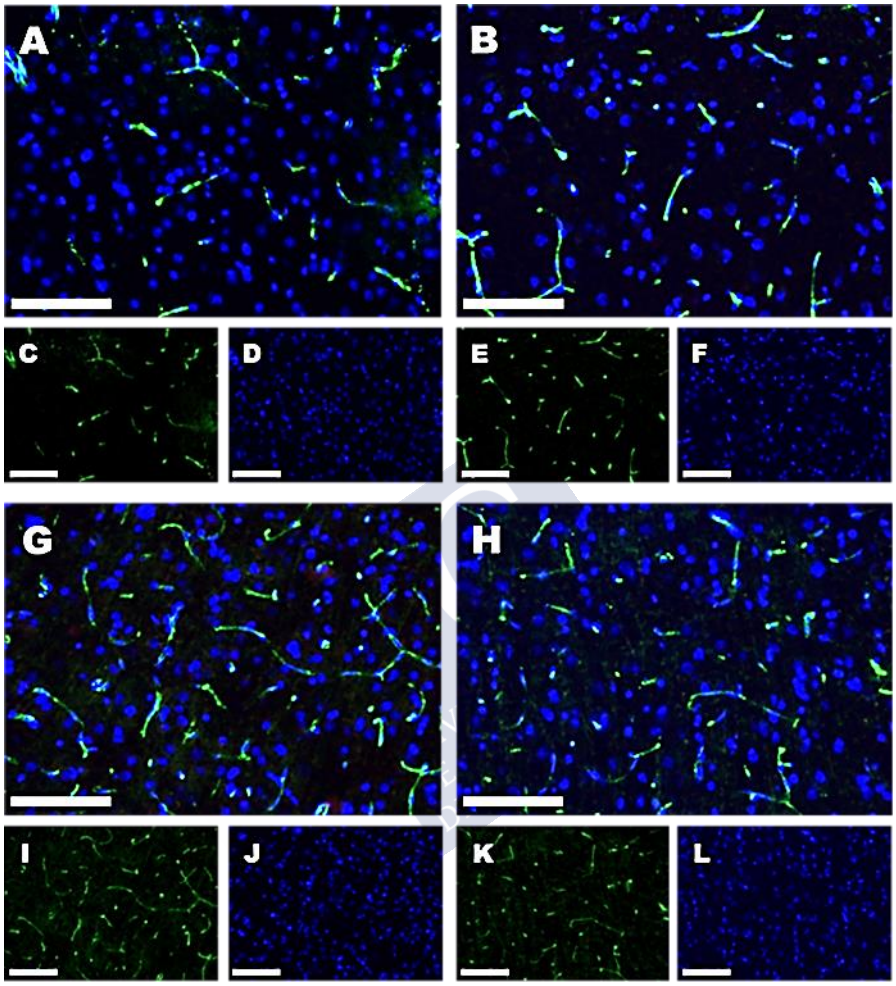

Figure 43: Images of cortex immunohistochemically stained for angiogenesis markers at 56 days after ICH, showing no differences between control and iPSCs treated group. (A) merge of PBS ic. (B) merge of iPSCs ic. (C) CD34 positive in green of PBS ic. (D) Hoescht in PBS ic. (E) CD31 positive in green in iPSC ic. (F) Hoechst in iPSC ic. (G) merge of PBS iv. (H) merge of iPSCs iv. (I) CD34 positive in green of PBS iv. (J) Hoechst in PBS iv. (K) CD31 positive in green of iPSCs iv. (L) Hoechst in iPSCs iv. Scale in all images is 100 μm.

6.2.5. EFFECT OF iPSCs TREATMENT ON TUMOR DEVELOPMENT

At day 56, all ICH rats included in iPSCs treated groups (intravenous and intracerebral) were scanned by microPET/CT. Likewise, two control rats were also scanned as negative control group. PET images did not show tumour or teratoma formation in any case (**Figure 44**).

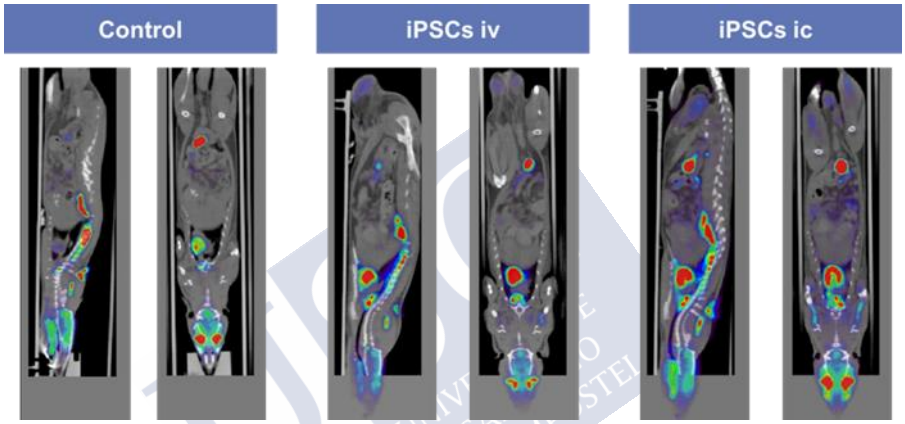

Figure 44: Representative PET/CT images for iPSCs treated (both intravenous and intracerebral) and control groups, showing no evidence of tumour or teratomas formation at 56 days after ICH.

7. SECTION IV: BIODISTRIBUTION OF iPSCs INTRAVENOUSLY ADMINISTERED AT EARLY STAGE

USC
UNIVERSIDADE
DE SANTIAGO
DE COMPOSTELA

The objective of this section is to study the *in vivo* biodistribution of iPSCs after its intravenous administration. One of the pending gaps of cell therapy is to determine the *in vivo* biodistribution of its intravenous administration in order to avoid side effects and determine the natural migration niches. For this purpose, a previous objective becomes imperative that is developing a method to label the cells and being able to detect them *in vivo* after intravenous administration.

7.1.MATERIALS AND METHODS

7.1.1. LABELLING OF iPSCs WITH MAGNETIC NANOPARTICLES

7.1.1.1. Procedure summary

Figure 45 shows the protocol for the *in vivo* study of the biodistribution of iPSCs. The experiments began with the synthesis of magnetic nanoparticles (MNPs) and its coating with dextran. MNPs were characterized to check size, and shape. iPSCs were incubated with MNPs and their integration inside the cells was also checked. Likewise, toxicity, pluripotency, and contrast in MRI was analysed. Finally, labelled iPSCs were intravenously injected in rats and iPSCs were search for in body by MRI and inductively coupled plasma mass spectrometry (ICP-MS) techniques. This same protocol was tested for other labelling methods such as CFSE, ^{18}F-FDG and finally AuNPs.

7.1.1.2. Synthesis of dextran coated superparamagnetic nanoparticles

Dextran magnetic nanoparticles (D-MNPs) were synthesised and characterized following the protocol described by Argibay *et al.* (109), based on Pardoe *et al.*(110) publication. Under N_2 atmosphere, Fe (II) 0.1 M and Fe (III) 0.1 M, both in water (Grifols, Barcelona, Spain), were mixed at 400 rpm and heating until 60 ºC. Then 20 mg/ml dextran (from *Leuconostoc* spp., Sigma-Aldrich, San Luis, USA) solution was

added until making double volume; this mixture was maintained for 15 minutes maintaining same temperature. Next, 1/6 of total volume of 70% ammonia solution were added and mixed for 15 min. The final solution was cooled down to room temperature maintaining the initial stirring. The suspension was dialyzed (D0530, Sigma-Aldrich, San Luis, USA) against distilled water. D-MNPs suspension was kept at 4ºC until further usage.

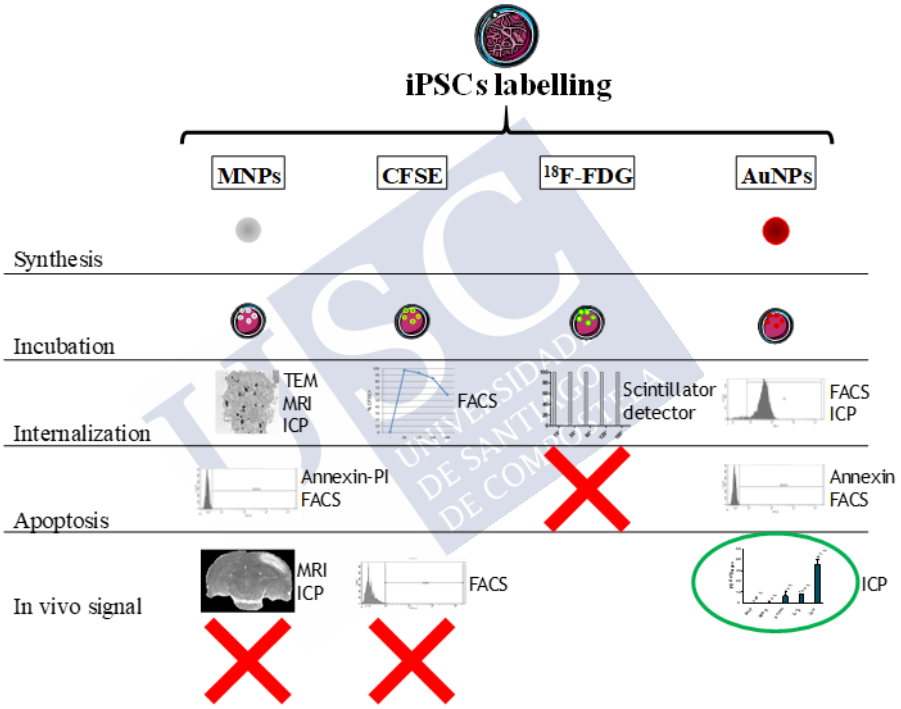

Figure 45: Protocol for the *in vivo* study of the biodistribution of iPSCs (self-created image using elements with creative commons license).

7.1.1.3. Cell labelling with D-NPMs

Prior to cell labelling, D-MNPs were coated with poly-L-lysine (PLL) in excess (5 µg/ml) in iPSCs medium. The solution was shacked at 1400 rpm for one hour at room temperature.

After two washes with PBS, iPSCs were incubated with the solution (medium and D-MNPs-PLL) for 24 h. Later, medium was

removed and cells were washed with PBS three times and incubated with normal iPSCs medium for 12 h before any experiment in order to let MNPs be internalized.(111)

7.1.1.4. Cellular quantification

To determine the proliferation rate, cells were counted with Trypan Blue (STEMCELL Technologies, Vancouver, Canada) staining on a Neubauer chamber.

7.1.1.5. Prussian Blue

To check uptake of MNPs by iPSCs, Prussian Blue staining was performed. Prussian Blue is a pigment formed by oxidation of ferrous salts. Cells were incubated with a mix of equal parts of aqueous solution of 20% HCl (Hydrochloric acid fuming 37% extra pure, Merk, Whitehouse Station, USA) and aqueous solution of 10% potassium ferrocyanide trihydrate ($KFe(CN)_6 \cdot 3H_2O$, Sigma-Aldrich) for 20 minutes.

7.1.1.6. Toxicity

In order to optimize the concentration of MNPs per cell, toxicity was evaluated using LDH kit and Annexin/Propidium iodide kit for FACS. LDH test measures the extracellular lactate dehydrogenase (LDH). This enzyme is out of cells only by cytolysis or cytotoxicity. Annexin binds to translocated phospholipid phosphatidylserine from the inner to the outer leaflet of the plasma membrane, and this occurs as a previous phase to apoptotic processes. Propidium iodide (PI) is a fluorescent intercalating agent that gets to nuclei when the plasmatic and nuclear membranes are broken by necrosis.

LDH tests were performed with Pierce™ LDH Cytotoxicity Assay Kit (ThermoFisher Scientific, Waltham, USA) following kit's instructions, we measured the LDH reactions in supernatants of cultures, namely the removed culture medium after 24 hours.

Annexin/PI tests were performed with DY634 Annexin V Apoptosis Detection Kit with PI (Immunostep, Salamanca, Spain)

following manufacturer's protocol. We washed the cells two times with PBS, detached with trypsin, washed one again after centrifugation, and incubated Annexin and PI 15 minutes in dark. The cellular suspension was analysed with flow cytometry by BD FACS Aria II (BD Bioscience, Franklin Lakes, USA).

Prior to assays, cellular quantification was performed to detect potential differences in proliferation. Control without cells, control cells without MNPs and death control were measured with sample in both tests.

7.1.1.7. Magnetic resonance imaging of labelled cells

Agar phantoms were done to detect MRI contrast of labelled cells. After detaching and counts cells, 100 µl of sample and another 100 µl of hot agar were mixed and deposited in wells of a cooled and solidified agar mould. When all wells are filled, hot agar was dumped on mould in order to cover all the surface. Mould with samples was left to cold at 4ºC before acquisition in MR.

Phantoms were scanned in a Bruker Biospec 9.4 T small animal MR scanner (Bruker, Biospin) equipped with actively shielded gradients (400 mT/m). A quadrature radiofrequency transmit-receive resonator was used for data acquisition. T2-weighted images was acquired using MSME sequence of 10.26 ms echo time, 3 s repetition time, 16 echoes, 14 slices, 1 average, FOV of 7.5 cm x 7.5cm and matrix size of 256 x 256. T2*-weighted images was acquired using MGE sequence of 4.44 ms echo time, 6.75 ms echo spacing, 1.8 s repetition time, 16 echoes, 14 slices, 2 averages, FOV of 7.5cm x 7.5cm and a matrix size of 256 x 256. Post-processing was performed using ImageJ software (Rasband).

Control with only medium and not labelled control cells were included in MRI acquisitions.

7.1.1.8. Pluripotency assay

BD Mouse Pluripotent Stem Cell Transcription Factor Analysis Kit (BD Bioscience) was used to analyse the pluripotency of cells in order to check the maintaining of their normal metabolism and phenotype

after incubation with MNPs. Pluripotency kit was used following the manufacturer's indications. After washing the cells two times with PBS, we detached them with trypsin, and after centrifugation and resuspension we incubated antibodies to Nanog, Oct3/4 and Sox2 for 20 minutes. Samples were analysed by BD FACS Aria II (BD, Bioscience). We analysed not labelled control cells, just labelled cells, cells one day after MNPs incubation and cells 3 days after MNPs incubation.

7.1.1.9. Transmission electron microscopy

For measuring the size and determining the shape of the MNPs, samples were evaporated on a carbon-coated cooper grid without staining. It was used a Philips CM-12 transmission electron microscope (TEM) operating at 120 kV. Diameters of 100 particles were measured with NIH ImageJ software to calculate the mean particle diameter.

To assess the localization of the MNPs in the cell, TEM images of cells were taken. Fixation and post-fixation of 500.000 cells were carried out in 2% glutaraldehyde in sodium cacodylate buffer and in 1% OsO_4 in the same buffer. Inclusion were done in Spurr's epoxy resin. Semithin sections (0.5 μm) were stained with Toluidine blue and ultrathin sections (100 nm) were stained with uranyl acetate and lead citrate.

7.1.1.10. Animal model

tMCAO was performed following the protocol described in section 5.1.2.

7.1.1.11. Cells administration

Cells were intravenously administrated following the same protocol in the previous sections 5.1.4. A dose of $3x10^6$ labelled iPSCs in 1 ml of PBS were injected in jugular of anesthetized rats at 24 h post-MCAO. The injection was administrated during at least 1 min.

7.1.1.12. Magnetic resonance imaging of animals

In vivo cell tracking was assessed by MRI. T2-weighted and T2*-weighted images were acquired at 24 h, 72 h and 7 days after cells administration. Whole body of the animal was scanned.

T2-weighted images were acquired using a multislice multiecho spin-echo sequence with the following acquisition parameters: FOV 19.2 x 19.2 mm^2, image matrix 192 x 192 (isotropic in-plane resolution of 100 μm/pixel x 100 μm/pixel), 14 consecutive slices of 1 mm thickness, repetition time of 3 s, and 16 echoes with 9 ms of echo time.T2*-weighted images were acquired using a multi gradient echo sequence with the following acquisition parameters: FOV 19.2 x 19.2 mm^2, image matrix 192 x 192 (isotropic inplane resolution of 100 μm/pixel x 100 μm/pixel), 14 consecutive slices of 1 mm thickness, repetition time of 1.5 s, and 16 echoes with 2.9 ms for the first echo time and 3.28 ms of echo spacing.

7.1.1.13. Inductively coupled plasma mass spectrometry

Rats were sacrificed and perfused with 80 ml PBS. Lungs, liver, spleen, kidneys and brain were extracted and weighted, immediately frozen with liquid nitrogen, and kept at 80 ºC until their digestion.

Between 0.5 and 0.6 g of each organ were soaked in 4 ml of 69% HNO_3 (Hiperpur, Panreac, Barcelona, Spain) and 1 ml of 33% H_2O_2 (Panreac), digested in heating plate (DK20, Velp Scientifica, Usmate. Italy) at 110 ºC for 2 h, and added milli-Q H_2O until a final volume of 25 ml.

Cell samples were detached from plate, washed twice with PBS, and kept at 80 ºC until the ICP-MS analysis. 0.5 ml of 69% HNO_3 (Hiperpur, Panreac) were added to cell samples, after one hour milli-Q H_2O was added until a final volume of 3 ml.

The equipment used was an ICP-MS (Agilent 7700x, Agilent Technologies, Santa Clara, CA, USA) with sample introduction system consisting of a micromist glass low-flow nebulizer, a double-pass glass spray chamber with Peltier system (2ªC) and a quartz torch. The determinations were performed in the Network of Infrastructures to

Support Research and Technological Development (RIAIDT) of Santiago de Compostela University.

7.1.1.14. Experimental design

The first step was to prove the correct size and shape of MNPs by TEM. Then, the labelling of iPSCs was performed with several concentrations of nanoparticles in culture medium: 100, 200, and 500 µg/ml. These concentrations and a control (cells incubated only with culture medium) were used: to prove the uptake of MNPs by images of TEM and optic microscope (after Prussian blue staining), to evaluate the cellular proliferation using a haemocytometer, apoptosis and necrosis by annexin/PI kit for flow cytometer, and cytotoxicity by LDH. In 200, 500 µg/ml and control the signal in MRI and the maintaining of pluripotency were assessed along different times: at day 1, 2 and 5, and at day 2, 5 and 7, respectively, after incubation with MNPs.

For *in vivo* study, two ischemic rats were intravenously injected with $3x10^6$ of MNPs-labelled iPSCs. MRI was acquired just after injection and two days later to track the biodistribution of cells. The doses of intravenous administration of iPSCs were $3x10^6$ cells, therefore we have tested $3x10^6$, $1.5x10^6$, $7.5x10^5$, 375,000 and 187,500 cells in each well. iPSCs-MNPs administrated ischemic rats and control ischemic rats were sacrificed at 12, 24 and 48 hours after labelled-iPSCs injection to measure the quantity of iron in their main organs by ICP-MS.

7.1.2. LABELLING iPSCs WITH CFSE

7.1.2.1. Procedure summary

With this method we tried to label iPSCs with carboxyfluorescein succinimidyl ester (CFSE), a fluorescent dye. iPSCs were labelled with CFSE and intravenously injected in rats; organs were extracted, disaggregated mechanically, diluted in PBS and analysed by flow cytometry.

7.1.2.2. CFSE labelling

CellTrace™ CFSE Cell Proliferation Kit (ThermoFisher Scientific, Waltham, MA, USA) was used to label cells following the kit's instruction. After removing the culture medium, iPSCs were incubated with CFSE 5µM dissolved in PBS for 20 minutes at 37ºC. Then CFSE-PBS was removed, cells were washed with PBS and incubated with culture medium for at least 10 minutes.

7.1.2.3. Flow cytometry *in vitro* analysis

Cells were detached with trypsin, washed with PBS and analysed by flow cytometry with BD FACS Aria II (BD, Bioscience, Franklin Lakes, NJ, USA). Control cells, just labelled cells, and cells 12, 24, and 48 hours after labelling were analysed.

7.1.2.4. Flow cytometry ex vivo analysis

A total of $3x10^6$ of labelled iPSCs in 1 ml of PBS were injected in jugular vein following the same protocol than in the previous section 5.1.4. Two SD rats was sacrificed at 12, 24 and 48 hours after the injection of CFSE-iPSCs and perfused with 80 ml PBS and 80 ml formaldehyde 4%. Lungs, liver, spleen and kidneys were extracted, disaggregated and filtered by 70 µm pore, and the filter washed with PBS. The cell suspension was analysed by flow cytometry with BD FACS Aria II (BD, Bioscience, Franklin Lakes, NJ, USA). A control rat, without any injection, was also perfused, and its organs analysed by flow cytometry by same protocol.

7.1.2.5. Experimental design

We quantified the CFSE positive cells by flow cytometry just after labelling and at 12, 24 and 48 hours. So, we were able to measure the decay of CFSE signal due to cell division. Rats were intravenously injected with these CFSE-labelled cells, sacrificed at the same time points, and their organs were disaggregated and filtered, and analysed by flow cytometry.

7.1.3. LABELLING MSCS WITH ^{18}F-FDG

7.1.3.1. Procedure summary

As probe of concept, we used MSCs to test labelling with ^{18}Fluor fludeoxyglucose (^{18}F-FDG). ^{18}F-FDG was incubated in MSCs culture, and after different times of incubation radioactivity was measured.

7.1.3.2. ^{18}F-FDG labelling and experimental design

We followed a previous protocol to label MSCs with ^{18}F-FDG.(112) Initially, radioactivity of vials with ^{18}F-FDG was measured. Culture medium was removed, MSCs were washed with PBS and fresh medium with FDG was incubated for several times: 15, 30, 60, 90, 120 and 180 minutes. After ^{18}F-FDG incubation, medium was removed, cells were washed twice with PBS (medium and washing PBS were set apart), and trypsinized (trypsin and neutralizing medium were also set apart). Radioactivity in pellet, trypsin, and medium-PBS were quantified.

The same protocol was applied incubating the ^{18}F-FDG with PBS for 15, 30, 60, and 120 minutes. Also, we tried incubating ^{18}F-FDG with DMEN glucose-free for 15, 30, 60, 90, 120, and 180 minutes. Finally, we incubated with MSCs medium based on DMEN glucose-free for 24 hours, and after that with DMEN glucose-free and ^{18}F-FDG for 1, 2 and 3 hours.

7.1.4. LABELLING iPSCs WITH GOLD NANOPARTICLES

7.1.4.1. Procedure summary

Firstly, we synthetized gold nanoparticles (AuNPs) of two different sizes (10 and 18 nm); then, these AuNPs were characterised to check size and shape. AuNPs were bound to bovine serum albumin (BSA) that previously was labelled with rhodamine b. iPSCs were incubated with AuNPs-BSA-R (0.1, 0.5 and 1 mg/ml using 3 times of incubation: 6, 12 and 24 h) and the integration in the cells was checked. Also, toxicity, and pluripotency were assessed at several times after incubation (0.1, 0.5 and 1 mg/ml using 3 times of incubation: 6, 12 and 24 h for toxicity and 1 mg/ml using 3 times of incubation: 1, 2 and 3 days). Finally, labelled iPSCs were intravenously injected ($3x10^6$ cells) in ischemic rats and cells were searched for in body by ICP-MS.

7.1.4.2. Synthesis of gold nanoparticles cores

The first step in AuNPs synthesis was to mix 26.042 ml of sodium citrate (60mM) and 8.681 ml of citric acid (60mM) in 1 l of milli-Q water with stirring on. This mixture was heating until soft boiling and maintained for 30 minutes. After that, 0.694 ml of EDTA (30mM) was added, and then 6.944 ml of $HAuCl_4$ (25mM). In 60 seconds, approximately, the solution got red wine colour. With this procedure we could get the seeds, to obtain them we let cooling to room temperature with stirring on. To grow these seeds the solution was kept with soft boiling and $HAuCl_4$ 25 mM was added two times.

7.1.4.3. Transmission electron microscopy

TEM was used to study the AuNPs morphology and size distribution. All TEM micrographs were obtained using a JEOL JEM-2010 electron microscope operated at an accelerating voltage of 120 kV. 3 µL of diluted sample was deposited on a carbon film supported on a 400 Mesh copper grid (Electric Microscopy Sciences, CF400-CU) and was air-dried. TEM images were acquired in the Network of

Infrastructures to Support Research and Technological Development (RIAIDT) of Santiago de Compostela University. Using ImageJ software, diameter of AuNPs were measured from TEM images.

7.1.4.4. Labelling of gold cores

A solution of 20 mg/ml of BSA (Sigma-Aldrich, San Luis, USA) in $NaCO_3$ buffer and 10 mg/ml of rhodamine b isothiocyanate (Sigma-Aldrich, San Luis, USA) in MetOH were mixed at a ratio of 10 rhodamines/BSA. It was kept at room temperature at least 2 hours before storing at 4ºC in the dark.

Once BSA is labelled by rhodamine b (BSA-R), the free dye is removed by desalting columns (Merk, Whitehouse Station, NJ, USA) following manufacturer's instructions.

Solutions of cores and BSA-R were mixed at ratios of 100 BSAs/NP (with Au seeds) and 500 BSAs/NP (with grown seeds). This mixture (AuNPs-BSA-R) was kept stirring overnight and concentrated by 100K centrifugal filters (Merk, Whitehouse Station, NJ, USA) centrifuging 5 minutes at 3000 rcf. The concentrated nanoparticles were filtered by 0.22 µm in order to sterilize, and ultra-centrifuging 30 minutes at 15000 rcf twice with seeds and once with grown seeds in order to remove free BSA-R.

For pluripotency tests, AuNPs were also functionalized with only BSA in order to avoid fluorescence that could interfere with pluripotency markers. BSA was mixed with grown AuNPs as indicated above at 500 BSAs/NP.

7.1.4.5. Labelling of iPSCs with AuNPs-BSA-R

At least 24 hours after seeding, iPSCs were incubating with AuNPs at selected concentrations (0.1, 0.5, and 1 mg/ml) in normal medium and with different times of incubation (6, 12, and 24 h) in order to choose the optimum condition.

7.1.4.6. Toxicity

In order to optimize the concentration of NPs in accordance with toxicity, we used DY634 Annexin V Apoptosis Detection Kit with PI (Immunostep, Salamanca, Spain) for flow cytometry. We didn't use PI because this marker is detected in the same channel than rhodamine b, instead we evaluated the labelling of rhodamine b.

Just after incubation with NPs, medium was removed and iPSCs were washed three times with PBS, detached with trypsin, washed twice with PBS after centrifugation, resuspended in the kit's binding buffer, and incubated with Annexin during 15 minutes in dark. The cellular suspension was analysed with flow cytometry by BD FACS Aria II (BD, Bioscience, Franklin Lakes, NJ, USA).

7.1.4.7. Inductively coupled plasma mass spectrometry (ICP-MS)

The equipment used was an ICP-MS (Agilent 7700x, Agilent Technologies, Santa Clara, CA, USA) with sample introduction system consisting of a Micromist glass low-flow nebulizer, a double-pass glass spray chamber with Peltier system (2ªC) and a quartz torch. The determinations were performed in the Network of Infrastructures to Support Research and Technological Development (RIAIDT) of Santiago de Compostela University.

Three ischemic rats (one control and two with previous intravenous injection of AuNPs-BSA-R-labelled iPSCs) were sacrificed and intracardially perfused with 80 ml PBS one day after the injection. Lungs, liver, spleen, kidneys and brain were extracted, weighted, immediately frozen with liquid nitrogen, and kept at 80ºC until their digestion. Ischemic lesions inductions and intravenous injections of cells were performed as described above.

Between 0.5 and 0.6 g of each organ were soaked in 4 ml of 69% HNO_3 (Hiperpur, Panreac, Barcelona, Spain) and 1 ml of 33% H_2O_2 (Panreac, Barcelona, Spain), digested in heating plate (DK20, Velp Scientifica, Usmate. ItalyDK20) at 110 ºC for 2 h, and added milli-Q H_2O until a final volume of 25 ml.

Cell samples (control iPSCs, just labelled iPSCs and iPSCs one and two days after AuNPs-BSA-R labelling) were detached from plate, washed twice with PBS, and kept at 80 ºC until the ICP-MS analysis. 0.5 ml of 69% HNO_3 (Hiperpur, Panreac) were added to cell samples, after one hour milli-Q H_2O was added until a final volume of 3 ml.

7.2.RESULTS

7.2.1. LABELLING OF iPSCs WITH MNPS

7.2.1.1. Nanoparticles synthesis and structural characterization

TEM images showed the spherical shape of D-MNPs (**Figure 46**). The mean of D-MNP diameter was 3.255 ± 0.66 nm.

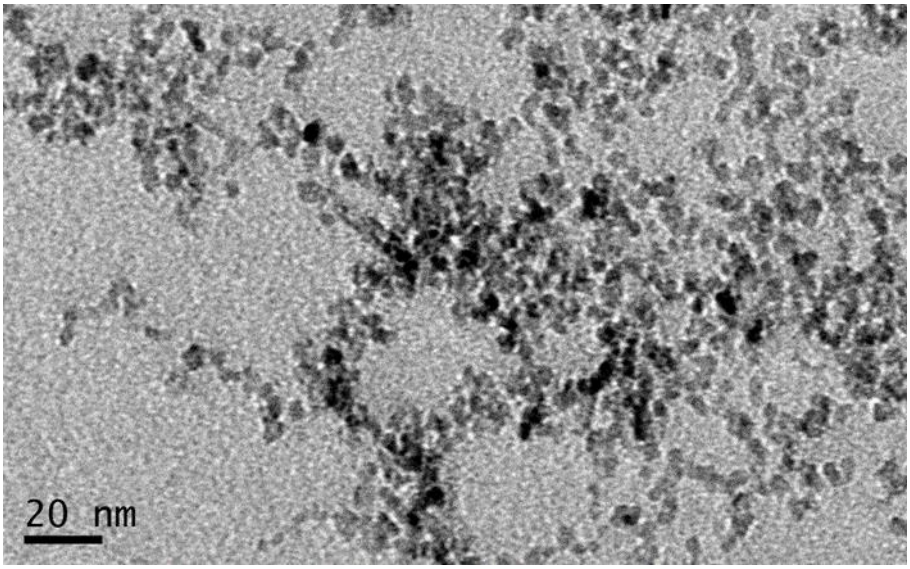

Figure 46: TEM image of dextran coated magnetic nanoparticle showing its spherical shape.

7.2.1.2. D-MNPs uptake by iPSCs

Prussian blue staining was performed after incubating iPSCs with D-MNPs at three different concentrations (100, 200 and 500 µg/ml) and in only culture medium. As shown in **Figure 47**, blue staining in D-MNPs-incubated iPSCs indicated the presence of iron inside the cells.

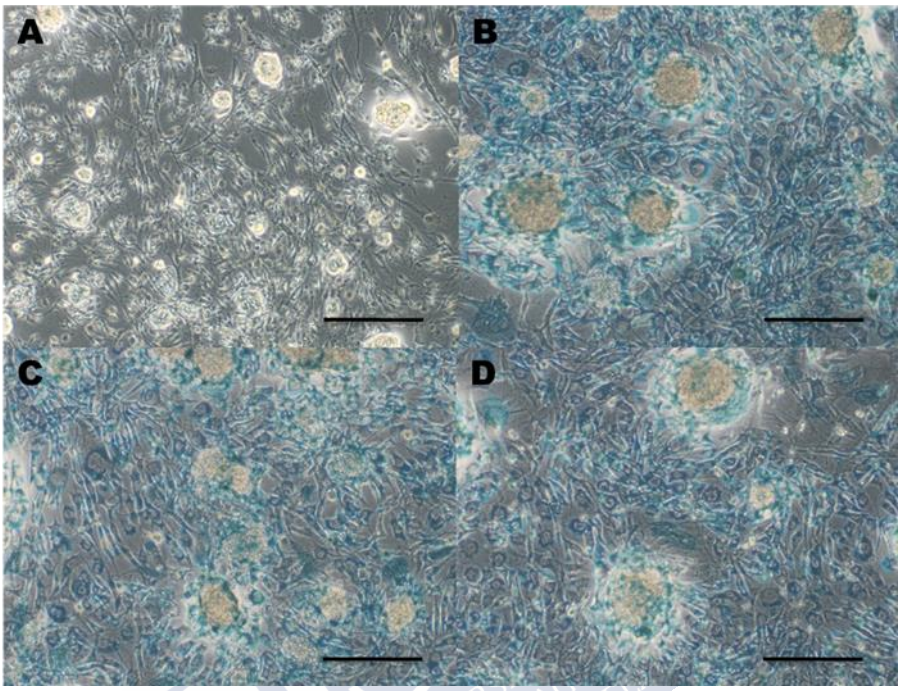

Figure 47: Prussian blue staining confirming the uptake of D-MNPs by iPSCs. (A) iPSCs control, incubated with only medium. (B) iPSCs incubated with 100 µg/ml D-MNPs. (C) iPSCs incubated with 200 µg/ml D-MNPs. (D) iPSCs incubated with 500 µg/ml D-MNPs. Scale: 200 µm.

Likewise, TEM images were acquired to check whether, indeed, there were nanoparticles into the cytoplasm of cells. **Figure 48** shows that the uptake of D-MNPs by iPSCs was successful in the three different concentrations (100, 200 and 500 µg/ml) by endocytosis of micro-clusters of nanoparticles. We observed clusters of iron nanoparticles into the cells, that are shown in **Figure 49** in detail.

7.2.1.3. Cellular proliferation

In order to check the proliferative capacity of iPSCs after MNPs incubation, we counted the number of cells at 24 hours after incubation in 6-wells plates with 100, 200 and 500 µg/ml of MNPs and a control incubated with only culture medium. In **Figure 50** we can observe a

significant reduction of cellular proliferation in those wells incubated with nanoparticles; however no differences were found between different concentrations of MNPs.

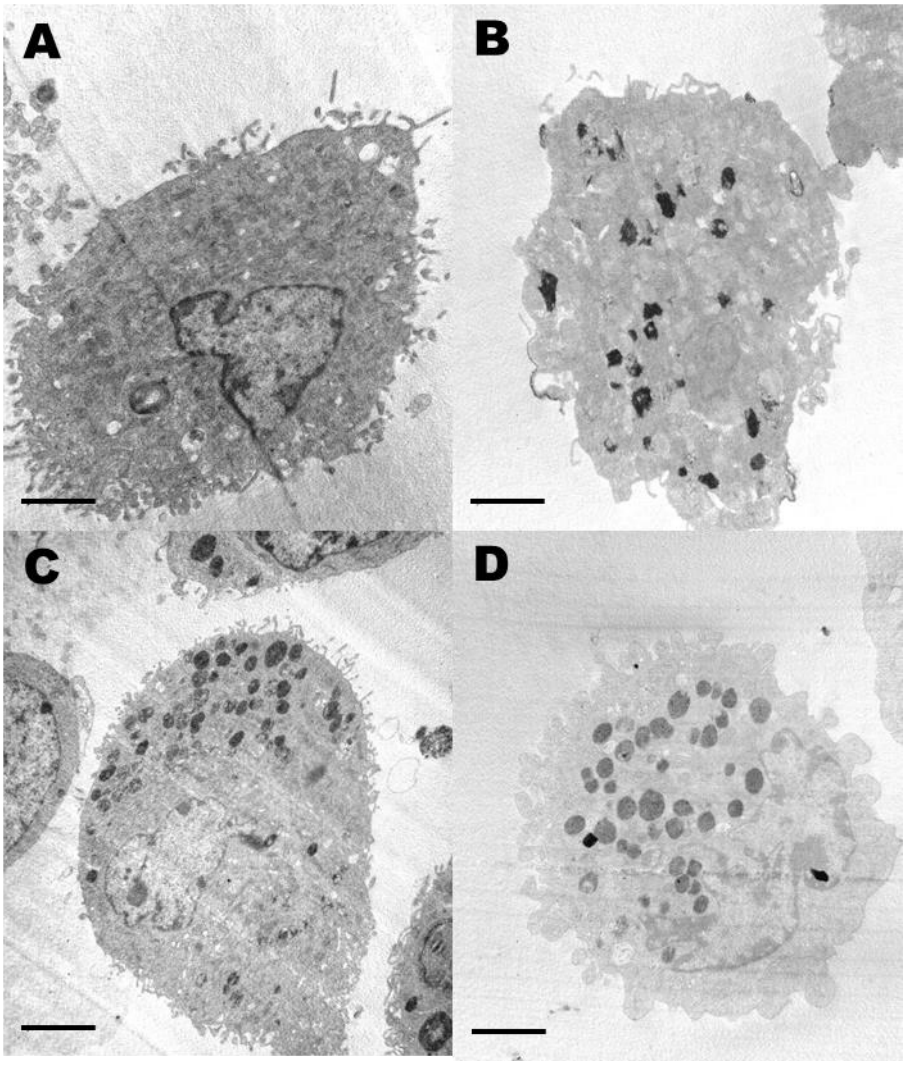

Figure 48: TEM images of iPSCs incubated with D-MNPs. (A) iPSCs control, incubated with only medium. (B) iPSCs incubated with 100 µg/ml D-MNPs. (C) iPSCs incubated with 200 µg/ml D-MNPs. (D) iPSCs incubated with 500 µg/ml D-MNPs. Scale: 2 µm.

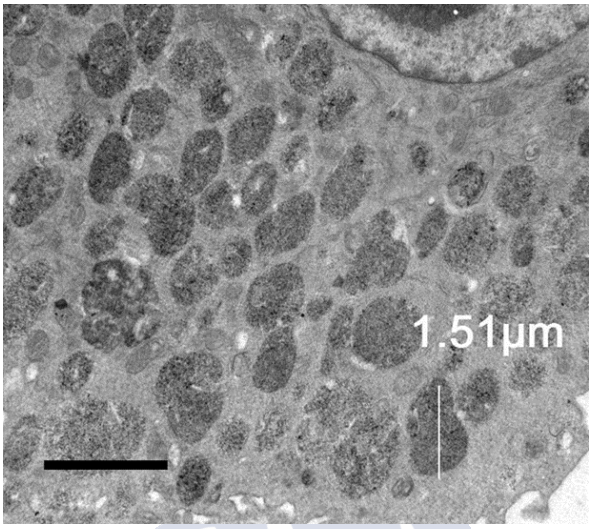

Figure 49: TEM images of iPSCs incubated with D-MNPs. Detail of nanoparticles clusters into the cytoplasm. Scale: 2 µm.

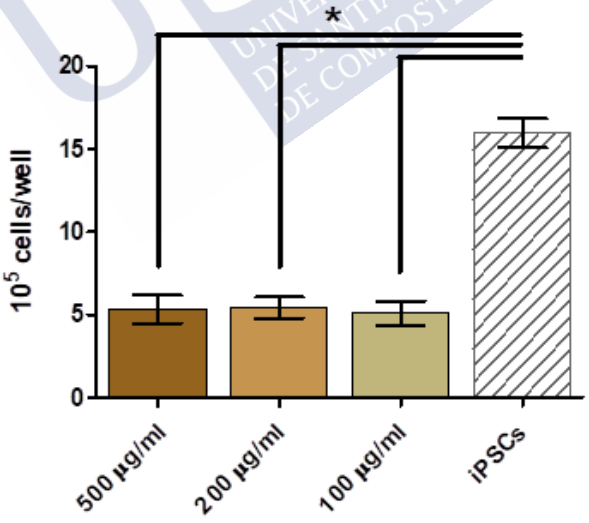

Figure 50: Number of iPSCs in 6-wells plates at 24 hours after incubation. A significant reduction of cellular proliferation was observed after MNPs incubation.

7.2.1.4. Toxicity

We evaluated apoptosis and necrosis by flow cytometry using annexin and propidium iodide markers, respectively. We did not find any difference between groups respect to apoptosis (**Figure 51**).

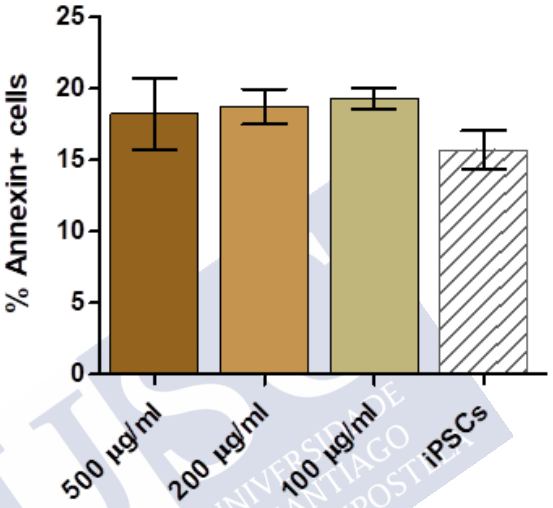

Figure 51: Percentage of annexin positive iPSCs after MNPs incubation at 3 different concentrations (100, 200 and 500 ug/ml) and iPSCs without MNPs. No differences were found between groups respect to apoptosis.

However, the percentage of positive iPSCs for propidium iodide was significant lower in control sample compared to those incubated with MNPs at 500 µg/ml (**Figure 52**). In any case, this difference was very small: the means were 13% *vs*. 15.2% for 500 µg/ml and control iPSCs, respectively; so, we conclude that incubation of iPSCs with MNPs was safe.

In addition, LDH viability assay was performed using the same conditions than those used in the other toxicity assays. There were no differences between groups (**Figure 53**) respect to % of absorbance; indeed we calculated the percentage of viability by the next equation: $\%\, Viability = \frac{A_{death} - A_{sample}}{A_{death} - A_{medium}} \cdot 100$ (being A_{death}: absorbance in death control, A_{sample}: absorbance in sample of interest, and A_{medium}:

absorbance in white control), showing percentages of viability between 70-73% for all tested groups.

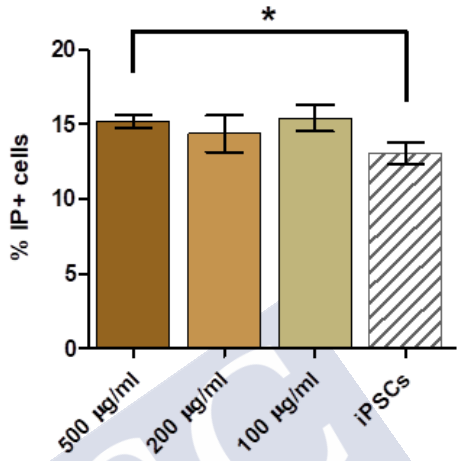

Figure 52: Percentage of propidium iodide positive iPSCs after MNPs incubation at 3 different concentrations (100, 200 and 500 ug/ml) and iPSCs without MNPs. A small increase of necrosis was found in the group of iPSCs incubated with the highest concentration of MNPs (500 ug/ml) respect to the control. (*p<0.05).

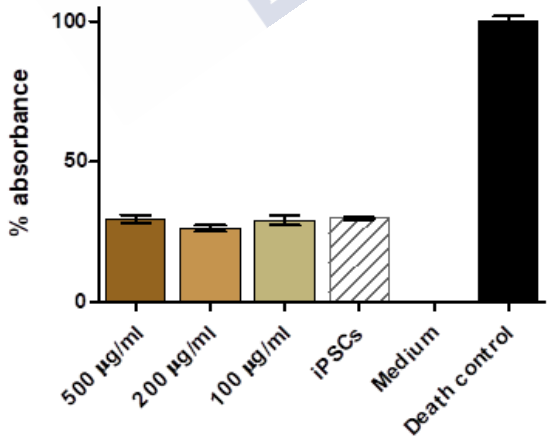

Figure 53: Percentage of absorbance for LDH assay. No differences were found between groups.

7.2.1.5. MRI contrast

MNPs are nice contrast agents for MRI. In order to test this feature, a phantom was performed with samples of only iPSCs, iPSCs incubated with MNPs (200 and 500 µg/ml) and PBS for MRI analysis. As shown in **Figure 54**, signals in T2 map were decreased in samples with the highest concentration of MNPs respect to the other lower concentration and controls. Likewise, we found a gradual decrease of signals in T2 map respect to que quantity of cells (the higher concentration of cells with MNPs, the lower the signal in T2 map of MRI) (**Figure 54**).

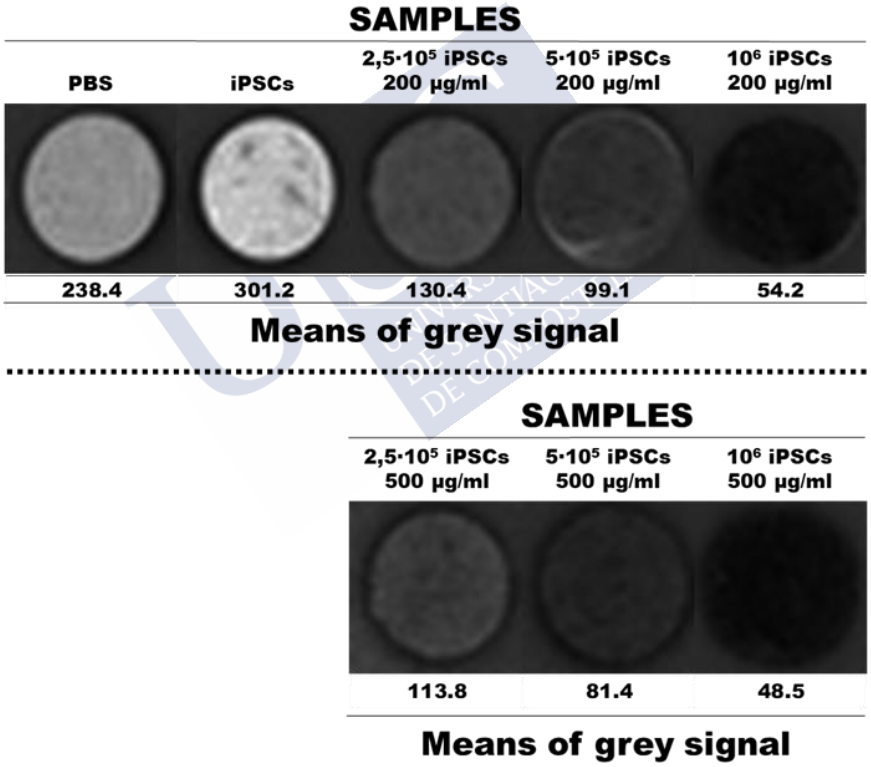

Figure 54: T2 map images by MR for phantoms of iPSCs with and without MNPs. Two different concentrations of MNPs (200 and 500 ug/ml) and three amounts of cells ($2.5x10^5$, $5x10^5$ and 10^6) were evaluated. A control with vehicle was also included. Numbers above images correspond to the mean signal in T2 maps of MRI.

On the other hand, MRIs *in vivo* were acquired in ischemic rats before and after intravenous injection of iPSCs incubated with 500 µg/ml of MNPs. T2 maps were obtained of whole brain. Unfortunately, signal uptake of nanoparticles was not detected in the brain (**Figure 55**).

Likewise, MRIs of whole body were acquired in order to check whether signal uptake was located in any other region, especially in liver, kidneys and spleen (**Figure 56**); however we could not observe any signal uptake as well.

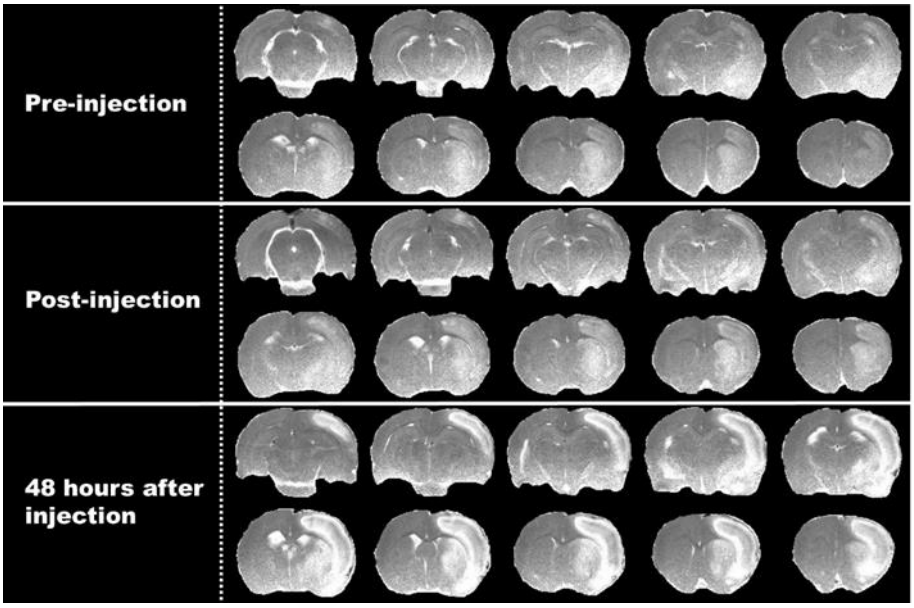

Figure 55: T2 maps of axial slices of representative ischemic rat brain before injection of iPSCs with MNPs, just after injection and 2 days after. Signal uptake of nanoparticles was not detected in the brain at any time.

7.2.1.6. Iron quantity *in vivo* analysis by ICP-MS

Given the possibility that the sensitivity of MRI was not sufficient to detect MNPs-iPSCs *in vivo*, an analysis of ICP-MS in the organs mostly involved in drug biodistribution was performed at 24 h after intravenous injection of iPSCs-MNPs (500 µg/ml) in ischemic rats. Animals were perfused in order to extract their organs (brain, liver,

lungs, kidneys, and spleen) and measure the quantity of iron by ICP-MS. The obtained results were close similar to the control group (ischemic rats without iPSCs administration) that would represent the baseline value in iron quantity. In addition, *in vitro* samples were measured to know how much iron we injected. The quantity of Fe per injection was 21.4 µg. In **Figure 57** we can see the comparative results of iron quantity in each organ in both control and MNPs-iPSCs treated rats. There were no differences between groups in any organ. One possible explanation is the fact that the Fe quantity per injection was, for example, 70 times smaller than the iron quantity in liver. Thus, the split of this little quantity of iron does not generate an enough difference in Fe levels in organs with high concentration of iron.

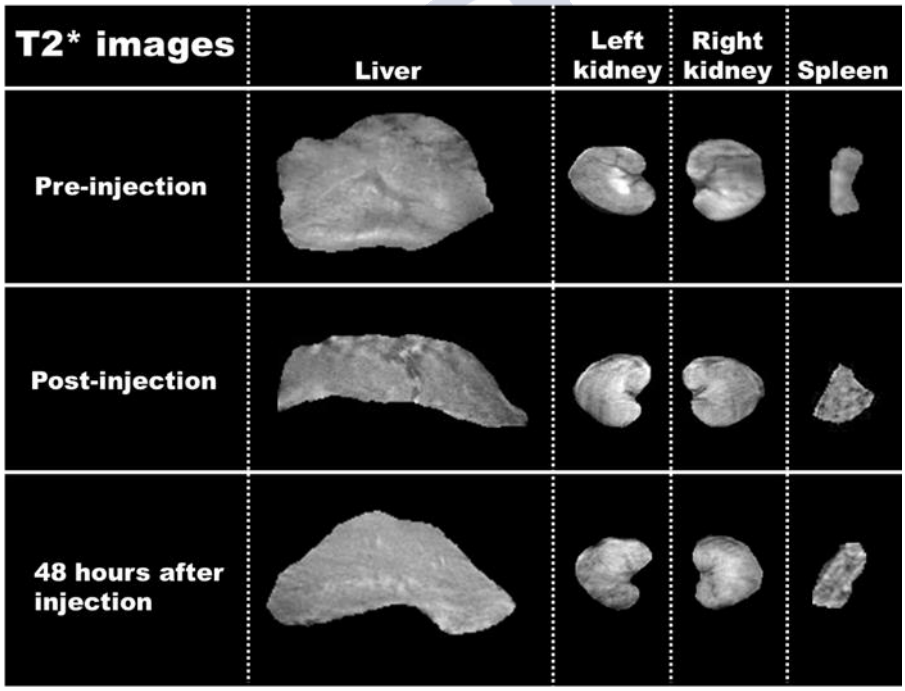

Figure 56: T2* MRI of liver, kidneys and spleen for a representative rat before intravenous treatment with MNPs-iPSCs, just after injection and 2 days after. Signal uptake of nanoparticles was not detected in any organ.

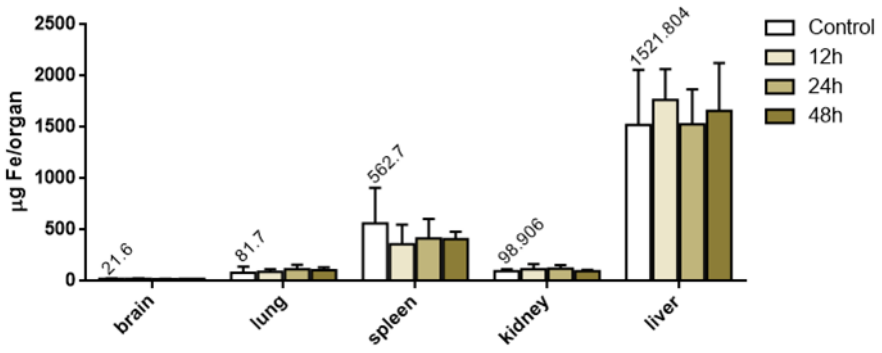

Figure 57: ICP-MS analysis showing the iron levels in brain, lungs, spleen, kidney, and liver in control group (ischemic rats), and in ischemic rats treated with MNPs-iPSCs that were sacrificed at 12, 24, and 48 hours after cell administration. Numbers in diagonal pattern above the control columns show normal levels (means in control group) of iron in each organ. No differences were found between groups.

7.2.2. LABELLING iPSCs WITH CFSE

7.2.2.1. CFSE labelling of iPSCs

Since the magnetic contrast for MRI did not work, we decided to use a fluorescent cell labelling method such as CSFE. Cells were analysed by flow cytometry just after labelling with CFSE, and at 12, 24 and 48 hours after this labelling; as reference we analysed control cells without CFSE. **Figure 58** showed a great efficiency of labelling (close to 100%) just after CFSE incubation. After that, a progressive decay of CFSE signal during the time was observed due to cellular proliferation. Therefore, in conclusion, CSFE labelling worked and cells maintained the capacity of proliferation.

7.2.2.2. CFSE labelling biodistribution

Just after CFSE labelling, cells were detached and injected in ischemic rats, and after 12 hours the organs were extracted, disaggregated and their cells analysed by flow cytometry. We didn't find any difference in histograms of organs between rats treated and non-treated with CFSE-iPSCs (**Figure 59**), so we could not discriminate an amount of labelled iPSCs in any organ, nor estimate a biodistribution of cells. Once more, the allocation of cells -in this case, the fluorescent label- was too spread out to be detected.

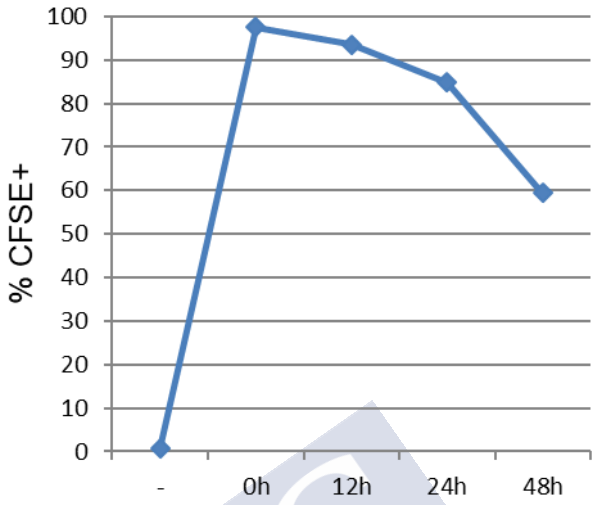

Figure 58: Percentage of CFSE-labelled cells during incubation of 48 hours. A great efficiency of labelling (close to 100%) just after CFSE incubation was obtained. After that, a progressive decay of CFSE signal during the time was observed due to cellular proliferation.

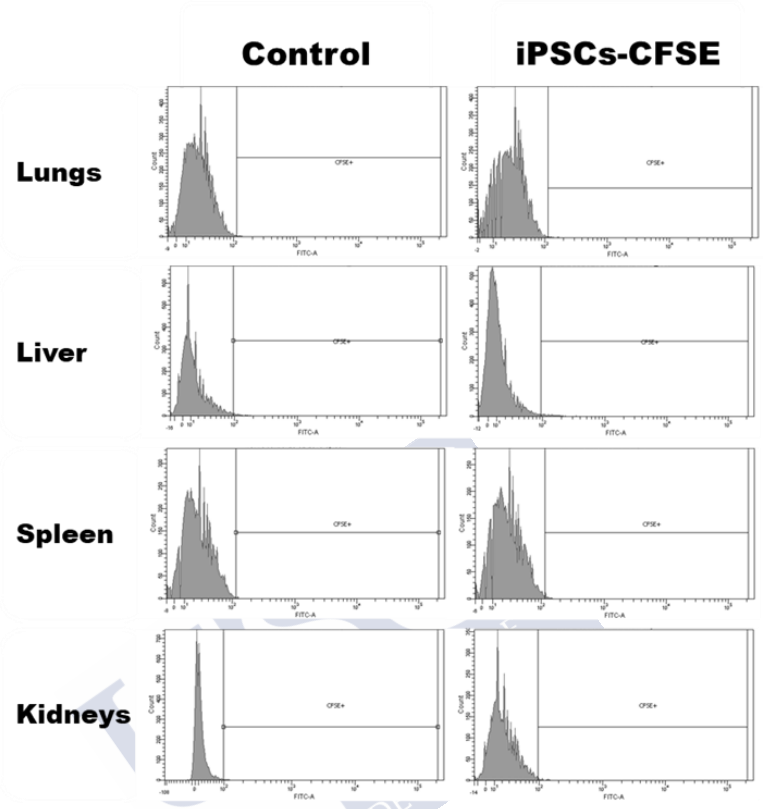

Figure 59: Flow cytometry histograms of disaggregated cells of different organs of rats treated or non-treated with CFSE-iPSCs. No differences were found between groups.

7.2.1. LABELLING MSCS WITH ^{18}F-FDG

7.2.1.1. Activity in cells

A powerful imaging tool for biodistribution analysis is PET. Due to this, we decided to carry out a proof of concept to test the viability or not of the cellular labelling with ^{18}F-FDG. ^{18}F-FDG incubation was applied in four different conditions. Firstly, MSCs were incubated with normal medium and ^{18}F-FDG, but all the activity stayed in medium. After that, we performed an incubation of ^{18}F-FDG with MSCs in only PBS, and the results showed a little uptake of activity by the cells; however, the percentage of this uptake was too small, and the time of incubation let the ^{18}F-FDG activity decayed. Likewise, ^{18}F-FDG was incubated with medium for MSCs based on free-glucose DMEN in order to facilitate the uptake of ^{18}F-FDG; unfortunately, cells didn't gain any radioactivity. Finally, the incubation of ^{18}F-FDG in free-glucose medium after glucose deprivation overnight resulted the strategy with higher activity percentage in cells; nevertheless, the required time of incubation was so long that the final activity in cells was very small for conducting *in vivo* studies. Therefore, this situation does not represent a useful cell labelling method for *in vivo* cell-tracking studies. **Figure 60** shows a summary of all explained results above.

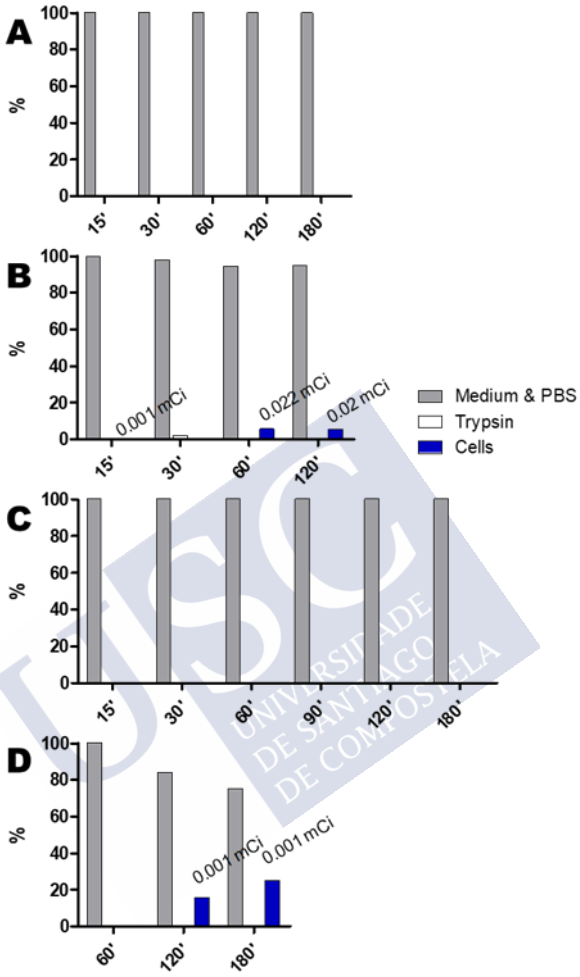

Figure 60: Percentage of ^{18}F-FDG activity in washing medium and PBS, trypsin and neutralizing medium, and cells after centrifugation. In all graphs the Y axis represents the percentage of total measured activity, and the X axis represents time of incubation of ^{18}F-FDG. The numbers above several columns indicate the absolute radioactivity measured at final point of incubation by cells in millicuries. (A) Results of ^{18}F-FDG incubation in normal medium for MSCs. (B) Results of incubating ^{18}F-FDG in PBS. (C) Results of ^{18}F-FDG incubation in medium for MSCs based in free-glucose DMEN. (D) ^{18}F-FDG incubation in glucose-free medium after glucose deprivation.

7.2.2. LABELLING iPSCs WITH AuNPs

At this point, we decided to use a cellular labelling through nanoparticles of a compound not present in the body or in trace amounts, and that could be detected by ICP-MS. The decision was to use AuNPs that meet these requirements.

7.2.2.1. AuNPs seeds

After synthesis of AuNPs, nanoparticles were analysed by UV-Vis in order to found out the maximal absorbance in spectrum and the absorbance at 450 nm. In this regard, TEM images of these seeds were acquired in order to measure the nanoparticles with more precision and check their shape. **Figure 61** shows TEM images of seeds; a total of 296 nanoparticles were measured and the mean of diameter was 10.69 nm with a standard deviation of 0.852.

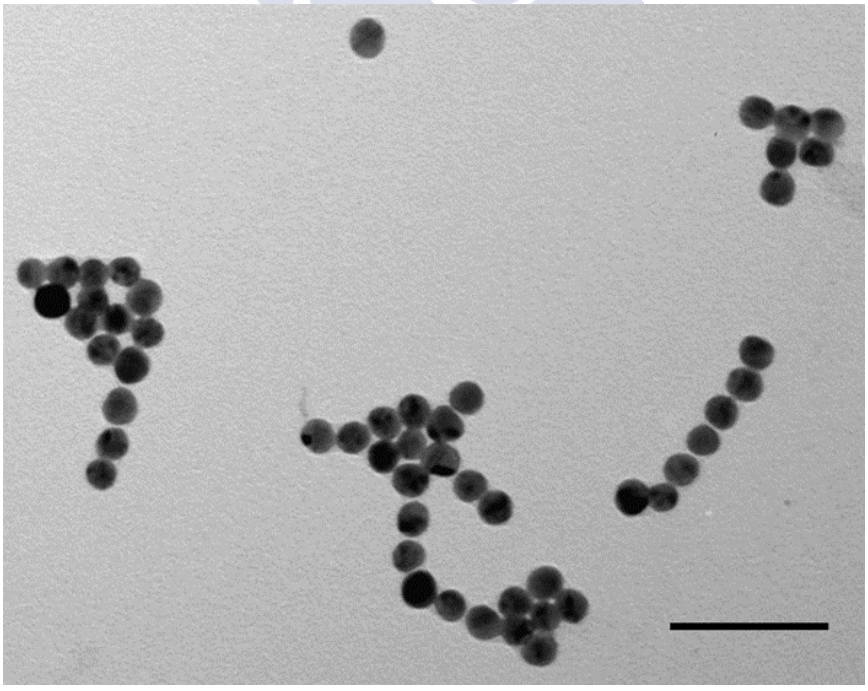

Figure 61: TEM image of AuNPs seeds. Scale: 50 nm.

7.2.2.2. Grown AuNPs

After two steps of growth, the same protocol to analyse the previous nanoparticles was applied. TEM was also used to measure the size and check the shape. The obtained result is shown in **Figure 62**, we measured the diameter of 332 nanoparticles with a mean of 18.39 nm and a standard deviation of 2.552.

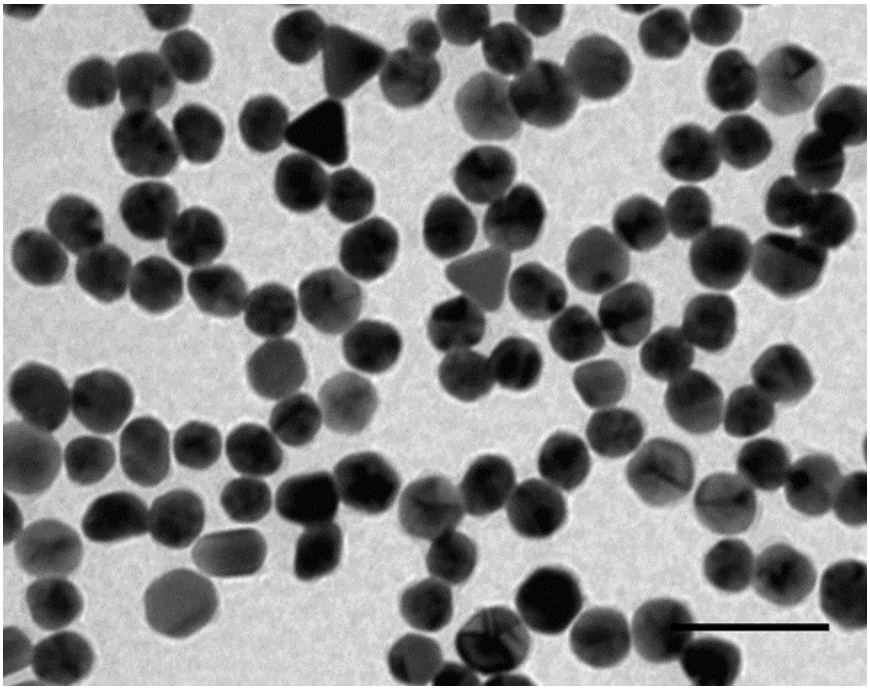

Figure 62: TEM image of AuNPs grown seeds. Scale: 50 nm.

7.2.2.3. Labelling of iPSCs

We analysed the percentage of rhodamine-labelled cells and the mean of fluorescent intensity after the incubation with AuNPs-BSA-R at different concentrations (0, 0.1, 0.5 and 1 mg/ml) and several times of incubation (6, 12 and 24 h). We can see results in **Table 3**. Both the mean of fluorescence and the percentage of cell positive for rhodamine b increase as time of incubation and concentration of AuNPs in culture

medium are larger. We observed great efficiency of labelling with 1 and 0.5 mg/ml with both sized of NPs, and with 0.1 mg/ml of 18 nm-NPs. The highest mean of fluorescence was obtained with 1 mg/ml of 18 nm-AuNPs incubated for 24 h. Generally, cells incubated with grown seeds showed better labelling.

Table 3: Results of percentages of labelled iPSCs in comparison with total amount of iPSCs and means of fluorescence intensity (MFI). Three times of incubation were tested: 6, 12 and 24 hours; and three concentrations of nanoparticles in culture medium were compared with a control with NPs.

Ø 10 nm			Ø 18 nm		
	Control			Control	
	Rhodamine b + (%)	MFI		Rhodamine b + (%)	MFI
6h	0.2	13	6h	0.1	10
12h	0.3	9	12h	0.2	8
24h	0.3	8	24h	0.2	7
	0.1 mg/ml			0.1 mg/ml	
	Rhodamine b + (%)	MFI		Rhodamine b + (%)	MFI
6h	13.3	813	6h	91.6	126
12h	16.5	140	12h	96.2	782
24h	17.9	151	24h	86.1	629
	0.5 mg/ml			0.5 mg/ml	
	Rhodamine b + (%)	MFI		Rhodamine b + (%)	MFI
6h	96.5	1290	6h	78.9	393
12h	93.6	487	12h	98.5	1207
24h	96.2	596	24h	98	1138
	1 mg/ml			1 mg/ml	
	Rhodamine b + (%)	MFI		Rhodamine b + (%)	MFI
6h	97.5	1421	6h	81.4	447
12h	96.8	539	12h	98.7	1263
24h	98.9	850	24h	99.4	1686

7.2.2.4. Analysis of apoptosis

We analysed apoptosis by flow cytometry of iPSCs incubated with AuNPs of 2 diameters (10 nm and 18 nm) at 3 different concentrations (0.1, 0.5 and 1 mg/ml) and using 3 times of incubation (6, 12 and 24 h).

No differences were found between iPSCs incubated or not with AuNPs for any concentration and time of incubation (**Table 4**).

Based on these results, we decided to use AuNPs at 1 mg/ml concentration and 24 hours for incubation with iPSCs for *in vivo* studies.

Table 4: Results of apoptosis test by flow cytometry. Numbers indicate the percentage of annexin positive cells. As in labelling assay, 6, 12 and 24 hours of incubation were tested comparing a control without nanoparticles and the following concentrations: 0.1, 0.5 and 1 mg of AuNPs per ml of culture medium.

Ø 10 nm		Ø 18 nm	
	Control		**Control**
	Annexin+ (%)		**Annexin+ (%)**
6h	2.6	6h	2
12h	1.3	12h	2.3
24h	6.4	24h	6.2
	0.1 mg/ml		**0.1 mg/ml**
	Annexin+ (%)		**Annexin+ (%)**
6h	2.2	6h	0.1
12h	1.7	12h	2
24h	3.5	24h	8.9
	0.5 mg/ml		**0.5 mg/ml**
	Annexin+ (%)		**Annexin+ (%)**
6h	2.3	6h	1.8
12h	2	12h	2.3
24h	2.2	24h	2.3
	1 mg/ml		**1 mg/ml**
	Annexin+ (%)		**Annexin+ (%)**
6h	2.5	6h	2.8
12h	2.5	12h	2.2
24h	2.1	24h	1.9

7.2.2.5. Analysis of pluripotency

Taking into the account the previous results, we chose the incubation of 18 nm-NPs at 1 mg/ml for 24 hours for final experiments. After the incubation, cells were analysed for pluripotency markers by flow cytometry. **Table 5** shows the percentage of positivity for pluripotency markers. The uptake of 18 nm-AuNPs did not affect the maintaining of pluripotency in culture up to 3 days.

Table 5: Percentage of expression for pluripotency markers: Oct3/4, Nanog, Sox2. Numbers mean the percentage of positive cells in whole population. No differences were found between iPSCs incubated or not with AuNPs.

iPSCs				
	Oct3/4+	Nanog+	Sox2+	Triple+
1 day	70.2	99.5	89.0	66.6
2 days	76.4	99.7	98.9	76.3
3 days	79.9	99.8	97.8	79.6
iPSCs + AuNPs-BSA				
	Oct3/4+	Nanog+	Sox2+	Triple+
1 day	80.8	99.5	99.7	80.7
2 days	86.7	99.7	99.9	86.7
3 days	86.8	99.4	98.1	86.5

7.2.2.6. *In vivo* biodistribution by ICP-MS analysis of gold quantity

Firstly, we measured gold quantity by ICP-MS in the following samples: iPSCs, iPSCs just after incubation with AuNPs (18 nm-NPs at 1 mg/ml), and 24 and 48 hours after this incubation.

Results showed in **Figure 63** indicated that a regular injection of $3x10^6$ iPSCs contained an average of 114 µg of gold that is split normally over time.

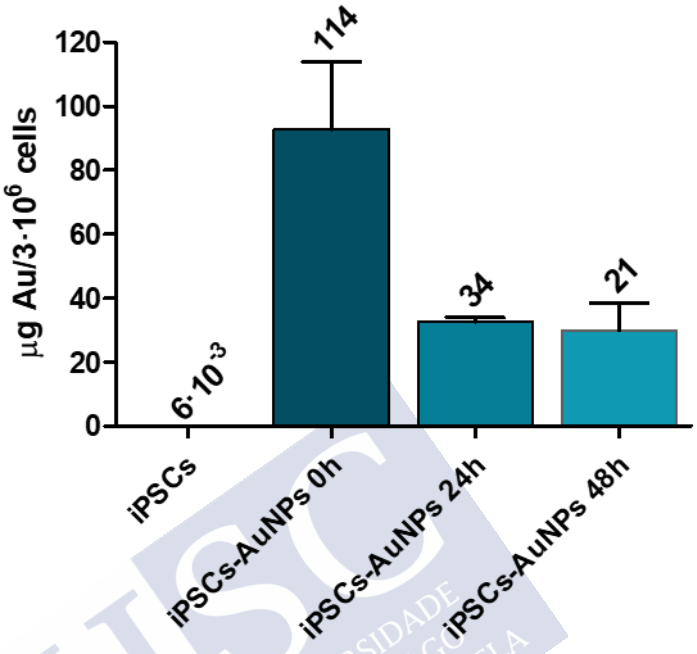

Figure 63: Gold quantity in $3x10^6$ of iPSCs incubated with AuNPs at three different times (basal, 24 and 48h) compared to a sample with only iPSCs as a control. Numbers above the bars indicate gold quantity (µg) in $3x10^6$ of iPSCs.

Finally, we performed an *in vivo* study in ischemic animals intravenously treated with $3x10^6$ iPSCs-AuNPs. Gold levels in main organs after iPSCs-AuNPs injection were also measured by ICP-MS (**Figure 64**). Gold quantity was mostly detected in liver: 35.3 $\mu g_{Au}/g_{organ}$ that represent 87.2% of total amount of gold, lung and spleen captured 10.3 and 2.2%, respectively. The amount of gold in the brain was minimal, so we can conclude that the potential therapeutic effects of iPSCs are not exerted directly on the brain but by pleiotropic effects.

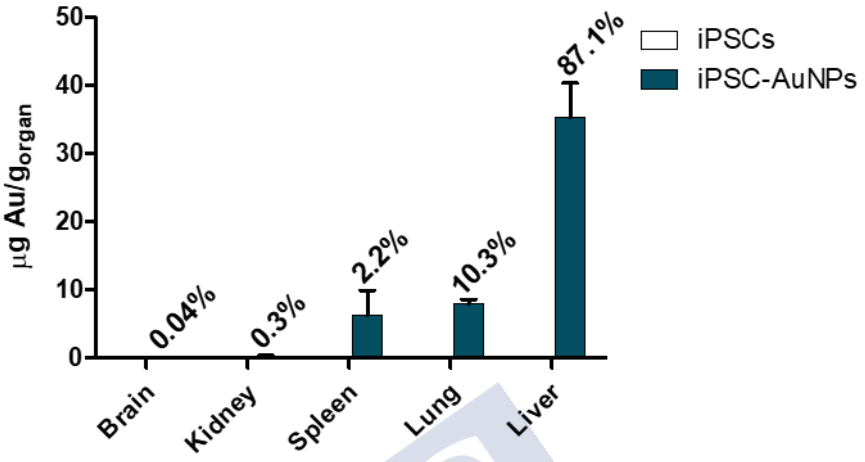

Figure 64: Gold concentrations, analysed by ICP-MS, in main organs at 24 hours after injection of $3 \cdot 10^6$ iPSCs-AuNPs. Columns represent µg of gold per gram of organ. Numbers above the columns indicate the percentage of gold respect to total amount of gold.

8. DISCUSSION

USC
UNIVERSIDADE
DE SANTIAGO
DE COMPOSTELA

Ischemic and haemorrhagic stroke remain as diseases without pharmacological treatment for recovery nor restauration of brain tissue, despite all the efforts of biomedical community to find out some neuroprotective or neurorestorative drug.

Nowadays, there is no specific pharmacological treatment for intracerebral haemorrhage; and early surgery, even if does not increase the rate of death or disability at 6 months, might have only a small but clinically relevant survival advantage for patients with spontaneous superficial ICH without intraventricular haemorrhage.(113) On the other hand, the only effective treatment for acute ischemic stroke is the recanalization procedures that due their short therapeutic window reaches a limited percentage of candidate patients. Therefore, it is high demand to search for new therapeutic options. During the last 2 decades, many efforts were aimed to search new therapeutic options for stroke based on neurorepair, especially through cellular therapy. In this regard, this study has evaluated the therapeutic effect of iPSCs treatment in preclinical models of the 2 major subtypes of cerebrovascular diseases, haemorrhagic and ischemic stroke, on the lesion volumes, sensorial-motor deficits, and neurogenesis/cerebral angiogenesis induction. Furthermore, due to the pluripotency properties of iPSCs, PET studies were performed in order to explore the development of tumours. Finally, a biodistribution study was conducted since one of the pending gaps of cell therapy is to determine the *in vivo* biodistribution of its intravenous administration in order to avoid side effects and determine the natural migration niches. Remarkably, we have demonstrated that iPSCs intravenous administration mediated recovery in haemorrhagic and ischemic stroke animal models. Specifically, improved motor function in the haemorrhagic model and better neurological function were in the ischemic model. By contrast, iPSCs intracranial administration aggravated both motor and neurological function in haemorrhagic stroke model. However, iPSCs treatment did not mediate protective effects on lesion volume. On the other hand, all iPSCs treatment increased endogenous neurogenesis in both ischemic and hemorrhagic preclinical stroke models, but no effects were observed for angiogenesis. Importantly, no evidence of tumour formation at two months after the intravenous administration nor the

intracranial graft of iPSCs. Finally, cell labelling of iPSCs with AuNPs demonstrated that these cells mostly migrated into the liver. The amount of gold, and therefore of iPSCs, in the brain was minimal, so we can conclude that the potential therapeutic effects of iPSCs are not exerted directly on the brain.

Several issues must be considered in the design of cell therapy studies; selection of the cellular type is essential, since they will be the promoter of beneficial or, even, harmful effects. Different cellular types were tested in pre-clinical and clinical trials. The current trend is to use more differentiated cells for local effect, and less differentiated ones for pleiotropic properties such as immunomodulation. iPSCs were discovered in 2006 and this fact meant a revolution in the way of getting stem cells. iPSCs are dedifferentiated as embryonic stem cells but can be obtained from somatic, adult and differentiated tissues, so may open big opportunities for cellular therapies based on autologous grafts. These unique characteristics of iPSCs, together with the lack of preclinical studies of intravenous administration of iPSCs in cerebrovascular diseases, were what motivated us to test the possible therapeutic effects of iPSCs in animal models of ischemia and cerebral haemorrhage.

Our results showed that intravenous administration of iPSCs induces recovery in both haemorrhagic and ischemic stroke model without migrating to any neurological niche. It is then possible to hypothesize that the beneficial effects of iPSCs are mediated by pleiotropic effects. In this regard, taking the pleiotropic effect up, it was demonstrated that stem cells are able to secrete inflammatory molecules and exosomes/microvesicles that can mediate therapeutic effects outside its cellular niche.(114) iPSCs also release microvesicles -around 5000 one cell in 24 hours- containing selected mRNAs and transcription factors as Oct3/4, Nanog, Klf4 and C-Myc,(115) that may have a role in maintaining of pluripotency and maybe a potential induction of tissue regeneration. In fact, microvesicles obtained from iPSCs culture are able to improve the wound repair in idiopathic pulmonary fibrosis animal model(116) or to inhibit apoptosis caused by oxidative stress.(117) That is one of the most original parts of this

project, since, as far as we know, we injected iPSCs intravenously in stroke animal models for the first time.

Moreover, we did not find a reduction in lesions volumes in any of used models, but we do observe an improvement in functional tests. Ischemic rats treated with iPSCs had better results in neurological tests; by contrast, there was not any improvement in functional outcome. Instead, haemorrhagic rats treated with intravenous iPSCs showed improvement in motor test, while neurological recovery was no so apparent. A possible explanation for these contradictory results can be focused on the location of the lesion that seems to be essential for the potential functional recovery. That is, the ischemic lesion, with its core in motor cortex, makes harder the recovery in motor functions; conversely, haematoma, located in striatum, increases the difficulty of a recovery in neurological functions.

It is also interesting that the intracranial injection of iPSCs exacerbated the functional deficits, despite good results in histological analysis showing an increased endogenous neurogenesis. Despite there are even some clinical trials about cell therapy in which cells were intracranially injected, this administration route implies certain risks; it was reported seizures, haematomas, worsening of motor deficits, headache, nauseas, fever, and, even, local ectopic tissue overgrowth.(118) Most of them are risks derived from surgical procedure. It is true that there are some trial that did not report adverse effects from intracranial injection,(119, 120) but it is important to note that the injections always were administrated several months or, even, years after stroke. Despite this, we decided to try intracranial injection of iPSCs in the haemorrhagic stroke model because some ICH are treated with decompressive craniotomy; in these cases, the intracerebral injection of cells is accessible.

On the other hand, we evaluated neuroplasticity -by the capacity of brain tissue to renewal neuroblasts- and the remodelling of the vascular system -by the density of vessels in brain. Like other studies with other types of stem cells,(121) we observed higher neurogenesis in animals treated with iPSCs. In both animal models, the number of double positive for DCX and Ki-67 was bigger in those groups treated with intravenous cells. Interestingly, intracranial administration of iPSCs did

not increase these double positive cells, but the positive area for DCX. Therefore, it seems that systemic iPSCs encourage the neurogenesis, and local iPSCs increase the migration of neuroblasts. This increased neurogenesis may be the responsible for the neurological improvement found in those groups treated with iPSCs.

Although it is known that certain stem cells enhance angiogenesis,(122) we did not find any differences in cerebral density of vessels nor angiogenesis processes between groups. However, the other histological effect (increased neurogenesis) appears enough to improve functional deficits.

It was also described that the iv injection of iPSCs in an acute lung injury animal model downregulates proinflammatory response, decreasing NF-κB, IL-6 levels among other inflammatory mediators.(123) Likewise, it was also demonstrated that the intravascular administration of iPSCs reduces the inducible NO synthase (iNOS) expression in an acute kidney injury animal model, that is induced by ischemia.(124) So, despite not many articles were published based on systemic administration of iPSCs, there is enough evidences that this kind of administration in animal models can modify inflammatory expression in a pleiotropic way.

The follow-up of period was close to two months after iPSCs administration. All animals from groups treated with cells were scanning to check tumour formation. No treated animals developed tumours. In addition, we did not notice any adverse effect; in fact, all rats survived the two months without any problem except the deficit causing by model. Therefore, we can conclude that both intravenous and intracerebral administration of iPSCs was safe.

To elucidate the potential mechanism how iPSCs may mediate therapeutic effects, we decided that the first step was to find out where they migrate and accumulate. For that, we had to label the cells and track them. There are several methods of labelling cells, namely different kinds of nanoparticle (quantum dots, silica NPs, polymer NPs, SPIO NPs, gold NPs…),(125) radioactive molecules,(126) or bioluminescence imaging (BLI).(127)

Firstly, we decided to test magnetic nanoparticles exploiting the previous experience and knowledge of our lab.(128, 129) After

synthesis of MNPs, nanoparticles were characterized to prove that they were of correct size, had a small dispersion and worked as contrast agent in MRI. MNPs were incubated with iPSCs and the resulted cells were also characterized to check the internalization of nanoparticles and regular behaviour of cells. All the experiments about MNPs synthesis and *in vitro* uptake showed positive results: nanoparticles had adequate size and shape, generated contrast in MRI, were internalized by iPSCs, no toxic effects were observed, and MNPs-iPSCs were detected by MRI. Unfortunately, *in vivo* results were unsatisfactory. Contrast in MRI signal was not enough to discriminate the location of MNPs in any region of the body. It is possible that the distribution of cells was so spread that not enough concentration of iron for generating contrast in MRI; or that the cells travelled to some place where the iron was undetectable, i.e. lung, where the air decrease MRI signal widely.

The next step was the repetition of the *in vivo* experiments in order to try to detect the quantity of iron by ICP-MS. Iron was measured in each organ separately, and they were compared with control organs. Each injection of $3x10^6$ iPSCs contained 21.4 μg_{Fe}, so each cell contained an average of around 7 pg_{Fe}; but the quantity of iron in the control organ with less iron -the brain- had an average of 21.6 μg_{Fe}, and a standard deviation of 1.7 μg_{Fe} (this quantity would imply near to 250,000 cells). And the control organ with most iron -liver- had 1,522 μg_{Fe} with a standard deviation of 540 μg_{Fe}, and lungs contained an average of 82 ± 58 μg_{Fe}. Therefore, both the quantity of iron and the standard deviation in control organs were so high; this supposed a big background, enough to hide a potential elevation of iron quantity due to MNPs.

Discarding iron nanoparticles to track iPSCs, we tried to track them with a fluorescent molecule. CFSE is a commercial and regular marker for cells that is mainly used to study the proliferation of cells. That is why, firstly, we evaluated the percentage of positive cells several days after labelling. Despite more than 90% of CFSE positive cells at 12 hours after labelling was found *in vitro*, CFSE-iPSCs were undetectable after intravenous administration in *in vivo* studies. Once again, it seems that the cells spread through the body in such way that the signal (in this case, fluorescent signal) is so low to be detected.

The next step was to follow the protocol from Wolfs *et al.*(112) to label cells with a radioactive tag in order to detect it by γ-counter or PET. ^{18}F-FDG, used to label cells, is a regular contrast in clinical PET practice; radioactive glucose is seized as normal glucose by cells but could not be metabolized, so it is accumulated. In this experiment we did not pass the *in vitro* part, because in no case signal from ^{18}F in cells was enough for a detection *in vivo*. Unlike in the article of Wolfs, our cells did not capture enough labelled glucose, even after an incubation without glucose. A personal advice from Wolfs´s group was to use cells in passes < 10, even so we could not get a properly uptake of ^{18}F-FDG by the iPSCs. Therefore, we concluded that this method is not the right one to label cell for *in vivo* tracking.

Finally, we performed some experiments similar to MNPs labelling, but in this case the nanoparticles were made of gold. The quantity of gold in the body is minimal, and this fact reduces to very low levels the background in ICP analysis. AuNPs were stable and no toxic or side effects were observer after their incubation with the iPSCs. After intravenous administration of AuNPs-labelled iPSCs in rats, almost totally of gold were found in liver, lungs and spleen, especially in the first one. The injection of labelled cells was performed at 24 hours after tMCAO; at this time brain-blood barrier is re-established, so the lack of cells in brain was not surprising. The experience of our lab with other types of cells like mesenchymal stem cells indicate that MSCs travel predominately to lungs, hence this great uptake by liver was astonishing.(109) This discrepancy in biodistribution between MSCs and iPSCs, probably, is due to the size of both. iPSCs are smaller than MSCs, so whereas mesenchymal cells get caught in very small pulmonary capillaries, iPSCs get away from lungs. Around 10% of iPSCs travel to the lungs. Lungs have a wide hematopoietic capacity,(130) and from liver several immunologic effects are initiated causing an anti-inflammatory immune response.(131) Additionally, iPSCs have got a great advantage in comparison with MSCs, that is they are pluripotent so they can differentiate in any cellular type meanwhile MSCs can differentiate only in mesodermal cells. In this way, iPSCs could be integrated in any tissue, i.e. in brain in the case some cells get pass through brain-blood barrier.

More studies must be carried out to understand deeply how iPSCs may induce recovery in stroke. In this way, we though that identifying migratory niches should be the first step, but their relationship to the environment and their potential pleiotropic effects must be further investigated in order to enable cell therapy with iPSCs in stroke patients.

USC
UNIVERSIDADE
DE SANTIAGO
DE COMPOSTELA

9. CONCLUSIONS

USC
UNIVERSIDADE
DE SANTIAGO
DE COMPOSTELA

9.1. THERAPEUTIC EFFECTS OF iPSCs IN CEREBRAL ISCHEMIA

1) iPSCs intravenous administration mediated recovery in ischemic stroke animal model in comparison with control group, specifically, in neurological function, and increased neurogenesis at two months after treatment.

2) Intravenous administration of iPSCs did not have effect on lesion volume or on vessels density in cerebral parenchyma at two months after treatment.

3) There was no evidence of tumour formation at two months after the intravenous administration of iPSCs.

9.2. THERAPEUTIC EFFECTS OF iPSCs IN INTRACEREBRAL HAEMORRHAGE

1) iPSCs intravenous administration mediated recovery in haemorrhagic stroke animal model in comparison with control group, specifically, in motor function, and increases neurogenesis at two months after treatment.

2) Intravenous or intracranial administration of iPSCs did not have effect on haematoma lesion volume or on vessels density in cerebral parenchyma at two months

3) iPSCs intracranial administration aggravated both motor and neurological function in haemorrhagic stroke model compared to control group.

4) There was no evidence of tumour formation at two months after the intravenous administration nor the intracranial graft of iPSCs.

9.3.BIODISTRIBUTION OF iPSCs INTRAVENOUSLY ADMINISTERED AT EARLY STAGE

1) D-MNPs were internalized by iPSCs without toxic or side effects. Likewise, D-MNPs decreased signal in MRI both alone and internalized by cells, so they can act as contrast agents for MRI *in vitro*, but D-MNPs-labelled iPSCs did not generated contrast in MRI *in vivo* after intravenous injection in ischemic rats.

2) Labelling cells with CFSE was not an adequate method for cell tracking after systemic administration of iPSCs.

3) AuNPs functionalized with Rhodamine B-labelled BSA were internalized by iPSCs, with no evidences of toxic or side effects, such affectation on pluripotency cell-surface markers.

4) Biodistribution *in vivo* studies in ischemic rats with AuNPs-iPSCs suggest that these cells travel mostly to the liver. The amount of gold, and therefore (theoretically) of iPSCs, was minimally detected in the brain; indicating that the potential therapeutic effects of iPSCs are not exerted directly on the brain.

10. CONCLUSIONES

USC
UNIVERSIDADE
DE SANTIAGO
DE COMPOSTELA

10.1.EFECTOS TERAPÉUTICOS DE LAS iPSCs EN LA ISQUEMIA CEREBRAL

1) La administración intravenosa de iPSCs medió recuperación funcional en el modelo animal de isquemia en comparación con el grupo de control, específicamente, en la función neurológica, y aumentó la neurogénesis dos meses después del tratamiento.

2) La administración intravenosa de iPSCs no tuvo efecto sobre el volumen de la lesión ni sobre la densidad de vasos en el parénquima cerebral dos meses después del tratamiento.

3) No hubo evidencias de formación de tumores dos meses después de la administración intravenosa de las iPSCs.

10.2.EFECTOS TERAPÉUTICOS DE LAS iPSCs EN LA HEMORRAGIA CEREBRAL

1) La administración intravenosa de iPSCs medió recuperación funcional en el modelo animal de hemorragia, concretamente en la función motora, y aumentó la neurogénesis a los dos meses después del tratamiento.

2) Las administraciones intravenosa e intracraneal de iPSCs no tuvieron efecto sobre el volumen de la lesión del hematoma ni sobre la densidad de vasos en el parénquima cerebral a los dos meses tras el tratamiento.

3) La administración intracraneal de iPSCs agravó tanto la función motora como la neurológica en comparación con el grupo control.

4) No hubo evidencias de formación de tumores a los dos meses después de la administración intravenosa o intracraneal de iPSCs.

10.3.BIODISTRIBUCIÓN EN FASE TEMPRANA DE LAS iPSCs TRAS SU ADMINISTRACIÓN SISTÉMICA

1) Las D-MNPs fueron internalizadas por las iPSCs sin efectos tóxicos o secundarios. Asimismo, las D-MNPs disminuyeron la señal en resonancia magnética tanto solas como internalizadas por las células, por lo que pueden actuar como agentes de contraste en resonancia *in vitro*; sin embargo, las iPSCs marcadas con D-MNPs no generaron contraste en resonancia *in vivo* después de su inyección intravenosa en ratas isquémicas.

2) El marcaje de las células con CFSE no fue un método adecuado para el seguimiento celular después de su administración sistémica.

3) Las AuNPs funcionalizadas con BSA y con rodamina B fueron internalizadas por las iPSCs, sin evidencias de efectos tóxicos o secundarios, como la afectación en marcadores de pluripotencia.

4) Los estudios de biodistribución *in vivo* en ratas isquémicas con AuNPs-iPSCs sugieren que estas células viajan principalmente al hígado. La cantidad de oro, y por lo tanto (teóricamente) de iPSCs, fue mínimamente detectada en el cerebro; sugiriendo que los potenciales efectos terapéuticos de las iPSCs no se ejercen directamente sobre él.

11. REFERENCES

USC
UNIVERSIDADE
DE SANTIAGO
DE COMPOSTELA

1. Sacco RL, Kasner SE, Broderick JP, Caplan LR, Culebras A, Elkind MS, George MG, Hamdan AD, Higashida RT, Hoh BL. An updated definition of stroke for the 21st century a statement for healthcare professionals from the American Heart Association/American Stroke Association. Stroke. 2013;44(7):2064-89.
2. Rodríguez-Yáñez M, Fernández Maiztegui C, Pérez-Concha T, Castillo J, Zarranz J. Enfermedades vasculares cerebrales. Neurología. Cuarta Edición ed. Madrid, España: Elsevier España; 2008. p. 337-411.
3. INE INdE. Defunciones según la Causa de Muerte. 2014.
4. Mérida-Rodrigo L, Poveda-Gómez F, Camafort-Babkowski M, Rivas-Ruiz F, Martín-Escalante M, Quirós-López R, García-Alegría J. Supervivencia a largo plazo del ictus isquémico. Revista clínica española. 2012;212(5):223-8.
5. Arias-Rivas S, Vivancos-Mora J, Castillo J. Epidemiología de los subtipos de ictus en pacientes hospitalizados atendidos por neurólogos: resultados del registro EPICES (I). Revista de neurología. 2012;54(7):385-93.
6. Wolfe CD. The impact of stroke. British medical bulletin. 2000;56(2):275-86.
7. Clua-Espuny J, Piñol-Moreso J, Panisello-Tafalla A, Lucas-Noll J, Gil-Guillen V, Orozco-Beltran D, Queralt-Tomas M. Estudio Ebrictus. Resultados funcionales, supervivencia y años potenciales de vida perdidos después del primer episodio de ictus. Atención Primaria. 2012;44(4):223-31.
8. Adamson J, Beswick A, Ebrahim S. Is stroke the most common cause of disability? Journal of Stroke and Cerebrovascular Diseases. 2004;13(4):171-7.
9. Feigin VL, Forouzanfar MH, Krishnamurthi R, Mensah GA, Connor M, Bennett DA, Moran AE, Sacco RL, Anderson L, Truelsen T. Global and regional burden of stroke during 1990–2010: findings from the Global Burden of Disease Study 2010. The Lancet. 2014;383(9913):245-55.

10. Sánchez CS. Informe del Impacto Sociosanitario de las Enfermedades Neurológicas en España. Fundación Española de Enfermedades Neurológicas (FEEN); 2006.
11. Carod-Artal FJ, Egido-Herrero JA, González-Gutiérrez JL, Varela de Seijas E. Coste directo de la enfermedad cerebrovascular en el primer año de seguimiento. Revista de neurología. 1999;28(12):1123-30.
12. Beguiristain JM, Mar J, Arrazola A. Coste de la enfermedad cerebrovascular aguda. Revista de neurología. 2005;40(07):0406-411.
13. de Economía Aplicada FdE. Los costes de los cuidados informales asociados a enfermedades neurológicas discapacitantes de alta prevalencia en España. Neurología. 2008;23(1):29-39.
14. Arboix A, Díaz J, Pérez-Sempere A, Álvarez-Sabín J. Ictus: Tipos etiológicos y criterios diagnósticos. Revista de neurología. 2002;17:3-12.
15. Del Zoppo GJ, Saver JL, Jauch EC, Adams HP, Jr., American Heart Association Stroke C. Expansion of the time window for treatment of acute ischemic stroke with intravenous tissue plasminogen activator: a science advisory from the American Heart Association/American Stroke Association. Stroke. 2009;40(8):2945-8.
16. Adams HP, Jr., Bendixen BH, Kappelle LJ, Biller J, Love BB, Gordon DL, Marsh EE, 3rd. Classification of subtype of acute ischemic stroke. Definitions for use in a multicenter clinical trial. TOAST. Trial of Org 10172 in Acute Stroke Treatment. Stroke. 1993;24(1):35-41.
17. Feinberg WM, Albers GW, Barnett HJ, Biller J, Caplan LR, Carter LP, Hart RG, Hobson II RW, Kronmal RA, Moore WS. Guidelines for the management of transient ischemic attacks. From the Ad Hoc Committee on Guidelines for the Management of Transient Ischemic Attacks of the Stroke Council of the American Heart Association. Circulation. 1994;89(6):2950-65.

18. Amarenco P, Bogousslavsky J, Caplan L, Donnan G, Hennerici M. Classification of stroke subtypes. Cerebrovascular diseases. 2009;27(5):493-501.
19. Astrup J, Symon L, Branston NM, Lassen NA. Cortical evoked potential and extracellular K+ and H+ at critical levels of brain ischemia. Stroke. 1977;8(1):51-7.
20. Hansen AJ. Effect of anoxia on ion distribution in the brain. Physiological reviews. 1985;65(1):101-48.
21. Kristian T, Siesjo BK. Calcium in Ischemic Cell Death. Stroke. 1998;29(3):705-18.
22. Choi DW. Ionic dependence of glutamate neurotoxicity. The Journal of neuroscience. 1987;7(2):369-79.
23. Choi DW, Rothman SM. The role of glutamate neurotoxicity in hypoxic-ischemic neuronal death. Annual review of neuroscience. 1990;13:171-82.
24. White BC, Sullivan JM, DeGracia DJ, O'Neil BJ, Neumar RW, Grossman LI, Rafols JA, Krause GS. Brain ischemia and reperfusion: molecular mechanisms of neuronal injury. Journal of the neurological sciences. 2000;179(S 1-2):1-33.
25. Grandati M, Verrecchia C, Revaud ML, Allix M, Boulu RG, Plotkine M. Calcium-independent NO-synthase activity and nitrites/nitrates production in transient focal cerebral ischaemia in mice. British journal of pharmacology. 1997;122(4):625-30.
26. Nogawa S, Zhang F, Ross ME, Iadecola C. Cyclo-oxygenase-2 gene expression in neurons contributes to ischemic brain damage. The Journal of neuroscience. 1997;17(8):2746-55.
27. McDonald ES, Windebank AJ. Mechanisms of neurotoxic injury and cell death. Neurologic clinics. 2000;18(3):525-40.
28. Jander S, Kraemer M, Schroeter M, Witte OW, Stoll G. Lymphocytic infiltration and expression of intercellular adhesion molecule-1 in photochemically induced ischemia of the rat cortex. Journal of cerebral blood flow and metabolism. 1995;15(1):42-51.

29. Banasiak KJ, Xia Y, Haddad GG. Mechanisms underlying hypoxia-induced neuronal apoptosis. Progress in neurobiology. 2000;62(3):215-49.
30. Rami A, Agarwal R, Botez G, Winckler J. mu-Calpain activation, DNA fragmentation, and synergistic effects of caspase and calpain inhibitors in protecting hippocampal neurons from ischemic damage. Brain research. 2000;866(1-2):299-312.
31. Back T. Pathophysiology of the ischemic penumbra--revision of a concept. Cellular and molecular neurobiology. 1998;18(6):621-38.
32. Castillo J. Fisiopatología de la isquemia cerebral. Revista de neurología. 2000;30(5):459.
33. Astrup J, Siesjö BK, Symon L. Thresholds in cerebral ischemia-the ischemic penumbra. Stroke. 1981;12(6):723-5.
34. Mies G, Ishimaru S, Xie Y, Seo K, Hossmann K-A. Ischemic thresholds of cerebral protein synthesis and energy state following middle cerebral artery occlusion in rat. Journal of Cerebral Blood Flow & Metabolism. 1991;11(5):753-61.
35. Rodríguez-Yáñez M, Castellanos M, Freijo M, Fernández JL, Martí-Fàbregas J, Nombela F, Simal P, Castillo J, Díez-Tejedor E, Fuentes B. Guías de actuación clínica en la hemorragia intracerebral. Neurología. 2013;28(4):236-49.
36. Xi G, Keep RF, Hoff JT. Mechanisms of brain injury after intracerebral haemorrhage. The Lancet Neurology. 2006;5(1):53-63.
37. Wagner KR, Sharp FR, Ardizzone TD, Lu A, Clark JF. Heme and iron metabolism: role in cerebral hemorrhage. Journal of cerebral blood flow and metabolism. 2003;23(6):629-52.
38. Aronowski J, Zhao X. Molecular pathophysiology of cerebral hemorrhage: secondary brain injury. Stroke. 2011;42(6):1781-6.
39. Adams HP, Jr., del Zoppo G, Alberts MJ, Bhatt DL, Brass L, Furlan A, Grubb RL, Higashida RT, Jauch EC, Kidwell C, Lyden PD, Morgenstern LB, Qureshi AI, Rosenwasser RH, Scott PA, Wijdicks EF, American Heart Association/American Stroke

Association Stroke C, American Heart Association/American Stroke Association Clinical Cardiology C, American Heart Association/American Stroke Association Cardiovascular R, Intervention C, Atherosclerotic Peripheral Vascular Disease Working G, Quality of Care Outcomes in Research Interdisciplinary Working G. Guidelines for the early management of adults with ischemic stroke: a guideline from the American Heart Association/American Stroke Association Stroke Council, Clinical Cardiology Council, Cardiovascular Radiology and Intervention Council, and the Atherosclerotic Peripheral Vascular Disease and Quality of Care Outcomes in Research Interdisciplinary Working Groups: The American Academy of Neurology affirms the value of this guideline as an educational tool for neurologists. Circulation. 2007;115(20):e478-534.
40. Dirks M, Niessen LW, van Wijngaarden JD, Koudstaal PJ, Franke CL, van Oostenbrugge RJ, Huijsman R, Lingsma HF, Minkman MM, Dippel DW, Investigators PRATiIS. Promoting thrombolysis in acute ischemic stroke. Stroke. 2011;42(5):1325-30.
41. Donnan GA, Davis SM, Parsons MW, Ma H, Dewey HM, Howells DW. How to make better use of thrombolytic therapy in acute ischemic stroke. Nature reviews neuroscience. 2011;7(7):400-9.
42. Lees KR, Bluhmki E, von Kummer R, Brott TG, Toni D, Grotta JC, Albers GW, Kaste M, Marler JR, Hamilton SA, Tilley BC, Davis SM, Donnan GA, Hacke W, Ecass AN, Group Er-PS, Allen K, Mau J, Meier D, del Zoppo G, De Silva DA, Butcher KS, Parsons MW, Barber PA, Levi C, Bladin C, Byrnes G. Time to treatment with intravenous alteplase and outcome in stroke: an updated pooled analysis of ECASS, ATLANTIS, NINDS, and EPITHET trials. Lancet. 2010;375(9727):1695-703.
43. Wahlgren N, Ahmed N, Davalos A, Ford GA, Grond M, Hacke W, Hennerici MG, Kaste M, Kuelkens S, Larrue V, Lees KR, Roine RO, Soinne L, Toni D, Vanhooren G, investigators S-M. Thrombolysis with alteplase for acute ischaemic stroke in the Safe Implementation of Thrombolysis in Stroke-Monitoring Study

(SITS-MOST): an observational study. Lancet. 2007;369(9558):275-82.
44. DeMers G, Meurer WJ, Shih R, Rosenbaum S, Vilke GM. Tissue plasminogen activator and stroke: review of the literature for the clinician. The Journal of emergency medicine. 2012;43(6):1149-54.
45. Rodriguez-Yáñez M, Sobrino T, Arias S, Vazquez-Herrero F, Brea D, Blanco M, Leira R, Castellanos M, Serena J, Vivancos J, Davalos A, Castillo J. Early biomarkers of clinical-diffusion mismatch in acute ischemic stroke. Stroke. 2011;42(10):2813-8.
46. Morgenstern LB, Hemphill JC, 3rd, Anderson C, Becker K, Broderick JP, Connolly ES, Jr., Greenberg SM, Huang JN, MacDonald RL, Messe SR, Mitchell PH, Selim M, Tamargo RJ, American Heart Association Stroke C, Council on Cardiovascular N. Guidelines for the management of spontaneous intracerebral hemorrhage: a guideline for healthcare professionals from the American Heart Association/American Stroke Association. Stroke. 2010;41(9):2108-29.
47. Kaur H, Prakash A, Medhi B. Drug therapy in stroke: from preclinical to clinical studies. Pharmacology. 2013;92(5-6):324-34.
48. Ginsberg MD. Current status of neuroprotection for cerebral ischemia: synoptic overview. Stroke. 2009;40(3 Suppl):S111-4.
49. Jia M, Njapo SA, Rastogi V, Hedna VS. Taming glutamate excitotoxicity: strategic pathway modulation for neuroprotection. CNS Drugs.29(2):153-62.
50. Shuaib A, Lees KR, Lyden P, Grotta J, Davalos A, Davis SM, Diener HC, Ashwood T, Wasiewski WW, Emeribe U. NXY-059 for the treatment of acute ischemic stroke. The New England Journal of medicine. 2007;357(6):562-71.
51. Chamorro A, Amaro S, Castellanos M, Segura T, Arenillas J, Marti-Fabregas J, Gallego J, Krupinski J, Gomis M, Canovas D, Carne X, Deulofeu R, Roman LS, Oleaga L, Torres F, Planas AM. Safety and efficacy of uric acid in patients with acute stroke

(URICO-ICTUS): a randomised, double-blind phase 2b/3 trial. Lancet neurology.13(5):453-60.
52. Secades JJ, Frontera G. CDP-choline: pharmacological and clinical review. Methods and findings in experimental and clinical pharmacology. 1995;17 Suppl B:1-54.
53. Hurtado O, Moro MA, Cardenas A, Sanchez V, Fernandez-Tome P, Leza JC, Lorenzo P, Secades JJ, Lozano R, Davalos A, Castillo J, Lizasoain I. Neuroprotection afforded by prior citicoline administration in experimental brain ischemia: effects on glutamate transport. Neurobiology of disease. 2005;18(2):336-45.
54. Hurtado O, Cardenas A, Pradillo JM, Morales JR, Ortego F, Sobrino T, Castillo J, Moro MA, Lizasoain I. A chronic treatment with CDP-choline improves functional recovery and increases neuronal plasticity after experimental stroke. Neurobiology of disesase. 2007;26(1):105-11.
55. Davalos A, Castillo J, Alvarez-Sabin J, Secades JJ, Mercadal J, Lopez S, Cobo E, Warach S, Sherman D, Clark WM, Lozano R. Oral citicoline in acute ischemic stroke: an individual patient data pooling analysis of clinical trials. Stroke. 2002;33(12):2850-7.
56. Davalos A, Alvarez-Sabin J, Castillo J, Diez-Tejedor E, Ferro J, Martinez-Vila E, Serena J, Segura T, Cruz VT, Masjuan J, Cobo E, Secades JJ. Citicoline in the treatment of acute ischaemic stroke: an international, randomised, multicentre, placebo-controlled study (ICTUS trial). Lancet. 2012;380(9839):349-57.
57. Montaner J. Capítulo 7. Estrategias neuroprotectoras. Tratamiento del ictus isquémico. 3: Marge Books; 2009.
58. Haseldonckx M, Van JR, de Ven Van M, Wouters L, Borgers M. Protection with lubeluzole against delayed ischemic brain damage in rats. A quantitative histopathologic study. Stroke. 1997;28(2):428-32.
59. Gandolfo C, Sandercock PA, Conti M. Lubeluzole for acute ischaemic stroke. Cochrane Database of Systematic Reviews. 2002;(1):CD001924.

60. Veltkamp R, Gill D. Clinical trials of immunomodulation in ischemic stroke. Neurotherapeutics. 2016;13(4):791-800.
61. da Silva-Candal A, Pérez-Díaz A, Santamaría M, Correa-Paz C, Rodríguez-Yáñez M, Ardá A, Pérez-Mato M, Iglesias-Rey R, Brea J, Azuaje J. Clinical validation of blood/brain glutamate grabbing in acute ischemic stroke. Annals of neurology. 2018;84(2):260-73.
62. Alvarez-Buylla A, Garcia-Verdugo JM. Neurogenesis in adult subventricular zone. The Journal of neuroscience. 2002;22(3):629-34.
63. Zhang ZG, Chopp M. Neurorestorative therapies for stroke: underlying mechanisms and translation to the clinic. The Lancet Neurology. 2009;8(5):491-500.
64. Marti-Fabregas J, Romaguera-Ros M, Gomez-Pinedo U, Martinez-Ramirez S, Jimenez-Xarrie E, Marin R, Marti-Vilalta JL, Garcia-Verdugo JM. Proliferation in the human ipsilateral subventricular zone after ischemic stroke. Neurology. 2010;74(5):357-65.
65. Wang L, Zhang Z, Wang Y, Zhang R, Chopp M. Treatment of stroke with erythropoietin enhances neurogenesis and angiogenesis and improves neurological function in rats. Stroke. 2004;35(7):1732-7.
66. Souvenir R, Doycheva D, H Zhang J, Tang J. Erythropoietin in stroke therapy: friend or foe. Current medicinal chemistry. 2015;22(10):1205-13.
67. Arenillas JF, Sobrino T, Castillo J, Davalos A. The role of angiogenesis in damage and recovery from ischemic stroke. Current treatment options in cardiovascular medicine. 2007;9(3):205-12.
68. Brea D, Sobrino T, Ramos-Cabrer P, Castillo J. Reorganización de la vasculatura cerebral tras la isquemia. Revista de neurología. 2009;49:645-54.
69. Seevinck PR, Deddens LH, Dijkhuizen RM. Magnetic resonance imaging of brain angiogenesis after stroke. Angiogenesis. 2010;13(2):101-11.

70. Sobrino T, Hurtado O, Moro MA, Rodriguez-Yanez M, Castellanos M, Brea D, Moldes O, Blanco M, Arenillas JF, Leira R, Davalos A, Lizasoain I, Castillo J. The increase of circulating endothelial progenitor cells after acute ischemic stroke is associated with good outcome. Stroke. 2007;38(10):2759-64.
71. Zacharek A, Chen J, Cui X, Li A, Li Y, Roberts C, Feng Y, Gao Q, Chopp M. Angiopoietin1/Tie2 and VEGF/Flk1 induced by MSC treatment amplifies angiogenesis and vascular stabilization after stroke. Journal of cerebral blood flow and metabolism. 2007;27(10):1684-91.
72. Font MA, Arboix A, Krupinski J. Angiogenesis, neurogenesis and neuroplasticity in ischemic stroke. Current cardiology reviews. 2010;6(3):238-44.
73. Liu XS, Chopp M, Zhang RL, Hozeska-Solgot A, Gregg SC, Buller B, Lu M, Zhang ZG. Angiopoietin 2 mediates the differentiation and migration of neural progenitor cells in the subventricular zone after stroke. The Journal of biological chemistry. 2009;284(34):22680-9.
74. Teng H, Zhang ZG, Wang L, Zhang RL, Zhang L, Morris D, Gregg SR, Wu Z, Jiang A, Lu M, Zlokovic BV, Chopp M. Coupling of angiogenesis and neurogenesis in cultured endothelial cells and neural progenitor cells after stroke. Journal of cerebral blood flow and metabolism. 2008;28(4):764-71.
75. Chopp M, Zhang ZG, Jiang Q. Neurogenesis, angiogenesis, and MRI indices of functional recovery from stroke. Stroke. 2007;38(2 Suppl):827-31.
76. Jiang Q, Zhang ZG, Ding GL, Zhang L, Ewing JR, Wang L, Zhang R, Li L, Lu M, Meng H, Arbab AS, Hu J, Li QJ, Pourabdollah Nejad DS, Athiraman H, Chopp M. Investigation of neural progenitor cell induced angiogenesis after embolic stroke in rat using MRI. Neuroimage. 2005;28(3):698-707.
77. Polezhaev L, Alexandrova M. Transplantation of embryonic brain tissue into the brain of adult rats after hypoxic hypoxia. Journal fur Hirnforschung. 1983;25(1):99-106.

78. Tae-Hoon L, Yoon-Seok L. Transplantation of mouse embryonic stem cell after middle cerebral artery occlusion. Acta Cirúrgica Brasileira. 2012;27(4):333-9.
79. Jafari SS, Aghaei AA, Asadi-Shekaari M, Nematollahi-Mahani S, Sheibani V. Investigating the effects of adult neural stem cell transplantation by lumbar puncture in transient cerebral ischemia. Neuroscience letters. 2011;495(1):1-5.
80. Chen J, Li Y, Wang L, Lu M, Zhang X, Chopp M. Therapeutic benefit of intracerebral transplantation of bone marrow stromal cells after cerebral ischemia in rats. Journal of the neurological sciences. 2001;189(1-2):49-57.
81. van Velthoven CT, Sheldon RA, Kavelaars A, Derugin N, Vexler ZS, Willemen HL, Maas M, Heijnen CJ, Ferriero DM. Mesenchymal stem cell transplantation attenuates brain injury after neonatal stroke. Stroke. 2013;44(5):1426-32.
82. Yamagata M, Yamamoto A, Kako E, Kaneko N, Matsubara K, Sakai K, Sawamoto K, Ueda M. Human dental pulp-derived stem cells protect against hypoxic-ischemic brain injury in neonatal mice. Stroke. 2013;44(2):551-4.
83. Chen J, Sanberg PR, Li Y, Wang L, Lu M, Willing AE, Sanchez-Ramos J, Chopp M. Intravenous administration of human umbilical cord blood reduces behavioral deficits after stroke in rats. Stroke. 2001;32(11):2682-8.
84. Borlongan CV, Kaneko Y, Maki M, Yu S-J, Ali M, Allickson JG, Sanberg CD, Kuzmin-Nichols N, Sanberg PR. Menstrual blood cells display stem cell-like phenotypic markers and exert neuroprotection following transplantation in experimental stroke. Stem cells and development. 2010;19(4):439-52.
85. Chen J, Shehadah A, Pal A, Zacharek A, Cui X, Cui Y, Roberts C, Lu M, Zeitlin A, Hariri R. Neuroprotective effect of human placenta-derived cell treatment of stroke in rats. Cell transplantation. 2013;22(5):871-9.
86. Takahashi K, Yamanaka S. Induction of pluripotent stem cells from mouse embryonic and adult fibroblast cultures by defined factors. Cell. 2006;126(4):663-76.

87. Kawai H, Yamashita T, Ohta Y, Deguchi K, Nagotani S, Zhang X, Ikeda Y, Matsuura T, Abe K. Tridermal tumorigenesis of induced pluripotent stem cells transplanted in ischemic brain. Journal of Cerebral Blood Flow & Metabolism. 2010;30(8):1487-93.
88. Jiang N, Chopp M, Chahwala S. Neutrophil inhibitory factor treatment of focal cerebral ischemia in the rat. Brain research. 1998;788(1):25-34.
89. Jensen MB, Yan H, Krishnaney-Davison R, Al Sawaf A, Zhang S-C. Survival and differentiation of transplanted neural stem cells derived from human induced pluripotent stem cells in a rat stroke model. Journal of Stroke and Cerebrovascular Diseases. 2013;22(4):304-8.
90. Qin J, Gong G, Sun S, Qi J, Zhang H, Wang Y, Wang N, Wang QM, Ji Y, Gao Y, Shi C, Yang B, Zhang Y, Song B, Xu Y. Functional recovery after transplantation of induced pluripotent stem cells in a rat hemorrhagic stroke model. Neuroscience letters. 2013;554:70-5.
91. Yuan T, Liao W, Feng N-H, Lou Y-L, Niu X, Zhang A-J, Wang Y, Deng Z-F. Human induced pluripotent stem cell-derived neural stem cells survive, migrate, differentiate, and improve neurologic function in a rat model of middle cerebral artery occlusion. Stem cell research & therapy. 2013;4(3):1.
92. Oki K, Tatarishvili J, Wood J, Koch P, Wattananit S, Mine Y, Monni E, Tornero D, Ahlenius H, Ladewig J. Human-induced pluripotent stem cells form functional neurons and improve recovery after grafting in stroke-damaged brain. Stem cells. 2012;30(6):1120-33.
93. Qin J, Song B, Zhang H, Wang Y, Wang N, Ji Y, Qi J, Chandra A, Yang B, Zhang Y, Gong G, Xu Y. Transplantation of human neuro-epithelial-like stem cells derived from induced pluripotent stem cells improves neurological function in rats with experimental intracerebral hemorrhage. Neuroscience letters. 2013;548:95-100.
94. Abad M, Mosteiro L, Pantoja C, Canamero M, Rayon T, Ors I, Grana O, Megías D, Domínguez O, Martínez D.

Reprogramming in vivo produces teratomas and iPS cells with totipotency features. Nature. 2013;502(7471):340.
95. Longa EZ, Weinstein PR, Carlson S, Cummins R. Reversible middle cerebral artery occlusion without craniectomy in rats. Stroke. 1989;20(1):84-91.
96. Agulla J, Argibay B, Pérez-Mato M, Brea D, Ramos-Cabrer P, Castillo J. Comparación de la lesión producida en tres modelos animales de isquemia cerebral focal permanente mediante resonancia magnética. Revista de neurología. 2011;53:265-74.
97. Saver JL, Albers GW, Dunn B, Johnston KC, Fisher M. Stroke Therapy Academic Industry Roundtable (STAIR) recommendations for extended window acute stroke therapy trials. Stroke. 2009;40(7):2594-600.
98. Fisher M, Feuerstein G, Howells DW, Hurn PD, Kent TA, Savitz SI, Lo EH. Update of the stroke therapy academic industry roundtable preclinical recommendations. Stroke. 2009;40(6):2244-50.
99. Waynforth HB, Flecknell PA. Experimental and surgical technique in the rat: Academic press London; 1980.
100. Nahhas MI, Hess DC. Stem Cell Therapy in Cerebrovascular Disease. Current treatment options in neurology. 2018;20(11):49.
101. Schallert T, Fleming SM, Leasure JL, Tillerson JL, Bland ST. CNS plasticity and assessment of forelimb sensorimotor outcome in unilateral rat models of stroke, cortical ablation, parkinsonism and spinal cord injury. Neuropharmacology. 2000;39(5):777-87.
102. Bederson JB, Pitts LH, Tsuji M, Nishimura M, Davis R, Bartkowski H. Rat middle cerebral artery occlusion: evaluation of the model and development of a neurologic examination. Stroke. 1986;17(3):472-6.
103. Wahl F, Allix M, Plotkine M, Boulu R. Neurological and behavioral outcomes of focal cerebral ischemia in rats. Stroke. 1992;23(2):267-72.

104. Seoane-Viaño I, Gómez-Lado N, Lázare-Iglesias H, Barreiro-de Acosta M, Silva-Rodríguez J, Luzardo-Álvarez A, Herranz M, Otero-Espinar F, Antúnez-López JR, Lamas MJ. Longitudinal PET/CT evaluation of TNBS-induced inflammatory bowel disease rat model. International journal of pharmaceutics. 2018;549(1-2):335-42.
105. Zhang L, Li Y, Zhang C, Chopp M, Gosiewska A, Hong K. Delayed administration of human umbilical tissue-derived cells improved neurological functional recovery in a rodent model of focal ischemia. Stroke. 2011;42(5):1437-44.
106. Liao SJ, Lin JW, Pei Z, Liu CL, Zeng JS, Huang RX. Enhanced angiogenesis with dl-3n-butylphthalide treatment after focal cerebral ischemia in RHRSP. Brain research. 2009;1289:69-78.
107. Rosenberg GA, Mun-Bryce S, Wesley M, Kornfeld M. Collagenase-induced intracerebral hemorrhage in rats. Stroke. 1990;21(5):801-7.
108. da Silva-Candal A, Vieites-Prado A, Gutiérrez-Fernández M, Rey RI, Argibay B, Mirelman D, Sobrino T, Rodríguez-Frutos B, Castillo J, Campos F. Blood glutamate grabbing does not reduce the hematoma in an intracerebral hemorrhage model but it is a safe excitotoxic treatment modality. Journal of Cerebral Blood Flow & Metabolism. 2015;35(7):1206-12.
109. Argibay B, Trekker J, Himmelreich U, Beiras A, Topete A, Taboada P, Perez-Mato M, Vieites-Prado A, Iglesias-Rey R, Rivas J, Planas AM, Sobrino T, Castillo J, Campos F. Intraarterial route increases the risk of cerebral lesions after mesenchymal cell administration in animal model of ischemia. Scientific reports. 2017;7:40758.
110. Pardoe H, Chua-Anusorn W, Pierre TGS, Dobson J. Structural and magnetic properties of nanoscale iron oxide particles synthesized in the presence of dextran or polyvinyl alcohol. Journal of magnetism and magnetic materials. 2001;225(1-2):41-6.
111. Suzuki J, Sasaki M, Harada K, Bando M, Kataoka Y, Onodera R, Mikami T, Wanibuchi M, Mikuni N, Kocsis JD.

Bilateral cortical hyperactivity detected by fMRI associates with improved motor function following intravenous infusion of mesenchymal stem cells in a rat stroke model. Brain research. 2013;1497:15-22.
112. Wolfs E, Struys T, Notelaers T, Roberts SJ, Sohni A, Bormans G, Van Laere K, Luyten FP, Gheysens O, Lambrichts I. 18F-FDG labeling of mesenchymal stem cells and multipotent adult progenitor cells for PET imaging: effects on ultrastructure and differentiation capacity. Journal of nuclear medicine. 2013;54(3):447-54.
113. Mendelow AD, Gregson BA, Rowan EN, Murray GD, Gholkar A, Mitchell PM, Investigators SI. Early surgery versus initial conservative treatment in patients with spontaneous supratentorial lobar intracerebral haematomas (STICH II): a randomised trial. The Lancet. 2013;382(9890):397-408.
114. Han C, Sun X, Liu L, Jiang H, Shen Y, Xu X, Li J, Zhang G, Huang J, Lin Z. Exosomes and their therapeutic potentials of stem cells. Stem cells international. 2016;2016.
115. Zhou J, Ghoroghi S, Benito-Martin A, Wu H, Unachukwu UJ, Einbond LS, Guariglia S, Peinado H, Redenti S. Characterization of induced pluripotent stem cell microvesicle genesis, morphology and pluripotent content. Scientific reports. 2016;6:19743.
116. Gazdhar A, Grad I, Tamò L, Gugger M, Feki A, Geiser T. The secretome of induced pluripotent stem cells reduces lung fibrosis in part by hepatocyte growth factor. Stem cell research & therapy. 2014;5(6):123.
117. Wang Y, Zhang L, Li Y, Chen L, Wang X, Guo W, Zhang X, Qin G, He S-h, Zimmerman A. Exosomes/microvesicles from induced pluripotent stem cells deliver cardioprotective miRNAs and prevent cardiomyocyte apoptosis in the ischemic myocardium. International journal of cardiology. 2015;192:61-9.
118. Boltze J, Arnold A, Walczak P, Jolkkonen J, Cui L, Wagner D-C. The dark side of the force–constraints and complications of cell therapies for stroke. Frontiers in neurology. 2015;6:155.

119. Suárez-Monteagudo C, Hernández-Ramírez P, Álvarez-González L, García-Maeso I, de la Cuétara-Bernal K, Castillo-Díaz L, Bringas-Vega ML, Martínez-Aching G, Morales-Chacón LM, Báez-Martín MM. Autologous bone marrow stem cell neurotransplantation in stroke patients. An open study. Restorative neurology and neuroscience. 2009;27(3):151-61.
120. Chen D-C, Lin S-Z, Fan J-R, Lin C-H, Lee W, Lin C-C, Liu Y-J, Tsai C-H, Chen J-C, Cho D-Y. Intracerebral implantation of autologous peripheral blood stem cells in stroke patients: a randomized phase II study. Cell transplantation. 2014;23(12):1599-612.
121. Yoo S-W, Kim S-S, Lee S-Y, Lee H-S, Kim H-S, Lee Y-D, Suh-Kim H. Mesenchymal stem cells promote proliferation of endogenous neural stem cells and survival of newborn cells in a rat stroke model. Experimental & molecular medicine. 2008;40(4):387.
122. Chen J, Zhang ZG, Li Y, Wang L, Xu YX, Gautam SC, Lu M, Zhu Z, Chopp M. Intravenous administration of human bone marrow stromal cells induces angiogenesis in the ischemic boundary zone after stroke in rats. Circulation research. 2003;92(6):692-9.
123. Yang KY, Shih HC, How CK, Chen CY, Hsu HS, Yang CW, Lee YC, Perng RP, Peng CH, Li HY, Chang CM, Mou CY, Chiou SH. IV delivery of induced pluripotent stem cells attenuates endotoxin-induced acute lung injury in mice. Chest. 2011;140(5):1243-53.
124. Lee P-Y, Chien Y, Chiou G-Y, Lin C-H, Chiou C-H, Tarng D-C. Induced pluripotent stem cells without c-Myc attenuate acute kidney injury via downregulating the signaling of oxidative stress and inflammation in ischemia–reperfusion rats. Cell transplantation. 2012;21(12):2569-85.
125. Accomasso L, Gallina C, Turinetto V, Giachino C. Stem cell tracking with nanoparticles for regenerative medicine purposes: an overview. Stem cells international. 2016;2016.
126. Matsusaka Y, Nakahara T, Takahashi K, Iwabuchi Y, Nishime C, Kajimura M, Jinzaki M. 18 F-FDG-labeled red blood

cell PET for blood-pool imaging: preclinical evaluation in rats. EJNMMI research. 2017;7(1):19.
127. Pendharkar AV, Chua JY, Andres RH, Wang N, Gaeta X, Wang H, De A, Choi R, Chen S, Rutt BK. Biodistribution of neural stem cells after intravascular therapy for hypoxic–ischemia. Stroke. 2010;41(9):2064-70.
128. Argibay B, Trekker J, Himmelreich U, Beiras A, Topete A, Taboada P, Pérez-Mato M, Iglesias-Rey R, Sobrino T, Rivas J. Easy and efficient cell tagging with block copolymer-based contrast agents for sensitive MRI detection in vivo. Cell transplantation. 2016;25(10):1787-800.
129. Argibay B, Trekker J, Himmelreich U, Beiras A, Topete A, Taboada P, Pérez-Mato M, Vieites-Prado A, Iglesias-Rey R, Rivas J. Intraarterial route increases the risk of cerebral lesions after mesenchymal cell administration in animal model of ischemia. Scientific reports. 2017;7:40758.
130. Lefrançais E, Ortiz-Muñoz G, Caudrillier A, Mallavia B, Liu F, Sayah DM, Thornton EE, Headley MB, David T, Coughlin SR. The lung is a site of platelet biogenesis and a reservoir for haematopoietic progenitors. Nature. 2017;544(7648):105.
131. Racanelli V, Rehermann B. The liver as an immunological organ. Hepatology. 2006;43(S1):S54-S62.

12. ANNEXES

USC
UNIVERSIDADE
DE SANTIAGO
DE COMPOSTELA

VICERREITORÍA DE INVESTIGACIÓN
E INNOVACIÓN
Oficina de Investigación e Tecnoloxía
Servizo de Convocatorias e Recursos Humanos de I+S
Edificio CACTUS – Campus Vida
15782 Santiago de Compostela
Tel. 981 547 040 - Fax 981 547 077
Correo electrónico: cittinfo@usc.es
http://imaisd.usc.es

JOSÉ MANUEL CIFUENTES MARTÍNEZ, PRESIDENTE DEL COMITÉ DE BIOÉTICA DE LA UNIVERSIDAD DE SANTIAGO DE COMPOSTELA, cuya Sección de Experimentación animal ha sido designada como Órgano Habilitado para la evaluación de proyectos de experimentación animal por resolución de la Xunta de Galicia, con fecha 11 de noviembre de 2013, de acuerdo con lo exigido por el RD 53/2013 de 1 de febrero, por el que se establecen las normas básicas aplicables para la protección de los animales utilizados en experimentación y otros fines científicos, incluyendo la docencia,

INFORMA:

Que el proyecto de investigación titulado: **"Nanopartículas biomiméticas para la administración dirigida de nanomedicinas"** del que es investigador responsable **D. Francisco Campos Pérez,** ha sido examinado por el Comité de Bioética de esta Universidad, Sección de Experimentación Animal, llegando a las siguientes conclusiones:

Con respecto a su finalidad, se trata de un proyecto de investigación traslacional o aplicada cuyo objetivo fundamentale el desarrollo de nanosistemas biomiméticos basados en cubiertas celulares (extraídas de células madre mesenquimales y/o plaquetas) para dirigir nanomedicinas a su lugar de acción (diana).

- Con respecto a los requisitos de las 3Rs,
    - No cabe la posibilidad de reemplazo ya que no se han encontrado otros métodos o estrategias de ensayo que permitan llevar a cabo los experimentos propuestos en este trabajo.
    - La experimentación se realizará en un centro registrado como usuario de animales de experimentación por lo que la manipulación, manejo y supervisión de los animales durante todo el proyecto será llevada a cabo por personas capacitadas. El grupo investigador lo componen personas con capacitaciones A, B y C, lo que asegura su preparación para garantizar el bienestar animales durante todos los procedimientos (requisito de refinamiento).
    - Finalmente, con respecto al requisito de reducción, se considera que el número de animales a utilizar es el mínimo imprescindible para la obtención de los resultados.

- La clasificación de los procedimientos en función de su grado de severidad es de "leve pa ra los procedimientos 1, 3 y "severo" para los procedimiento 2 y 4.
- Con respecto al balance de los daños y los beneficios, los procedimientos se efectúan bajo analgesia y anestesia previa a la administración de sustancias e intervenciones quirúrgicas por lo que se minimiza el dolor, angustia y sufrimiento. Los métodos de sacrificio descritos (sobredosis de anestesia) se encuentran entre los indicados por el propio RD 53/2013.
- Se han examinado las situaciones y excepciones previstas en el punto e) del artículo 34. 2 encontrando que ninguna de ellas es aplicable en este proyecto.
- El el proyecto se clasifica como tipo III y por tanto debe ser sometido a evaluación retrospectiva. Este Comité considera que dicha evaluación debería efectuarse a los dos años de la concesión de la autorización.

VICERREITORÍA DE INVESTIGACIÓN
E INNOVACIÓN
Oficina de Investigación e Tecnoloxía
Servizo de Convocatorias e Recursos Humanos de I+S
Edificio CACTUS – Campus Vida
15782 Santiago de Compostela
Tel. 981 547 040 - Fax 981 547 077
Correo electrónico: cittinfo@usc.es
http://imaisd.usc.es

Por todas estas razones, este Comité acordó emitir un **INFORME FAVORABLE.**

En la evaluación de este proyecto NO HA EXISTIDO CONFLICTO DE INTERESES.

Lugo, 17 de abril de 2018

Departamento Territorial
Edificio Administrativo de Servizos Múltiples
Vicente Ferrer, 2
15071 – A Coruña

RESOLUCIÓN DE AUTORIZACIÓN DE PROXECTOS DE EXPERIMENTACIÓN ANIMAL

Expediente núm.: 15010/2019/004 **Data de inicio:** 05.02.2019
Persoa interesada: Francisco Campos Pérez **Procedemento:** resolución de autorización
Forma de inicio: solicitude da persoa interesada

ANTECEDENTES

A persoa interesada, como representante do centro CIMUS (Universidade de Santiago de Compostela), presentou con data 05.02.2019 unha solicitude para a realización do proxecto de experimentación animal (entrada no Rexistro Electrónico da Xunta de Galicia 2019/246024), cuxos datos se detallan a continuación:

Denominación do proxecto: *Nanopartículas biomiméticas para a administración dirixida de nanomedicinas*
Nome do centro usuario: Animalario do CIMUS
Persoa responsable do proxecto: Francisco Campos Pérez
Establecemento onde se realizarán os procedementos do proxecto (ou lugar xeográfico no caso de traballos de campo): Animalario do CIMUS
Clasificación do proxecto : Tipo I ☐ Tipo II ☐ Tipo III ☒

CONSIDERACIÓNS LEGAIS E TÉCNICAS

1 O Real decreto 53/2013, de 1 de febreiro (BOE 34, do 8 de febreiro), polo que se establecen as normas básicas aplicables para a protección dos animais utilizados en experimentación e outros fins científicos, incluíndo a docencia, establece no seu artigo 33 as condicións de autorizacións dos proxectos con animais de experimentación.

2 O artigo 88 da Lei 39/2015, de 1 de outubro, do procedemento administrativo común das administracións públicas (BOE 236, do 2 de outubro de 2015) establece que a resolución que poña fin o procedemento decidirá todas as cuestións expostas polos interesados e aquelas outras derivadas deste.

3 O Servizo de Gandaría da Coruña revisou a documentación achegada na solicitude e o resultado favorable da avaliación do proxecto, realizada polo órgano habilitado da Sección de Experimentación Animal do Comité de Bioética da Universidade de Santiago de Compostela.

Esta xefatura territorial é competente para ditar unha resolución, de conformidade co Decreto 149/2018, do 5 de decembro, polo que se establece a estrutura orgánica da

Departamento Territorial
Edificio Administrativo de Servizos Múltiples
Vicente Ferrer, 2
15071 – A Coruña

Consellería do Medio Rural e se modifica parcialmente o Decreto 177/2016, do 15 de decembro, polo que se fixa a estrutura orgánica da Vicepresidencia e das consellerías da Xunta de Galicia (DOG 235, do 11 de novembro).

De acordo con todo o indicado, RESOLVO:

1 Autorizar o proxecto solicitado.
2 O mencionado proxecto precisa someterse a unha avaliación retrospectiva tras finalizar a súa autorización.
3 A autorización deste proxecto terá unha duración de dous anos e unha vez transcorrido este tempo deberá ser autorizado de novo.

A citada autorización é unicamente válida nas condicións que figuran no expediente. Ante calquera cambio significativo no proxecto que poida ter efectos negativos sobre o benestar dos animais, deberá solicitar a confirmación da autorización ao Servizo Provincial de Gandaría.

Esta autorización poderá ser suspendida, no caso de que o proxecto non se leve a cabo de acordo coas condicións de autorización e retirala, previo expediente tramitado ao que se lle dará audiencia.

Contra a presente resolución, que non lle pon fin á vía administrativa, poderá interpoñer un recurso de alzada ante o conselleiro de Medio Rural. O prazo comezará a contar dende o día seguinte ao da recepción desta resolución. Todo isto, segundo o disposto nos artigos 121 e 122 da citada Lei 39/2015.

Mediante este escrito notifícaselle ao CIMUS da USC esta resolución segundo o esixido no artigo 40.1 da antedita Lei 39/2015.

XUNTA DE GALICIA
CONSELLERÍA DO MEDIO RURAL

Dirección Xeral de Ordenación Forestal

San Lázaro, s/n
15781 Santiago de Compostela
Teléfono: 981 546 108 Fax: 981 546 101
mediorural.montesgalicia@xunta.es

galicia

Certificado de capacitación en materia de protección de animais utilizados, criados ou subministrados con fins de experimentación e otros fins científicos, incluíndo a docencia conforme coa Orde ECC/566/2015 de 20 de marzo.

Certificado de capacitación en materia de protección de animales utilizados, criados o suministrados con fines de experimentación y otros fines científicos, incluyendo la docencia conforme con la Orden ECC/566/2015 de 20 de marzo.

1. IDENTIFICACIÓN

1.1. Apelidos / *Apellidos / Surname:*

LÓPEZ ARIAS

1.2. Nome / *Nombre / First names:*	DNI / *IDNI / Identity card number:*
ESTEBAN	**47363783K**

1.3. Categoría/*Categoría/Category:*	1.4. Especies/*Especies/Species:*	1.5. Válido ata/ *válido hasta/expires:*
"c"	*Todas*	***2.04.2023***

2. Nº DO CERTIFICADO / *Nº DEL CERTIFICADO / CERTIFICATE NUMBER*

c366

3.ORGANISMO QUE EXPIDE O CERTIFICADO / *ORGANISMO QUE EXPIDE EL CERTIFICADO / BODY ISSUING THE CERTIFICATE:*

3.1. Nome e enderezo do organismo que expide o certificado / *Nombre y dirección del organismo que expide el certificado / Name and address of the body issuing the certificate:*

Dirección Xeral de Ordenación Forestal
CONSELLERÍA DO MEDIO RURAL – XUNTA DE GALICIA
San Lázaro, s/n
15781 Santiago de Compostela
A Coruña (España)

3.2. Teléfono / *Teléfono / Telephone:*	3.3. Fax / *Fax / Fax:*	3.4. Correo electrónico / *Correo electrónico / Email:*
981 546 654	981 546 651	formacion.cmrm@xunta.es

3.5. Data / *Fecha / Date:*	3.6. Lugar / *Lugar / Place:*
18/05/2018	**Santiago de Compostela**

3.7. Nome e sinatura / *Nombre y firma / Name and signature*	3.8. Selo / Sello / Stamp
Asdo.: **Tomás Fernández-Couto Juanas** **Director Xeral de Ordenación Forestal**	

galicia

MÓDULOS FUNDAMENTAIS OU TRONCAIS E ESPECÍFICOS CORRESPONDENTES Á CATEGORÍA "C" REALIZACIÓN DOS PROCEDEMENTOS – ORDE ECC/566/2015, DE 20 DE MARZO

MÓDULOS FUNDAMENTAIS OU TRONCAIS

1.- Lexislación nacional (1 hora).

2.- Ética, benestar animal e as "tres erres", nivel 1 (2 horas).

3.- Bioloxía básica e adecuada, nivel 1 (3 horas).

4.- Coidado, saúde e manexo dos animais, nivel 1 (5 horas).

5.- Recoñecemento do dolor, o sufrimento e a angustia (3 horas).

6.- Métodos incruentos de sacrificio, nivel 1 (2 horas)

MÓDULOS ESPECÍFICOS DA CATEGORÍA "C"

1.- Bioloxía básica e adecuada, nivel 2 (3 horas)

2.- Procedementos minimamente invasores sen anestesia, nivel 1 (5 horas)

3.- Procedementos minimamente invasores sen anestesia, nivel 2 (10 horas)

4.- Anestesia para procedementos menores (5 horas)

5.- Anestesia avanzada para intervencións cirúrxicas ou procedementos prolongados (8 horas)

6.- Principios de cirurxía (5 horas)

.....

MÓDULOS FUNDAMENTALES O TRONCALES

1.- Legislación nacional (1 hora).

2.- Ética, bienestar animal y las "tres erres", nivel 1 (2 horas).

3.- Biología básica y adecuada, nivel 1 (3 horas).

4.- Cuidado, salud y manejo de los animales, nivel 1 (5 horas).

5.- Reconocimiento del dolor, el sufrimiento y la angustia (3 horas).

6.- Métodos incruentos de sacrificio, nivel 1 (2 horas)

MÓDULOS ESPECÍFICOS DE LA CATEGORÍA "C"

1.- Biología básica y adecuada, nivel 2 (3 horas)

2.- Procedimientos mínimamente invasivos sin anestesia, nivel 1 (5 horas)

3.- Procedimientos mínimamente invasivos sin anestesia, nivel 2 (10 horas)

4.- Anestesia para procedementos menores (5 horas)

5.- Anestesia avanzada para intervenciones quirúrgicas o procedimientos prolongados (8 horas)

6.- Principios de cirugía (5 horas)

XUNTA DE GALICIA
CONSELLERÍA DO MEDIO RURAL
Dirección Xeral de Ordenación Forestal

San Lázaro, s/n
15781 Santiago de Compostela
Teléfono: 981 546 108 Fax: 981 546 101
mediorural.montesgalicia@xunta.es

Certificado de capacitación en materia de protección de animais utilizados, criados ou subministrados con fins de experimentación e otros fins científicos, incluíndo a docencia conforme coa Orde ECC/566/2015 de 20 de marzo.

Certificado de capacitación en materia de protección de animales utilizados, criados o suministrados con fines de experimentación y otros fines científicos, incluyendo la docencia conforme con la Orden ECC/566/2015 de 20 de marzo.

1. IDENTIFICACIÓN

1.1. Apelidos / *Apellidos / Surname:*
LÓPEZ ARIAS

1.2. Nome / *Nombre / First names:*	DNI /*DNI / Identity card number*
ESTEBAN	**47363783K**

1.3 Categoría/*Categoría/Category:*	1.4. Especies/*Especies/Species:*	1.5. Válido ata/ *válido hasta/expires:*
"d"	*Todas*	***2.04.2023***

2. Nº DO CERTIFICADO / *Nº DEL CERTIFICADO / CERTIFICATE NUMBER*

d231

3.ORGANISMO QUE EXPIDE O CERTIFICADO / *ORGANISMO QUE EXPIDE EL CERTIFICADO / BODY ISSUING THE CERTIFICATE:*

3.1. Nome e enderezo do organismo que expide o certificado / *Nombre y dirección del organismo que expide el certificado / Name and address of the body issuing the certificate:*

Dirección Xeral de Ordenación Forestal
CONSELLERÍA DO MEDIO RURAL – XUNTA DE GALICIA
San Lázaro, s/n
15781 Santiago de Compostela
A Coruña (España)

3.2. Teléfono / *Teléfono / Telephone:*	3.3. Fax / *Fax / Fax:*	3.4. Correo electrónico / *Correo electrónico / Email:*
981 546 654	981 546 651	formacion.cmrm@xunta.es

3.5. Data / *Fecha / Date:*	3.6. Lugar / *Lugar / Place:*
18/05/2018	**Santiago de Compostela**

3.7. Nome e sinatura / *Nombre y firma / Name and signature*	3.8. Selo / Sello / Stamp
Asdo.: **Tomás Fernández-Couto Juanas** **Director Xeral de Ordenación Forestal**	

galicia

MÓDULOS FUNDAMENTAIS OU TRONCAIS E ESPECÍFICOS CORRESPONDENTES Á CATEGORÍA "D" DESEÑO DOS PROXECTOS E PROCEDEMENTOS – ORDE ECC/566/2015, DE 20 DE MARZO

MÓDULOS FUNDAMENTAIS OU TRONCAIS

1.- Lexislación nacional (1 hora).

2.- Ética, benestar animal e as "tres erres", nivel 1 (2 horas).

3.- Bioloxía básica e adecuada, nivel 1 (3 horas).

4.- Coidado, saúde e manexo dos animais, nivel 1 (5 horas).

5.- Recoñecemento do dolor, o sufrimento e a angustia (3 horas).

6.- Métodos incruentos de sacrificio, nivel 1 (2 horas)

MÓDULOS ESPECÍFICOS DA CATEGORÍA "D"

1.- Ética, benestar animal e as "tres erres", nivel 2 (10 horas)

2.- Fundamentos de bioloxía e fisioloxía animal (20 horas)

3.- Procedementos minimamente invasores sen anestesia, nivel 1 (5 horas)

4.- Deseño de proxectos e procedementos, nivel 1 (5 horas)

5.- Deseño de proxectos e procedementos, nivel 2 (10 horas)

.....

MÓDULOS FUNDAMENTALES O TRONCALES

1.- Legislación nacional (1 hora).

2.- Ética, bienestar animal y las "tres erres", nivel 1 (2 horas).

3.- Biología básica y adecuada, nivel 1 (3 horas).

4.- Cuidado, salud y manejo de los animales, nivel 1 (5 horas).

5.- Reconocimiento del dolor, el sufrimiento y la angustia (3 horas).

6.- Métodos incruentos de sacrificio, nivel 1 (2 horas)

MÓDULOS ESPECÍFICOS DE LA CATEGORÍA "D"

1.- Ética, bienestar animal y las "tres erres", nivel 2 (10 horas)

2.- Fundamentos de biología y fisiología animal (20 horas)

3.- Procedimientos minimamente invasores sin anestesia, nivel 1 (5 horas)

4.- Diseño de proyectos y procedimientos, nivel 1 (5 horas)

5.- Diseño de proyectos y procedimientos, nivel 2 (10 horas)